UNIVERSITÄTSKLINIKUM HAMBURG-EPPENDORF

Institut für Systemimmunologie

Prof. Dr. Immo Prinz

Investigation of functional γδ and αβ T cell persistence through clonal tracking

Kumulative Dissertation

zur Erlangung des Doktorgrades PhD

an der Medizinischen Fakultät der Universität Hamburg.

vorgelegt von:

Zheng Song

Aus

Anhui, China

Hamburg 2026

Angenommen von der

Medizinischen Fakultät der Universität Hamburg am:

Veröffentlicht mit Genehmigung der

Medizinischen Fakultät der Universität Hamburg.

Betreuer:	Prof. Dr. Immo Prinz

Mitglieder des Thesis-Komitees:

Mitglied:	Prof. Dr. med. Christian F. Krebs
Mitglied:	Prof. Dr. Nicola Gagliani

Gutachtende:

Gutachter:	Prof. Dr. Immo Prinz
Gutachterin:	Prof. Dr. Eva Tolosa
Gutachter:	Prof. Axel Kallies

Mitglieder der Prüfungskommission:

Vorsitz der Prüfungskommission:	Prof. Dr. Immo Prinz
Mitglied der Prüfungskommission:	Prof. Dr. Eva Tolosa
Mitglied der Prüfungskommission:	Prof. Dr. med. Christian F. Krebs

Datum der Disputation: 11. September 2026

Table of Contents

List of Abbreviations 1

Summary 3

Zusammenfassung 5

Chapter 1: Introduction 7

1.1 T Cells 7

1.1.1 αβ T Cells 7

1.1.2 γδ T Cells 9

1.1.3 TCR 12

1.2 AML and AlloHSCT 13

1.3 Malaria 14

1.3.1 $CD4^+$ and $CD8^+$ T Cell Responses to Malaria 14

1.3.2 γδ T Cell Responses to Malaria 14

1.4 Single Cell RNA Sequencing 15

1.4.1 Library Generation 15

1.4.2 Single Cell TCR Sequencing 20

1.4.3 Analysis Workflow 23

1.5 Research Objectives 24

Chapter 2: Publication in *Journal of Leukocyte Biology*, November 2023 25

Chapter 3: Publication in *Biomarker Research*, December 2025 47

Chapter 4: Unpublished Manuscript 79

Chapter 5: Discussion 110

5.1 Clonal Tracking Unlocks Novel Insights into Immunity 110

5.2 T Cell Composition and TCR Repertoire Predict AlloHSCT Outcomes 112

5.3 The Need for a Cross-Tissue, Pan-Disease Human γδ T Cell Atlas 114

References for Introduction and Discussion 116

Curriculum Vitae and List of Publications 137

Erklärung des Eigenanteils **140**

Eidesstattliche Versicherung **141**

Danksagung **142**

List of Abbreviations

ADCC — antibody-dependent cellular cytotoxicity

ADGRG1 — adhesion G protein-coupled receptor G1

AML — acute myeloid leukemia

alloHSCT — allogeneic hematopoietic stem cell transplantation

BTN2A1 — butyrophilin subfamily 2 member A1

BTN3A1 — butyrophilin subfamily 3 member A1

CAR T cell — chimeric antigen receptor T cell

CHMI — controlled human malaria infection

CMV — cytomegalovirus

CTL — cytotoxic T lymphocyte

FACS — fluorescence-activated cell sorting

GRFS — graft-versus-host disease-free, relapse-free survival

GvHD — graft-versus-host disease

GvL — graft-versus-leukemia

HCMV — human cytomegalovirus

HMBPP — (E)-4-hydroxy-3-methyl-but-2-enyl pyrophosphate

HVG — highly variable gene

IFN-γ — interferon gamma

IL — interleukin

IPP — isopentenyl pyrophosphate

iTreg — inducible regulatory T cell

KNN — k-nearest-neighbor

LVIS — lentiviral vector integration site

MHC — major histocompatibility complex

MMLV — Moloney murine leukemia virus

NGS — next-generation sequencing

NK cell — natural killer cell

nTreg — natural regulatory T cell

NSCLC — non-small cell lung cancer

PCA — principal component analysis

pAg — phosphoantigen

PTCy — post-transplant cyclophosphamide

rATG — rabbit anti-thymocyte globulin

scRNA-seq — single-cell RNA sequencing

scTCR-seq — single-cell T cell receptor sequencing

TCR — T cell receptor

Tex — exhausted T cell

Tfh — T follicular helper cell

Th — T helper cell

TNF-α — tumor necrosis factor alpha

Tr1 — type 1 regulatory T cell

TSO — Template-switch oligo

Treg — regulatory T cell

Trm — tissue-resident memory T cell

UMAP — Uniform Manifold Approximation and Projection

UMI — unique molecular identifier

Summary

Human T cells are divided into αβ and γδ lineages based on T cell receptor (TCR) chain usage. Despite distinct developmental trajectories and antigen-recognition patterns, both can mount adaptive responses to infection and cancer through clonal expansion. However, limited integrated phenotypic-clonotypic information has hindered our understanding of how expanded T cell clones evolve and persist to sustain long-term immune surveillance. The advent of single-cell RNA sequencing (scRNA-seq) combined with single-cell TCR sequencing (scTCR-seq) enables unbiased characterization of T cell phenotypes while linking transcriptional states to clonotypes. This framework allows longitudinal tracking of phenotypic plasticity within individual expanded clonotypes, supporting precise dissection of effector and memory programs and the durability of functional T cell responses over time.

In this dissertation, we developed a robust computational strategy to dissect αβ and γδ T cells from scRNA-seq data and applied it to two longitudinal clinical cohorts, revealing persistent, disease-associated, functionally competent αβ and γδ T cell responses in acute myeloid leukemia (AML) patients undergoing allogeneic hematopoietic stem-cell transplantation (alloHSCT) and in children exposed to repeated seasonal malaria.

In the AML cohort, we used scRNA-seq to profile T cells from graft samples and two post-transplant follow-up blood samples (day 30 and day 100) from ten AML patients undergoing alloHSCT. Using TCR-based clonal tracking, we found that graft-derived $CD8^+$ αβ and γδ T cells persist after transplantation, accompanied by increased proliferation, clonal expansion, and transcriptional signatures potentially linked to alloreactivity. Transcriptome-wide screening further identified cellular biomarkers of engrafted T cells associated with beneficial graft-versus-leukemia (GvL) and detrimental acute graft-versus-host disease (aGvHD).

In the malaria cohort, we employed scRNA-seq and scTCR-seq to profile peripheral γδ T cell phenotypes and clonotypes in a 10-year longitudinal cohort of four Malian children (aged 4–5 years at enrollment) exposed to annual seasonal malaria transmission. Repeated infections drove clonal expansion of two distinct adaptive $V\delta1^+$ effector populations with either regulatory (*CX3CR1*, *PDCD1*, *IL10*) or cytotoxic (*CX3CR1*, *GNLY*, *IFNG*, *PRF1*) programs, alongside the emergence of a previously unrecognized precursor-like $V\delta1^+$ subset co-expressing self-renewal (*TCF7*) and exhaustion-associated markers (*TOX*, *PDCD1*, *TIGIT*, *HAVCR2*). TCR-based clonal tracking showed that dominant $V\delta1^+$ clonotypes in each

individual persisted over the decade with largely stable effector phenotypes, maintained by self-renewal and involving a precursor-like memory pool.

In conclusion, this dissertation presents a computational framework for longitudinal single-cell analysis of αβ and γδ T cells, uncovering durable, disease-associated T cell immunity in AML and malaria.

Zusammenfassung

Humane T-Zellen werden anhand ihrer T-Zell-Rezeptor-Ketten (TCR) in αβ- und γδ-Linien unterteilt. Trotz unterschiedlicher Entwicklungsverläufe und Antigenerkennungsmuster können beide durch klonale Expansion adaptive Reaktionen auf Infektionen und Krebs auslösen. Bisher hat die begrenzte Verfügbarkeit an integrierten phänotypisch-klonotypischen Informationen unser Verständnis davon eingeschränkt, wie expandierte T-Zell-Klone sich entwickeln und persistieren, um eine langfristige Immunüberwachung aufrechtzuerhalten. Die Kombination aus Einzelzell-RNA-Sequenzierung (scRNA-seq) und Einzelzell-TCR-Sequenzierung (scTCR-seq) ermöglicht eine unvoreingenommene Charakterisierung von T-Zell-Phänotypen und verknüpft dabei Transkriptionszustände mit Klonotypen. Dieser Ansatz erlaubt die longitudinale Verfolgung der phänotypischen Plastizität innerhalb einzelner expandierter Klonotypen und unterstützt so die präzise Analyse von Effektor- und Gedächtnisprogrammen sowie die Nachhaltigkeit funktioneller T-Zell-Reaktionen im Zeitverlauf.

In dieser Dissertation entwickelten wir eine robuste computergestützte Strategie zur Charakterisierung von αβ- und γδ-T-Zellen aus scRNA-seq-Daten und wendeten sie auf zwei longitudinale klinische Kohorten an. Dadurch konnten wir persistierende, krankheitsassoziierte und funktionell kompetente αβ- und γδ-T-Zell-Antworten bei Patientinnen und Patienten mit akuter myeloischer Leukämie (AML) nach allogener hämatopoetischer Stammzelltransplantation (alloHSCT) sowie bei Kindern mit wiederholter saisonaler Malariaexposition nachweisen.

In der AML-Kohorte nutzten wir scRNA-seq, um T-Zellen aus Graft-Proben sowie aus zwei Blutproben nach Transplantation (Tag 30 und Tag 100) von zehn AML-Patientinnen und -Patienten nach alloHSCT zu profilieren. Mithilfe von TCR-basiertem klonalem Tracking stellten wir fest, dass aus dem Transplantat stammende $CD8^+$-αβ- und γδ-T-Zellen nach der Transplantation fortbestehen, begleitet von erhöhter Proliferation, klonaler Expansion und Transkriptionssignaturen, die potenziell mit Alloreaktivität in Verbindung stehen. Ein transkriptomweites Screening identifizierte darüber hinaus zelluläre Biomarker von Spender-T-Zellen, die mit vorteilhafter Graft-versus-Leukämie (GvL) und schädlicher akuter Graft-versus-Host-Reaktion (aGvHD) assoziiert sind.

In der Malaria-Kohorte verwendeten wir scRNA-seq und scTCR-seq zur Analyse peripherer γδ-T-Zell-Phänotypen und -Klonotypen in einer zehnjährigen longitudinalen Kohorte von vier

malischen Kindern (im Alter von 4–5 Jahren bei Studieneinschluss), die einer jährlichen saisonalen Malariaübertragung ausgesetzt waren. Wiederholte Infektionen führten zur klonalen Expansion zweier unterschiedlicher adaptiver Vδ1$^+$-Effektorpopulationen mit entweder regulatorischem (CX3CR1, PDCD1, IL10) oder zytotoxischem (CX3CR1, GNLY, IFNG, PRF1) Programm sowie zum Auftreten einer zuvor nicht beschriebenen vorläuferähnlichen Vδ1$^+$-Subpopulation, die sowohl mit Selbsterneuerung assoziierte Marker (TCF7) als auch Erschöpfungsmarker (TOX, PDCD1, TIGIT, HAVCR2) exprimierten. Die TCR-basierte klonale Verfolgung zeigte, dass dominante Vδ1$^+$-Klonotypen in jedem Individuum über ein Jahrzehnt hinweg persistierten und dabei weitgehend stabile Effektorphänotypen beibehielten, die durch Selbsterneuerung und unter Beteiligung eines vorläuferähnlichen Gedächtnispools aufrechterhalten wurden.

Zusammenfassend präsentiert diese Dissertation einen bioinformatischen Worflow für die longitudinale Einzelzellanalyse von αβ- und γδ-T-Zellen und nutzt diesen, um eine dauerhafte, krankheitsassoziierte T-Zell-Immunität bei AML und Malaria zu identifizieren. Diese Ergebnisse vertiefen unser Verständnis persistenter T-Zell-Reaktionen und lassen sich direkt auf die Erforschung neuartiger therapeutischer Ansätze für Krebserkrankungen und Infektionskrankheiten anwenden.

Chapter 1: Introduction

1.1 T Cells

Human T lymphocytes (T cells) play a central role in cellular immunity, coordinating protective responses, maintaining tissue homeostasis, enforcing self-tolerance, and establishing long-term immunological memory[1,2]. These functions are principally mediated by T cell receptors (TCRs), which recognize antigens derived from pathogens, tumors, or environmental sources[3-9]. However, when regulation fails, T cells can contribute to autoimmunity and chronic inflammation by responding to self-antigens and driving harmful immune activation[10,11].

T cells are broadly divided into two main lineages—αβ and γδ T cells—based on the TCR chain usage[3]. Although both lineages can expand clonally and mount adaptive responses, they differ in their developmental trajectories and antigens-recognition patterns[3,5,12-15]. The following sections provide an overview of these two T cell types and the unique features of their antigen recognition and immune functions.

1.1.1 αβ T Cells

αβ T cells constitute the predominant T cell population in humans, comprising over 90% of circulating T cells[1]. They express a TCR composed of an alpha (α) and beta (β) chain[3]. During thymic development, $CD4^+CD8^+$ double-positive progenitors undergo positive and negative selection to ensure self-tolerance and the ability to recognize foreign peptides presented by major histocompatibility complex (MHC) molecules[16]. Following thymic selection, most mature αβ T cells differentiate into either $CD4^+$ helper T cells or $CD8^+$ cytotoxic T cells. αβ T cells are MHC-restricted, with $CD8^+$ T cells recognizing antigens presented by MHC class I and $CD4^+$ T cells responding to MHC class II[4]. In addition to these conventional subsets, a specialized population of $CD4^+$ αβ T cells differentiates into regulatory T cells (Tregs), characterized by expression of the transcription factor Foxp3[11]. Tregs are essential for maintaining immune tolerance by suppressing aberrant or excessive immune responses to self-antigens, thereby preventing autoimmunity[10].

1.1.1.1 $CD4^+$ T Cells

$CD4^+$ T cells play a central role in orchestrating adaptive immune responses by producing cytokines, providing help to other immune cells, and maintaining immune homeostasis[1,17,18]. Upon activation through their TCR in the presence of polarizing cytokines, naïve $CD4^+$ T cells differentiate into distinct effector lineages, each defined by unique transcriptional programs, cytokine profiles, and immunological functions[17,18]. Th1 cells, driven by IL-12 and the

transcription factor T-bet[19], characterized by secreting interferon-gamma (IFN-γ), lymphotoxin, IL-2, and TNF-α[20]. They activate macrophages and support $CD8^+$ T cell responses, making them essential for immunity against intracellular pathogens such as viruses and certain bacteria[17]. Th2 cells, induced by IL-4 and regulated by GATA3[21], produce IL-4, IL-5, IL-13, and IL-9[22]. They promote class switching in B cells (especially to IgE), activate eosinophils, and are critical for mediating allergic responses[17,22]. Th17 cells, differentiated under the influence of IL-6, IL-1β, and TGF-β with the transcription factor RORγt[23], secrete IL-17A, IL-17F, and IL-22[23,24]. They recruit and activate neutrophils and are important for mucosal immunity and defense against extracellular bacteria and fungi, especially at barrier surfaces[23]. T follicular helper (Tfh) cells, guided by IL-6 and IL-21 and expressing the transcription factor Bcl6[25], localize to germinal centers and provide help to B cells through IL-21 and CD40L signaling[26]. They are crucial for germinal center formation, antibody affinity maturation, and isotype switching[26].

Inducible regulatory T cells (iTregs), generated in the periphery in response to TGF-β and IL-2, express the transcription factor Foxp3 and function to suppress immune responses and maintain peripheral tolerance, particularly at mucosal sites[27,28]. Natural regulatory T cells (nTregs) develop in the thymus and are selected for intermediate affinity to self-antigens. They constitutively express Foxp3, CD25, and CTLA-4, and are stably committed to a suppressive lineage[10,11,27]. nTregs play a key role in central tolerance by controlling autoreactive T cells that escape thymic deletion. Unlike iTregs, they maintain stable Foxp3 expression and function even in inflammatory environments[10,27].

Type 1 regulatory T cells (Tr1) are peripherally induced in response to persistent antigen exposure, particularly under inflammatory conditions enriched in IL-10 and antigen-presenting cell-derived signals such as IL-27[29,30]. Unlike $Foxp3^+$ Tregs, Tr1 cells do not originate in the thymus and lack stable Foxp3 expression. Instead, they differentiate from conventional $CD4^+$ T cells in peripheral tissues, especially during chronic immune activation. Tr1 cells are defined by their high production of IL-10 and co-expression of inhibitory molecules such as LAG-3 and CD49b, which mediate contact-dependent and cytokine-driven suppression of effector T cell responses[29,31]. Through these mechanisms, Tr1 cells contribute to the resolution of inflammation and promote long-term immune homeostasis[32].

1.1.1.2 CD8$^+$ T Cells

CD8$^+$ T cells (cytotoxic T lymphocytes, CTLs) are specialized in detecting and eliminating infected or transformed cells[33,34]. After thymic selection, naïve CD8$^+$ T cells patrol secondary lymphoid tissues and peripheral compartments, where they detect peptide antigens presented on major histocompatibility complex class I (MHC I) molecules. CTLs activation typically requires coordinated signals delivered by professional antigen-presenting cells—TCR engagement with peptide–MHC I, costimulation, and inflammatory cytokines—together instructing clonal expansion and differentiation into effector states[34]. Activated effector CD8$^+$ T cells kill target cells through perforin- and granzyme-mediated cytolysis and through death receptor pathways such as Fas–FasL, while also producing cytokines including IFN-γ and TNF-α that amplify antimicrobial and antitumor immunity[1,33-35]. Following antigen clearance, most effector cells undergo a contraction phase, whereas a fraction persists as long-lived memory CD8$^+$ T cells capable of rapid recall responses[1,2,33,36,37]. This differentiation continuum encompasses circulating and tissue-resident programs and is governed by transcriptional and epigenetic mechanisms that balance immediate cytotoxicity against longevity, self-renewal, and proliferative potential[38,39].

In chronic viral infection and cancer, persistent antigen exposure and chronic TCR stimulation can drive CD8$^+$ T cells into dysfunctional states termed exhaustion, characterized by distinct constrained proliferative capacity, reduced effector function, increased surface checkpoint receptor expression and transcriptional factor TOX[35,40-45]. Such dysfunctional states are epigenetically imprinted that limits full reinvigoration of CTL functions in the presence of immune checkpoint blockade[44,46]. A key conceptual advance in the last decade is the recognition of TCF1$^+$ 'stem-like' or 'memory-precursor' CD8$^+$ T cell populations (Tpex) that maintain long-term responses under chronic antigen stimulations[47-54]. These cells typically retain self-renewal capacity, proliferate robustly, and generate downstream effector-like progeny, thereby acting as the renewable source that sustains CTLs pool[47]. In cancer and chronic infectious disease, these precursor-like subsets are strongly linked to clinical benefit from immune checkpoint blockade[35,47,52,55,56].

1.1.2 γδ T Cells

Human γδ T cells are defined by γδ TCR chain usage and comprise two major compartments: Vγ9Vδ2 (Vδ2$^+$) cells, which dominate the peripheral blood at steady states, and non-Vγ9Vδ2 γδ T cells (commonly Vδ1$^+$ and Vδ3$^+$), which are enriched in organs and mucosal tissues[3,6,7,15,57]. A hallmark of human γδ T cells is their non-classical antigen-recognition

patterns: γδ TCRs can recognize targets in a peptide–MHC independent way, which enables them for rapid, stress-focused immune surveillance[3,12-14].

1.1.2.1 Vγ9Vδ2 γδ T Cells

Human Vγ9Vδ2 T cells are defined by expression of a semi-invariant Vγ9Vδ2 TCR, characterized by "public" germline CDR3γ sequences exclusively using Vγ9JP segment paired with a "private/shared" CDR3δ repertoire, and are developmentally pre-programmed in utero, undergo polyclonal expansion after birth, and can persist stably into adulthood[15,58-61]. Vγ9Vδ2 T cells sense phosphoantigens (pAgs)—including the microbial metabolite (E)-4-Hydroxy-3-methyl-but-2-enyl pyrophosphate HMBPP and the host-derived metabolite isopentenyl pyrophosphate IPP of infected or transformed cells[62,63]. These pAgs function as "molecular glues" that promote heteromeric association between the intracellular domains of butyrophilin BTN3A1 and the structurally related BTN2A1 to form a heterodimer, enabling Vγ9Vδ2 TCR engagement and inducing innate-like, peptide–MHC-independent activation of Vγ9Vδ2 T cells[64-68].

In infections, Vγ9Vδ2 T cells exert direct antimicrobial activity through perforin/granzyme-dependent cytotoxicity against diverse pathogens, such as *Mycobacterium tuberculosis*[69]. They can also kill target cells via death-receptor pathways such as Fas/FasL and TRAIL, with effector potency further tuned by innate-like activating receptors (e.g., NKG2D)[70]. Beyond direct cytotoxicity, they can also eliminate target cells, such as *Plasmodium falciparum*–infected red blood cells, through antibody-dependent cellular cytotoxicity (ADCC)[71].

In cancer, Vγ9Vδ2 T cells provide a complementary antitumor mechanism to αβ T cells because their recognition is not constrained by peptide–MHC, enabling responses against tumors with low neoantigen burden or MHC-I downregulation[8]. They detect transformation-associated metabolic dysregulation—particularly the accumulation of isopentenyl pyrophosphate (IPP)—through the BTN3A1/BTN2A1 axis, mediate potent cytotoxicity, and integrate stress surveillance signals through NKG2D[8,62,65,67,68,72]. These intrinsic features have provided the rationale for several translational cancer immunotherapy strategies, including ex vivo expansion and adoptive transfer, in vivo activation with aminobisphosphonates or BTN3A agonists, and engineered redirection approaches such as T cell engagers and CAR-based platforms[8,73-77].

1.1.2.2 Non-Vγ9Vδ2 γδ T Cells

Non-Vγ9Vδ2 γδ T cells predominantly use Vδ1 or Vδ3 chains paired with diverse TCRγ chains and are enriched in tissues such as the gut epithelium, skin, spleen, and liver, where they contribute to tissue homeostasis and immune surveillance against infection and cell transformation[6,57,78-81]. This compartment is dominated by Vδ1 and Vδ3 cells, with smaller contributions from Vγ9-negative Vδ2 populations[82]. Compared with innate-like pAg-reactive Vγ9Vδ2 T cells, non-Vγ9Vδ2 subsets display greater TCR diversity. Their more private TCR repertoires are shaped by postnatal antigen exposure, showing individualized clonal expansions later in life[15,83-85]. These responses are thought to arise through clonal selection from a naïve-like pool characterized by high expression of CD27, CD28, CCR7, IL7R, and CD62L, followed by focused expansion, effector differentiation, and long-term persistence[83,84]. Such adaptive-like responses have been observed in the context of CMV, *Mycobacterium tuberculosis*, and *Plasmodium falciparum* infections[83,84,86-94]. The ligands of non-Vγ9Vδ2 γδ T cells remain largely unknown. Current evidence suggests that these cells recognize a broad spectrum of predominantly host-derived ligands, including classical or MHC-like molecules[92,95,96], lipid antigens presented by CD1 family members[97-99], and stress-associated self-proteins such as Annexin A2[100]. Reported ligand specificities are mostly clonotype-restricted, thereby hindering the establishment of general principles underlying antigen recognition by non-Vγ9Vδ2 γδ T cells[13,14]. Non-Vγ9Vδ2 γδ T cells can eliminate infected or transformed cells through perforin- and granzyme-mediated cytotoxicity and can also mediate antibody-dependent cellular cytotoxicity (ADCC). Beyond direct target-cell killing, these cells can also produce inflammatory cytokines and shape broader immune responses within tissues[6,57,81].

Accumulating evidences show that increased abundance of tumor-infiltrating non-Vγ9Vδ2 γδ T cells is associated with favorable outcomes in human cancer such as NSCLC[101], CRC[102-105], and kidney cancer[106]. Similarly, the long-term clinical remission of leukemia patients post-HSCT positively correlated with robust and durable γδ T cell reconstitution[107-110]. A prospective clinical trial demonstrated that haploidentical HSCT following ex vivo αβ T- and B-cell depletion is a clinically effective and well-tolerated strategy for children with acute leukemia, with improved GRFS[109,111]. This is partially due to the MHC-independent recognition the cancer cells through γδ TCR and NK receptors[109,112]. More importantly, the intratumoral non-Vγ9Vδ2 γδ T cells exhibit retained effector functions even though with elevated inhibitory receptor expression on the cell surface and blockade of inhibitory receptors on non-Vγ9Vδ2 γδ T cells has been showed to enhance the killing of tumor cells in

vitro[103,105,106]. These intrinsic tumor-reactive properties of non-Vγ9Vδ2 γδ T cells position them as outstanding candidates for cancer immunotherapy and several preclinical studies have shown promising results[8,113,114].

1.1.3 TCR

The T cell receptor (TCR) mediates the antigen recognition and T cell responses through the TCR-CD3 complex. TCR is composed of two chains, TCRα and TCRβ for αβ T cells, and TCRγ and TCRδ for γδ T cells[3]. TCR repertoires are generated through combinatorial somatic rearrangement of multiple variable (V), diversity (D) (for the β-chain and δ-chain only), joining (J) and constant (C) gene segments along with Palindromic (P) nucleotides addition and non-templated (N) nucleotides addition or deletion between spliced gene segments[3,115-117]. The complementary determining region 3 (CDR3) is the most informative part and defines the specificity of a TCR. The vast diversity of TCR repertoires underlies the specificity of adaptive immunity, as each T cell typically expresses a unique TCR that is selected to recognize a defined peptide–MHC complex to initiate immune responses regarding protecting the host through eliminating of infected cells or transformed cells[3], with an exception of the regulatory T cells which specialize in peripheral tolerance in contrast to canonical effector responses[10]. The TCR repertoire collectively enables recognition of a broad range of foreign and self-derived antigens[3,4,116].

In addition to the biological functions of TCR complex, the sequences of TCR can serve as molecular identifiers of individual T cell clones, as the probability of generating the same V(D)J rearrangement more than once is exceedingly low due to the immense diversity of TCR pairs (up to 10^15 for αβ pairs[115] and 10^18 for γδ pairs[117]). TCR repertoire profiling therefore provides a powerful framework to quantify antigen-driven clonal expansion, track longitudinal clonal persistence and dynamics, and resolve the heterogeneity of T cell responses[83,84,118-121]. This is closely linked to the well-defined continuum of T cell activation from naïve to effector states, during which antigen-specific clones undergo extensive proliferation to mount effective immune responses. Integrating TCR information with single-cell transcriptional phenotypes further enables reconstruction of the differentiation trajectories of individual T cell clones, providing a precise framework to resolve their activation states, functional plasticity, and disease relevance[85,116,118-121].

1.2 AML and AlloHSCT

Acute myeloid leukemia (AML) is a heterogeneous hematologic malignancy defined by the clonal accumulation of immature myeloid cells in the bone marrow and peripheral blood[122,123]. Although intensive chemotherapy has long served as the standard therapeutic solution, the outcomes remain to be improved, particularly in older patients accounting for a large proportion of AML cases[122-124]. Advances in the understanding of AML molecular pathobiology have recently accelerated the development of targeted therapies, including agents directed against mutated *BCL2*, *FLT3*, and *IDH1/2* genes, shifting the field toward more biologically informed and subtype-specific treatment strategies[122,123]. However, many patients eventually relapse in the absence of effective consolidation therapy[124,125]. Thus, allogeneic hematopoietic stem cell transplantation (alloHSCT) remains a cornerstone of AML therapy because of its potent anti-leukemic activity mediated by the graft-versus-leukemia (GvL) effect[126-130].

T cells are the major players of GvL effects with clinical trials showing that depletion of T cells from the graft significantly increased the probability of relapse post-alloHSCT[126]. The mechanisms of GvL are the recognition of antigens presented by the MHC complex on the leukemia cells by donor-derived T cells[131]. However, because minor histocompatibility antigens are also expressed on healthy cells, donor-derived graft T cells may also mediate the detrimental graft-versus-host disease (GvHD), which primarily affects the skin, gastrointestinal tract, and liver, even in MHC-matched transplants[132-134].

Clinical GvHD prophylaxis strategies, including rabbit anti-thymocyte globulin (rATG) and post-transplant cyclophosphamide (PTCy), have substantially reduced the risk of GvHD. However, these approaches may also compromise graft-versus-leukemia (GvL) activity because current prophylactic regimens suppress T cell responses in a broadly non-specific manner[135]. To overcome this, graft engineering and especially T cell composition manipulation should be employed to augment GvL while minimize GvHD[135,136]. Recent studies have shown that negative depletion of αβ T and B cells from graft has significantly improved 5-year probability of chronic GvHD-free, relapse-free survival (GRFS) in pediatric acute leukemia[111,137]. This is consistent with intrinsic features revealed by in vitro studies demonstrating the potent anti-leukemic activity of both Vγ9Vδ2 and non-Vγ9Vδ2 γδ T cells[109,112]. Further improvement of alloHSCT is limited by the lack of clearly defined T cell populations associated with GvL versus GvHD.

1.3 Malaria

Malaria is caused by infection with Plasmodium parasites, with *Plasmodium falciparum* responsible for the most severe and often fatal forms of the disease[138]. Following transmission by *Anopheles* mosquitoes, Plasmodium parasites first establish an asymptomatic liver stage, during which they replicate and differentiate into merozoites. Merozoites then target host erythrocytes to establish blood stage infection that causes the clinical symptoms of malaria[139].

1.3.1 $CD4^+$ and $CD8^+$ T Cell Responses to Malaria

Malaria elicits complex and stage-specific T cell immune responses that contribute both to host protection and to immune regulation[138]. During the liver stage, $CD8^+$ T cells are particularly important for recognizing and eliminating infected hepatocytes and may establish tissue-resident memory populations that support rapid recall responses upon reinfection[140-146]. Due to the lack of MHC class I on erythrocytes, $CD8^+$ T cells are thought to contribute little to limit the blood stage of malaria infection, although malaria parasite-specific $CD8^+$ T cells have been described in the blood of humans living in endemic areas and after vaccination[147]. In parallel, $CD4^+$ T cells play broader helper and regulatory roles by coordinating inflammatory responses, activating myeloid cells, and providing essential support for humoral immunity[148-150]. Notably, regulatory Th1 (Tr1) cells, characterized by high levels of BLIMP1, T- bet, IFNγ and IL-10 function as adaptive IL-10-producing regulatory $CD4^+$ T cells that limit TNF- and Th1-driven immunopathology during blood-stage infection, but this protective anti-inflammatory role may also restrain efficient parasite clearance and humoral immunity[94,118,151-156]. Tr1-mediated immune regulation may contribute to the establishment of naturally acquired clinical immunity to malaria, which is a non-sterilizing, exposure-dependent form of protection that develops progressively in individuals residing in endemic areas through repeated Plasmodium exposure and primarily limits symptomatic disease and severe outcomes without fully preventing reinfection[138,156,157].

1.3.2 γδ T Cell Responses to Malaria

γδ T cells contribute to both anti-parasite immunity and anti-disease tolerance during malaria. $V\delta2^+$ γδ T cells can directly kill *P. falciparum*–infected erythrocytes through both TCR-dependent cytotoxicity and antibody-dependent cellular cytotoxicity (ADCC)[158-160]. However, these Vδ2-mediated anti-parasites responses may be accompanied by excessive inflammation, as repeated exposure with progressive loss and dysfunction of $V\delta2^+$ cells correlate with the development of asymptomatic infection in endemic settings[161]. In controlled human malaria infection (CHMI), repeated *P. falciparum* infection consistently drives clonal expansion of an

adaptive γδ repertoire, highlighting the potential roles of Vδ1$^+$ T cells in acquiring long-term immunity to malaria[162]. This is further supported by the evidence that *P. falciparum*-challenged γδ T cells are able to mount recall responses that were largely maintained ~14 months after a single *P. falciparum* episode[163]. Also, in clinically immune individuals, expanded circulating Vδ1$^+$ T cells produce IL-10 alongside IFN-γ in response to *P. falciparum* antigens, mirroring the type 1 regulatory (Tr1)–like cytokine profile[164].

1.4 Single Cell RNA Sequencing

Single-cell RNA sequencing (scRNA-seq) has greatly improved our ability to dissect cellular and molecular complexity by enabling transcriptome profiling at single-cell resolution and large scale. Recent advances in experimental platforms and computational methods are further expanding the scope of single-cell analysis through multimodal approaches that integrate transcriptomic information with immune repertoires[116,165,166], cell surface protein expression[167], chromatin accessibility[168], and epigenetic states[169], thereby providing a more comprehensive view of cellular heterogeneity and dynamic biological processes.

1.4.1 Library Generation

The most critical step of scRNA-seq is cellular barcoding which enables the qualification of thousands of gene expression levels for individual cells[170]. Currently, there are two mainstream strategies to perform cell barcoding, namely droplet-based with a microfluidic device[171] and plate-based[172]. The former method employs a microfluidic device to encapsulate single cell with single oligonucleotides-barcoded gel bead and reagents for reverse transcription into one oil droplet[171]. After cell lysis within the droplet, released transcripts are captured by the oligonucleotide barcodes and reverse-transcribed into cDNA (**Fig. 1**). The later platform uses a plate with microwells to isolate single cell and introduces cell-barcodes (**Fig. 2**)[172]. The limitations of both platforms are the low throughput regarding sample and cell number[173-175].

The development of combinatorial barcoding unmeshed the throughput of single-cell experiments[176-186]. In single-cell combinatorial barcoding methods, the cell membrane functions as a physical barrier and intracellular reaction compartment, allowing cellular contents to remain associated during fixation, permeabilization, and barcoding without requiring cell isolation (**Fig. 3**). This enables in-cell enzymatic reactions such as reverse transcription and sequential barcode ligation, while multiple rounds of barcoding generate a unique combinatorial barcode for each cell. In addition, these approaches facilitate large-scale

sample multiplexing through pre-labeling cells from different samples for parallel profiling. The downstream process post-barcoding is the same including cDNA amplification, fragmentation, introducing sequencing adaptors compatible with the next-generation sequencing (NGS) platforms.

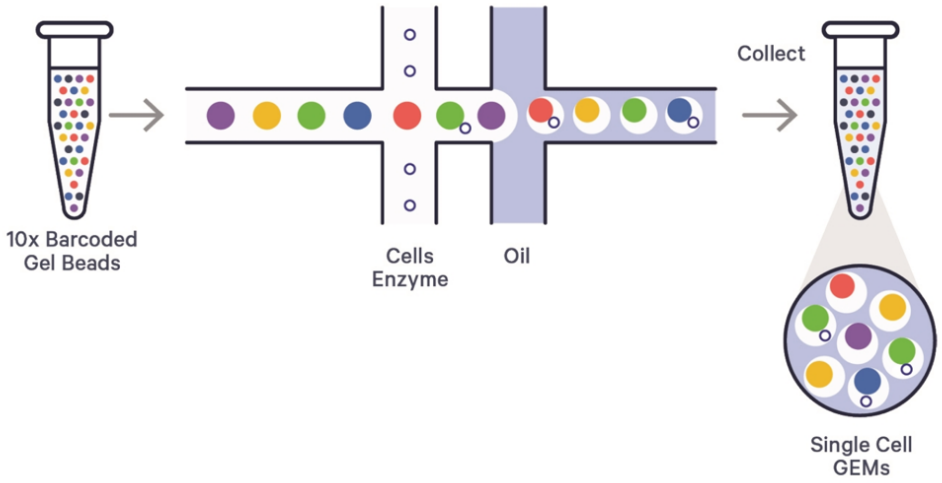


Fig. 1 Workflow of droplet-based single-cell platform (adapted from 10x Genomics)

Single cells and uniquely barcoded gel beads are partitioned together into oil droplets, known as Gel Beads-in-Emulsion (GEMs), in the presence of enzymes and reverse transcription reagents. Each GEM serves as an individual reaction chamber in which the gel bead dissolves and cellular target molecules are captured and barcoded to identify their cell of origin.

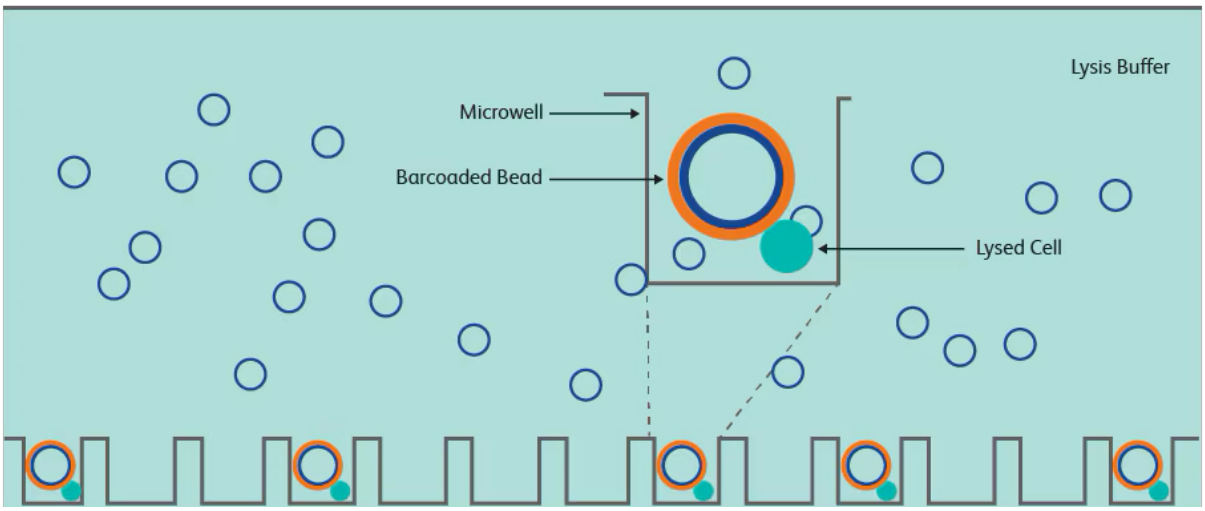


Fig. 2 Workflow of plate-based single-cell platform (adapted from BD Biosciences)

Single cells are loaded into a microwell cartridge and paired with barcoded beads after optional sample staining. Following imaging-based quality control, cells are lysed, transcripts are captured on the beads, and the beads are recovered for reverse transcription, cDNA synthesis, library preparation, sequencing, and downstream analysis.

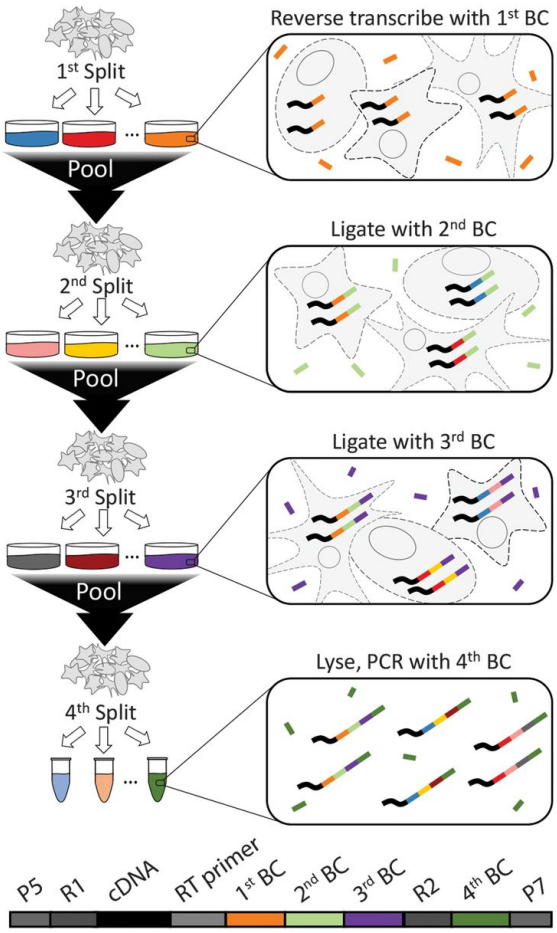


Fig. 3 Workflow of combinatorial barcoding single-cell platform (adapted from Rosenberg, *Science*, 2018)

Combinatorial barcoding labels single-cell transcriptomes through repeated random distribution of fixed cells or nuclei into wells, where transcripts receive well-specific barcodes in each round. The first barcode is introduced by barcoded reverse transcription primers, the second and third by ligation to cDNA, and the fourth during PCR in library preparation. The bottom schematic depicts the final fully barcoded cDNA molecule.

1.4.2 Single Cell TCR Sequencing

Because the informative CDR3 region of TCR transcripts is located at the 5′ end of the mRNA[3], conventional single-cell barcoding strategies that rely on poly(A)-tail capture are generally not efficient for TCR recovery, particularly given the limited read length of current next-generation sequencing (NGS) platforms. To overcome this limitation, template switching is employed to introduce barcodes at the 5′ end during reverse transcription by employing the intrinsic properties of Moloney murine leukemia virus (MMLV) reverse transcriptase (**Fig. 4**)[116,166]. Nested PCR was used to enrich the barcoded TCR transcripts. For the combinatorial barcoding, multiplexing PCR using a set of primers targeting the variable TCR gene segments was employed to enrich TCR transcripts (**Fig. 5**). The combination of scTCR-seq and scRNA-seq enables T cells profiling at phenotypic-clonotypic resolution[116].

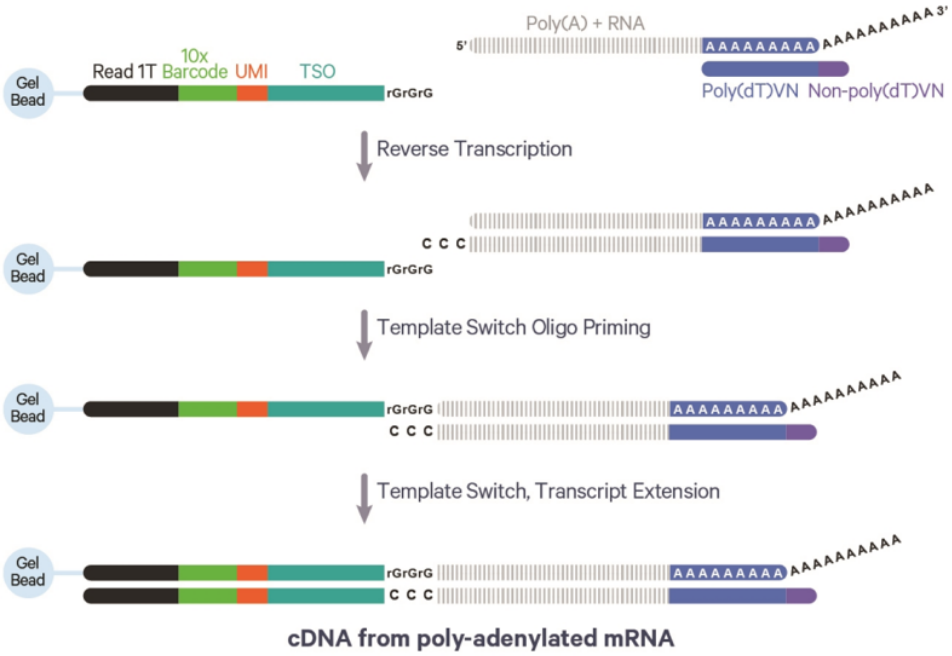


Fig. 4 Schematic of template switching during reverse transcription (adapted from 10x Genomics)

At the end of reverse transcription, the MMLV reverse transcriptase adds non-templated cytosines to the cDNA, which allows the template-switch oligo (TSO) to anneal. The enzyme then switches templates and extends the cDNA using the TSO, thereby introducing a known sequence at the 5′ end for subsequent amplification.

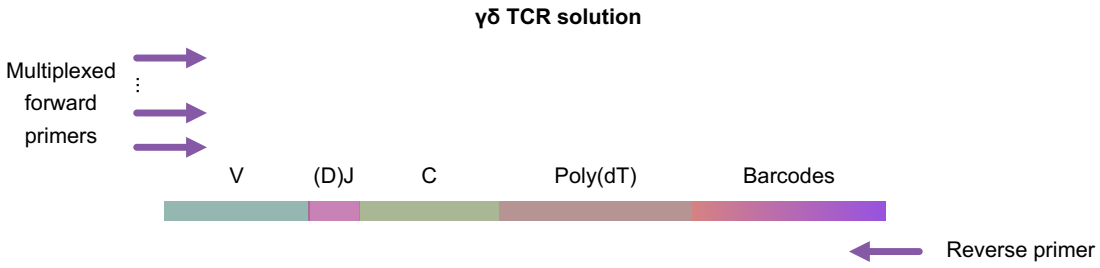


Fig. 5 Schematic of multiplexed PCR to enrich γδ TCR transcripts

Following cDNA synthesis, multiplex PCR is performed using primer sets targeting TCR γ and δ variable region to selectively enrich TCR-derived transcripts.

1.4.3 Analysis Workflow

The analysis workflow of single-cell data has been well-established with toolkit such as Scanpy[187] and Seurat[188]. A typical scRNA-seq analysis workflow starts with preprocessing and quality control of the raw count matrix[189]. This usually includes removal of low-quality cells based on metrics such as low gene counts, low UMI counts, or high mitochondrial transcript fractions, followed by correction for technical artifacts such as ambient RNA contamination (SoupX[190], CellBender[191], and DecontX[192]) and doublets (DoubletFinder[193], and Scrublet[194]). After QC, the expression matrix is normalized and transformed, for example by library-size normalization followed by log-transformation. The next stage is feature selection and dimensionality reduction[187,188,195]. Analysts typically identify highly variable genes (HVGs)[196] to focus on informative biological variation, then perform principal component analysis (PCA) on the normalized expression matrix. In practice, PCA provides a low-dimensional representation that is then used to construct a k-nearest-neighbor (KNN) graph[195], which is a central structure for downstream clustering and visualization. If multiple donors, batches, chemistries, or studies are combined, data integration or batch correction is often performed before graph construction or clustering. Harmony[197], reciprocal PCA (RPCA)[188], and Scanorama[198] are among widely used integration methods, and benchmark studies have evaluated their performance at atlas scale[199].

After the graph is built, cells are grouped by graph-based clustering, most commonly with the Leiden algorithm, which is an improved community-detection method derived from Louvain and is widely adopted for scRNA-seq because it operates directly on the neighborhood graph and tends to produce well-connected clusters[200]. For visualization, the high-dimensional structure is usually embedded in two dimensions with UMAP, which aims to preserve local neighborhood relationships from the graph and is now standard for displaying cellular structure and cluster relationships[201].

The resulting clusters are then assigned biological identities through cell-type annotation, either manually using canonical marker genes or with automated reference-based methods[202,203]. Once annotation is established, the main downstream analyses include differential gene expression, differential abundance, trajectory or pseudotime inference, RNA velocity, and cell–cell communication analysis, depending on the biological questions. For multimodal datasets, these steps may also be extended to integrate surface protein, chromatin accessibility, or adaptive immune receptor information[187,188].

1.5 Research Objectives

The advancement of scRNA-seq technologies has boosted the pace of biological discovery while generating an unprecedented scale of single-cell datasets. Due to the intrinsic phenotype similarities between human adaptive γδ T cells and $CD8^+$ αβ T cells[204], a robust strategy to identify γδ T cells from single-cell dataset generated based on pan-T cells without TCR information remained to be developed. To address this, we generated a ground-truth single-cell dataset including both αβ and γδ TCR information and revealed that the combination of TRD and TRA/B gene modules from transcriptome robustly distinguishes γδ T cells and αβ T cells as presented in **chapter 2**.

Graft T cells mediate the beneficial GvL and detrimental GvHD effects of alloHSCT treatment. However, the direct evidence of graft T cell persistence post-alloHSCT is still missing. To address this, we employed mega-scale scRNA-seq on 25 graft and post-alloHSCT PBMC samples obtained from a longitudinal cohort of ten AML patients. TCR clonal tracking revealed the persistence of graft γδ T cells and $CD8^+$ αβ T cells while displaying alloreactivity. Transcriptome-wide screening identified novel cellular biomarkers of T cells associated with GvL and GvHD as presented in **chapter 3**.

Human adaptive γδ T cells participate in immune responses to infections and cancer, showing durable clonal expansion and sustained functional competence. However, the lack of longitudinal studies with integrated clonal-phenotypic resolution limits our understanding of their functional plasticity, and longevity mechanisms. We used scRNA-seq and sc-γδTCR-seq to profile peripheral γδ T cell phenotypes and clonotypes in a 10–year longitudinal cohort of four Malian children (aged 4–5 years at enrollment) exposed to yearly seasonal malaria transmission. Clonal tracking revealed decade-long persistence of expanded clonotypes with distinct regulatory or cytotoxic phenotypes maintained by self-proliferation and involving a stem-like memory pool as presented in **chapter 4**.

Overall, our goal was to develop novel single-cell sequencing methods and a computational framework for longitudinal single-cell analysis of αβ and γδ T cells to uncover the dynamics of disease-associated long-term T cell immunity.

Chapter 2: Publication in *Journal of Leukocyte Biology*, November 2023

Human γδ T cell identification from single-cell RNA sequencing datasets by modular TCR expression

Specific contributions:

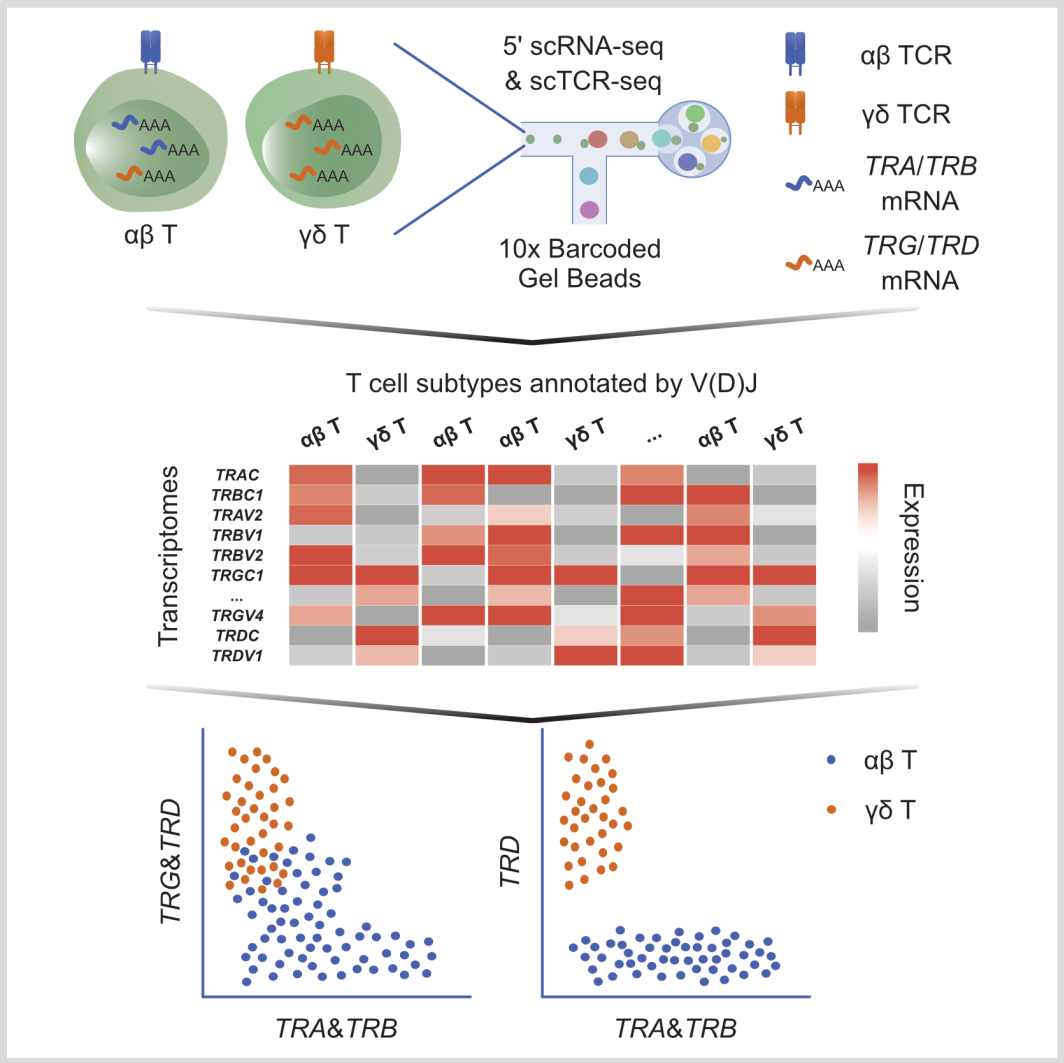
The following research article has been published in *Journal of Leukocyte Biology*. I am the first author of the publication. I conducted the computational analyses, generated the figures, drafted the manuscript, and contributed to the conceptual development of the study.

I, Immo Prinz, agree with the above statements as the direct supervisor.

Signature 

Date & Place 30.03.2026, Hamburg

Graphic Abstract



OXFORD JLB JOURNAL OF LEUKOCYTE BIOLOGY

Journal of Leukocyte Biology, 2023, **114**, 630–638

https://doi.org/10.1093/jleuko/qiad069
Advance access publication 12 July 2023
Article

Human γδ T cell identification from single-cell RNA sequencing datasets by modular TCR expression

Zheng Song,[1] Lara Henze,[2] Christian Casar,[2,3] Dorothee Schwinge,[2] Christoph Schramm,[2,4,5] Johannes Fuss,[6] Likai Tan,[1,7,*] and Immo Prinz[1,4,*]

[1]Institute of Systems Immunology, University Medical Center Hamburg-Eppendorf, Falkenried 94, 20251 Hamburg, Germany
[2]I. Department of Medicine, University Medical Center Hamburg-Eppendorf, Martinistrasse 52, 20246 Hamburg, Germany
[3]Bioinformatics Core, University Medical Center Hamburg-Eppendorf, Martinistrasse 52, 20246 Hamburg, Germany
[4]Hamburg Center for Translational Immunology, University Medical Center Hamburg-Eppendorf, Martinistrasse 52, 20246 Hamburg, Germany
[5]Martin Zeitz Center for Rare Diseases, University Medical Center Hamburg-Eppendorf, Martinistrasse 52, 20246 Hamburg, Germany
[6]Center for Translational Neuro- and Behavioral Sciences, Institute of Forensic Psychiatry and Sex Research, University of Duisburg-Essen, Alfredstrasse 68-72, 45130 Essen, Germany
[7]Department of Anaesthesia and Intensive Care (AIC), Prince of Wales Hospital, Shatin, The Chinese University of Hong Kong, New Territories, 4/F Main Clinical Block and Trauma Centre, Hong Kong, China
*Corresponding authors: Falkenried 94, 20251 Hamburg, Germany. Email: likaitan@cuhk.edu.hk; Falkenried 94, 20251 Hamburg, Germany. Email: i.prinz@uke.de

Abstract

Accurately identifying γδ T cells in large single-cell RNA sequencing (scRNA-seq) datasets without additional single-cell γδ T cell receptor sequencing (sc-γδTCR-seq) or CITE-seq (cellular indexing of transcriptomes and epitopes sequencing) data remains challenging. In this study, we developed a TCR module scoring strategy for human γδ T cell identification (i.e. based on modular gene expression of constant and variable *TRA/TRB* and *TRD* genes). We evaluated our method using 5′ scRNA-seq datasets comprising both sc-αβTCR-seq and sc-γδTCR-seq as references and demonstrated that it can identify γδ T cells in scRNA-seq datasets with high sensitivity and accuracy. We observed a stable performance of this strategy across datasets from different tissues and different subtypes of γδ T cells. Thus, we propose this analysis method, based on TCR gene module scores, as a standardized tool for identifying and reanalyzing γδ T cells from 5′-end scRNA-seq datasets.

Keywords: TCR genes, TCR module scores, scRNA-seq, scTCR-seq, γδ t cells

1 Introduction

Single-cell RNA sequencing (scRNA-seq) has become a widely used technology in immunology.[1] This technology has led to an explosion of published datasets, providing a wealth of data to be reanalyzed from different angles and depths. Reanalyzing existing data is even more important for γδ T cell research, due to the fact that many studies which had sequenced total immune cells or enriched T cells did not perform a throughout analysis on γδ T cells. However, how to accurately identify γδ T cells from a large T cell dataset is still challenging. The most precise way (the golden standard) to distinguish between γδ T cells and αβ T cells is through the use of single-cell γδ T cell receptor sequencing (sc-γδTCR-seq) or anti-γδTCR CITE-seq (cellular indexing of transcriptomes and epitopes).[2] However, these methods have not been widely incorporated into published scRNA-seq datasets. While some studies have attempted to distinguish between αβ T cells and γδ T cells by using the constant genes of *TRG/TRD* (*TRGC1*, *TRGC2*, and *TRDC*),[3] this approach may not be adequate to identify sufficient γδ T cells due to a high dropout rate of TCR transcripts in scRNA-seq data.[4] Moreover, *TRG* genes are frequently expressed in αβ T cells, which may lead to false positives in γδ T cell identification.[5,6]

In humans, γδ T cells are categorized into two major groups based on the variable genes (*TRGV* and *TRDV*) of their γδ TCRs. The intrathymically preprogrammed Vγ9Vδ2$^+$ T cells are characterized by innate immunity gene programs such as *ZBTB16* (encoding PLZF) and *NCR3*, and they do not express CD4 and CD8 molecules.[2,7–11] On the other hand, the non-Vδ2 γδ T cells are more similar to CD8$^+$ αβ T cells, with most of them expressing a TCR consisting of a Vδ1 or Vδ3 chain paired with a variable (V) γ chain.[12] They exit the thymus as naive γδ T cells and have the ability to recognize a diverse range of antigenic targets.[10,12–16] Upon antigen stimulation, non-Vδ2 T cells undergo massive clonal expansion and differentiate into cytotoxic effector cells.[15,16] These cells share a similar gene expression program with cytotoxic CD8$^+$ αβ T cells, including the expression of *CD8A/B*, *FCGR3A* (encoding CD16), *EOMES*, and *TBX21* (encoding T-bet).[2,17,18] The shared gene programs further complicate the distinction between αβ T cells and γδ T cells in scRNA-seq analysis.

To develop a γδ T classifier for scRNA-seq datasets, we postulated that the variable TCR genes (*TRAV*, *TRBV*, *TRGV*, and *TRDV*) and constant TCR genes captured by the 5′-end scRNA-seq chemistry (10x Genomics) would be sufficient to distinguish between αβ and γδ T cells in the transcriptome. We calculated the modular TCR expression of the constant and variable TCR genes (hereafter named TCR module score). We defined high γδTCR module score and low αβTCR module score population as putative γδ T cells. Our strategy was proved to be highly specific and sensitive when comparing to the genuine γδ T cells in the reference datasets. Therefore, our approach offers a practical solution for reanalyzing public scRNA-seq data of T cells with a focus on γδ T cells.

2 Materials and methods

2.1 Human samples and isolation of CD3$^+$ T cells

Before sample collection, healthy donors provided written informed consent and the study was approved by the local ethics committee Hamburger Ärztekammer (PV5982).

Received: March 27, 2023. **Revised:** June 2, 2023. **Accepted:** June 11, 2023. **Corrected and Typeset:** July 24, 2023
© The Author(s) 2023. Published by Oxford University Press on behalf of Society for Leukocyte Biology. All rights reserved. For permissions, please e-mail: journals.permissions@oup.com

Downloaded from https://academic.oup.com/jleukbio/article/114/6/630/7223408 by Universitaets-Krankenhaus Eppendorf user on 03 February 2026

Whole EDTA blood from 4 healthy female donors was collected. Peripheral blood mononuclear cells (PBMCs) were isolated via a density gradient centrifugation (Biocoll; Biochrom) and stored a nitrogen tank in 90% fetal calf serum and 10% DMSO (6–10 × 10^6 cells/mL). PBMCs were thawed and stained with Live/Death-PacO, Live/Death-APC-Cy7, and aCD3-BV650 (BioLegend). For each sample, live $CD3^+$ T cells were sorted with the BD Aria Fusion, and 15,000 cells were then used for the preparation of single-cell libraries. The Chromium Next GEM Single Cell 5′ Library and Gel Bead Kit v1.1 (10x Genomics) were used. Upon completion of reverse transcription but prior to fragmentation, the single-cell barcoded full-length complementary DNA was divided into three parts. Each part was used separately to prepare the libraries for scRNA, sc-αβTCR, and sc-γδTCR. For the sc-αβTCR and scRNA libraries, we followed the manufacturer's instructions. For the sc-γδTCR libraries, we used custom primers to enrich γδTCR transcripts. During the first target enrichment, we used primers RV_TRG1: ATCCCAGAATCGTGTTGCTC and RV_TRD1: CCCACTGGGAGAGATGACAA. For the second target enrichment, we used RV_TRG2: GGGGAAACATCTGCATCAAG and RV_TRD2: GACAAAAACGGATGGTTTGG as custom primers.[2] We sequenced each library, including scRNA, sc-αβTCR, and sc-γδTCR, on the Illumina NovaSeq6000.

2.2 Data processing and analysis of scRNA-seq libraries

The scRNA-seq reads were aligned to the human reference genome GRCh38-2020-A, and feature-barcode matrices were generated via the Cell Ranger pipeline (version 4.0.0; 10x Genomics). Further analysis including dimensional reduction and cell clustering was performed in R (version 4.2.2; R Foundation for Statistical Computing) using the R package Seurat (version 4.3.0). The quality control criteria were set as follows: (1) the number of UMI counts per cell is between 2,000 and 7,000; (2) the number of genes per cell is between 500 and 3,000; and (3) the percentage of mitochondrial genes is lower than 15%. After integration of 4 libraries, dimensional reduction analysis and unsupervised clustering were performed. The identities of clusters were annotated by gene expression profile.

Publicly available scRNA-seq datasets were reanalyzed according to the method in the original publications.[19–22]

2.3 scTCR-seq analysis

Cell Ranger VDJ pipeline (version 4.0.0; 10x Genomics) was used to align the scTCR-seq reads to the human reference genome (vdj_GRCh38_alts_ensembl-4.0.0.) and annotate productiveness of the TCR sequences. After excluding nonproductive TCR sequences and duplicates, scTCR-seq data were introduced to the metadata of the corresponding scRNA-seq Seurat object by identical barcodes. CDR3 was used to annotate genuine γδ and αβ T cell subtypes.

2.4 TCR module scores calculation

Constant or/and variable TCR genes (Supplementary Table 1) detected in the transcriptome were used to compute the TCR module scores using the AddModuleScore function (nbin = 24, ctrl = 100) from Seurat (version 4.3.0). Briefly, all genes were binned into 24 bins based on their average expression level across all cells. For each gene in the TCR gene sets, 100 random genes from the same expression bin were selected as the control gene sets. Within each cell, the TCR gene module scores were computed by averaging the expression of each gene from the TCR gene sets after subtracting the average expression of the corresponding control gene sets.

2.5 Data availability

scRNA and scTCR datasets to generate Fig. 1 are available at https://zenodo.org/deposit/7989561. Data used in Fig. 2 are available in the original publication.[19] Raw sequencing data used in Fig. 3 are deposited in the Gene Expression Omnibus repository under accession number GSE200173.[20] Raw sequencing data used in Supplementary Fig. 4 are deposited at the Genome Sequence Archive at the National Genomics Data Center (Beijing, China) under the BioProject ID PRJCA007744.[21] Raw sequencing data used in Fig. 4 are deposited in the ArrayExpress database at EMBL-EBI under accession number E-MTAB-11536.[22]

3 Results

3.1 Classifying γδ T cells in peripheral blood by modular TCR expression analysis

To obtain genuine γδ T cells and αβ T cells as a reference, we generated a dataset by performing 5′-end scRNA-seq and paired sc-αβ and γδTCR-seq (10x Genomics) on $CD3^+$ T cells collected from PBMCs of 4 healthy donors. Cells that passed quality control were visualized using UMAP (Uniform Manifold Approximation and Projection). Four major clusters, $CD4^+$ T cells, $CD8^+$ T cells, MAIT cells, and $V\gamma9V\delta2^+$ T cells were identified by gene expression profile (Supplementary Fig. 1A and B). A total of 1,755 cells detected with productive TCR-γ/TCR-δ chains were marked as genuine γδ T cells and 20,544 cells with productive TCR-α/TCR-β chains were marked as genuine αβ T cells. Cells without a productive TCR were removed (Supplementary Fig. 1A and C). Most non-Vδ2 γδ T cells collocated with $CD8^+$ αβ T cells, suggesting they have similar phenotypes (Supplementary Fig. 1D and E). *TRA/TRB* and *TRG/TRD* gene expression from the transcriptome of each cell were calculated as TCR module scores–αβTCR module score and γδTCR module score, respectively, using the AddModuleScore function from Seurat v4.3.[23] Cells with high γδTCR module scores and low αβTCR module scores were marked as putative γδ T cells and validated by genuine γδ T cells (Fig. 1A). Initially, only constant genes *TRDC*, *TRGC1*, and *TRGC2* were used to calculate γδTCR module scores, while *TRAC*, *TRBC1*, and *TRBC2* were used to calculate αβTCR module scores (Supplementary Table 1). However, this model yielded poor accuracy and sensitivity, with 40.1% of genuine γδ T cells locating within the putative αβ T population, while 42.2% of putative γδ T cells by this classifier were genuine αβ T cells (Fig. 1B–D). To improve the efficiency of γδ T cells identification, TCR module scores were recalculated by introducing variable TCR genes (*TRDV*, *TRGV*, *TRAV*, and *TRBV*) together with the constant TCR genes (Supplementary Table 1). Using this strategy, the genuine γδ T cells formed a population with a high γδTCR module score and a low αβTCR module score, largely separated from the genuine αβ T cells (Fig. 1E–G). However, a subpopulation of genuine αβ T cells showed intermediate γδTCR module scores ($\gamma\delta^{Int}$), leading to an ambiguous boundary between genuine γδ T cells and αβ T cells. Quantification analysis showed that 11.0% of genuine γδ T cells were not defined as putative γδ T cells (Fig. 1G). This confounder mainly resulted from the *TRG* gene expression by genuine αβ T cells (Supplementary Fig. 1F and G). Therefore, the γδTCR module score was recomputed using only the *TRDC* and *TRDV* genes (Supplementary Table 1). The genuine αβ T cells with $\gamma\delta^{Int}$ score were largely reduced under this strategy (Fig. 1H and Supplementary Fig. 1H). Up to 95.9% of genuine γδ T

Downloaded from https://academic.oup.com/jleukbio/article/114/6/630/7223408 by Universitaets-Krankenhaus Eppendorf user on 03 February 2026

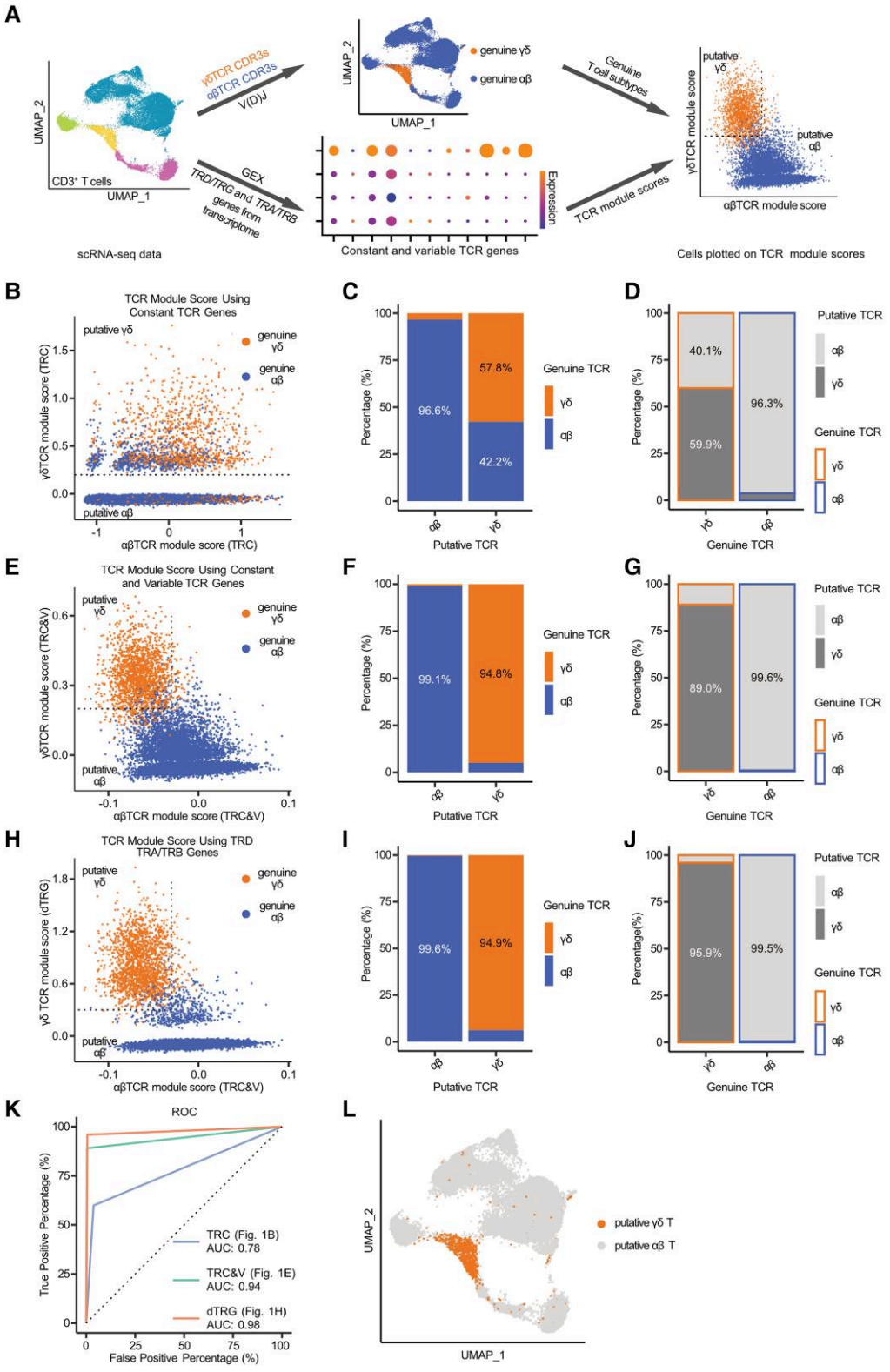


Fig. 1. Identification of genuine γδ T cells in PBMCs. scRNA-seq and scTCR-seq (γδ and αβ) of CD3⁺ T lymphocytes (22,883 cells) from PBMCs in 4 donors. (**A**) Schematic of workflow: genuine T cell subtypes were annotated with the detected CDR3 types and putative T subtypes were identified by TCR gene module scores. (**B–D**) Cells on TCR module scores calculated based on the constant TCR genes. (**E–G**) Cells on TCR module scores incorporating variable TCR (*TRD/TRG* vs *TRA/TRB*) genes. (**H–J**) Cells on TCR module scores computed on *TRD* vs *TRA/TRB* genes. (**C**, **F**, and **I**) Proportions of genuine T subtypes in putative T cell populations. (**D**, **G**, and **J**) Proportions of putative T subtypes in genuine T cell populations. (**K**) Receiver-operating characteristic curve (ROC) of 3 analysis models (**B**, **E**, and **H**). (**L**) Putative γδ T cells and αβ T cells on UMAP. (**A**, **B**, **E**, and **H**) The dashed line shows the threshold for high and low TCR module scores. (**A**, **B**, **E**, **H**, and **L**) Each dot represents 1 cell.

Downloaded from https://academic.oup.com/jleukbio/article/114/6/630/7223408 by Universitaets-Krankenhaus Eppendorf user on 03 February 2026

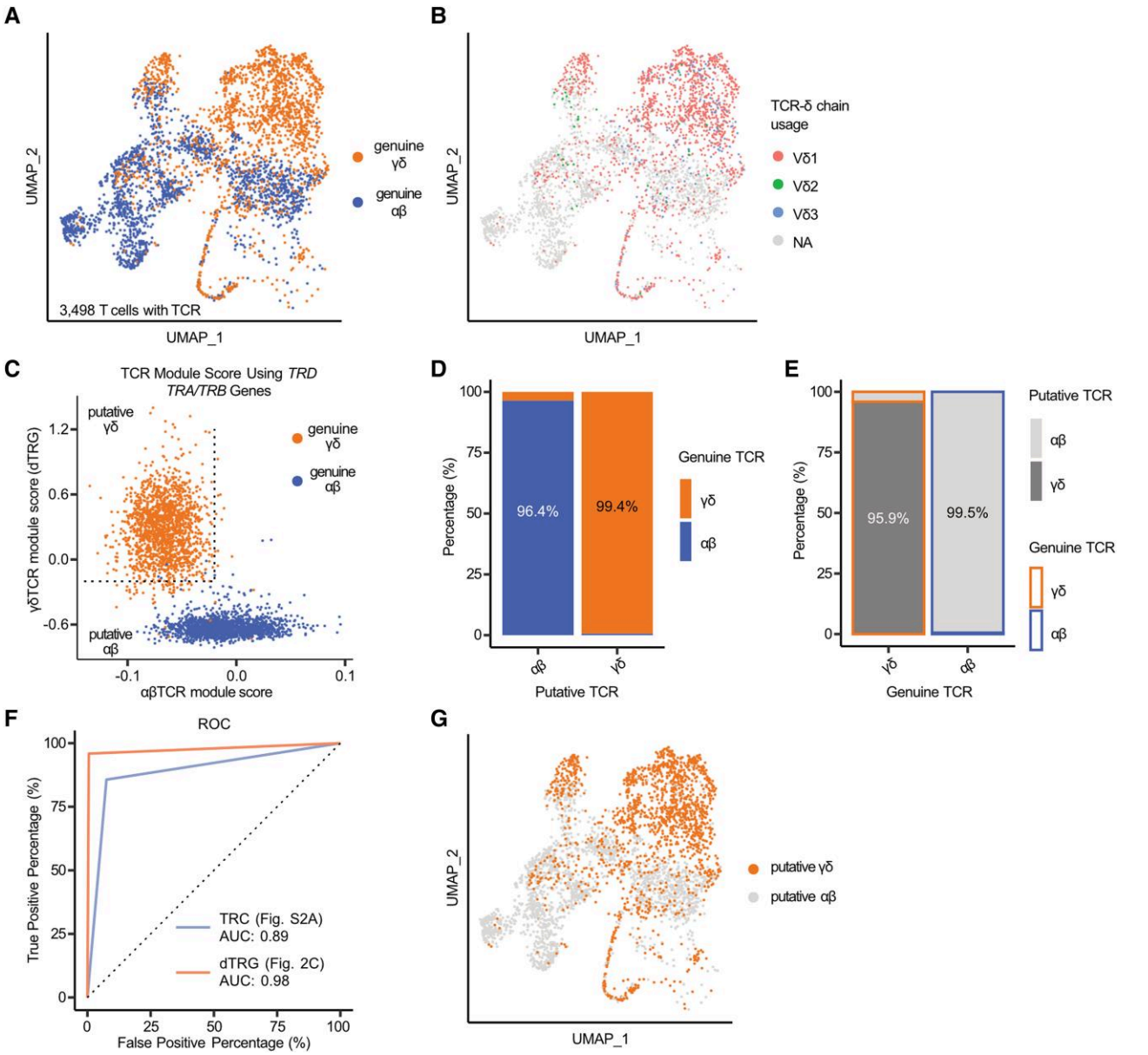


Fig. 2. Identification of tissue-resident genuine γδ T lymphocytes. Reanalysis of the Merkel cell carcinoma tumor-infiltrating CD3$^+$ T lymphocytes (3,498 cells) dataset. (**A**) Genuine T cell subtypes on UMAP. (**B**) TCR-δ chain usage on UMAP. (**C**) TCR module scores calculated on *TRA/TRB* vs *TRD* genes. (**D**) Proportions of genuine T subtypes in putative T cell populations. (**E**) Proportions of putative T subtypes in genuine T cell populations. (**F**) Receiver-operating characteristic curve of 2 models (Supplementary Fig. 2A and C). (**G**) Putative γδ T cells and αβ T cells on UMAP.

cells were recovered as putative γδ T cells, demonstrating a lower false negative rate (Fig. 1I and J). The reliability of the combination of γδTCR module score by *TRD* genes and αβTCR module score was confirmed by area under the receiver-operating characteristic curve (AUC), which reaches as high as 0.98 (Fig. 1K). Moreover, the putative γδ T cells were nearly overlapped with genuine γδ T cells on the phenotypic UMAP (Fig. 1L and Supplementary Fig. 1C).

3.2 Modular TCR expression analysis detects tissue-resident γδ T cells

Given that most of γδ T cells in peripheral blood are Vγ9Vδ2$^+$, while the non-Vδ2 γδ T cells are enriched in tissues,[10,11] we extended our analysis to a published scRNA-seq dataset that profiled the transcriptome with paired sc-αβ and γδTCR-seq of tumor-infiltrating T cells in human Merkel cell carcinomas.[19] In that study, 1,659 genuine γδ T cells and 1,839 genuine αβ T cells were defined by scTCR-seq (Fig. 2A). Notably, γδ T cells, with the majority of γδ T cells expressing Vδ1 TCR, were partially clustered together with αβ T cells (Fig. 2A and B). When the TCR module score analysis was performed on the constant TCR genes (Supplementary Table 1), the αβTCR score could not distinguish between αβ and γδ T cells, and 14.3% of genuine γδ T cells were defined as putative αβ T cells (Supplementary Fig. 2A–C). In contrast, after incorporating the constant and variable *TRA/TRB* and *TRD* genes into the analysis (Supplementary Table 1), the genuine γδ T cells and αβ T cells formed two distinct populations on TCR scores (Fig. 2C–E), and the area under the receiver-operating characteristic curve value of this classifier is 0.98 (Fig. 2F). The vast majority of genuine and putative γδ T cells were overlapped on the UMAP (Fig. 2A and G).

Downloaded from https://academic.oup.com/jleukbio/article/114/6/630/7223408 by Universitaets-Krankenhaus Eppendorf user on 03 February 2026

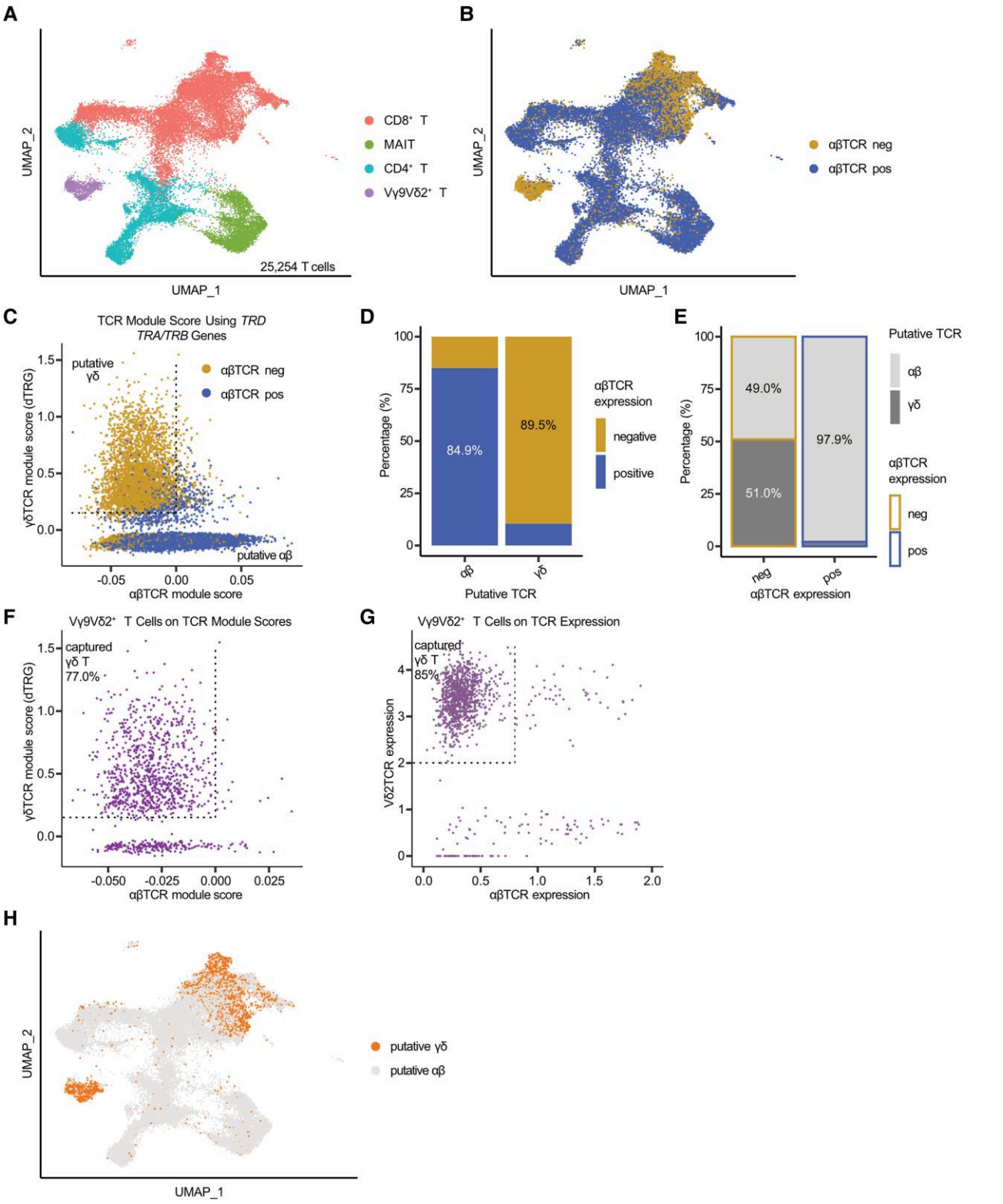


Fig. 3. Evaluation of γδ T lymphocytes identification strategy on a 5′-end dataset. Reanalysis of the human liver perfusates CD3⁺ T lymphocytes (25,254 cells) dataset (GSE200173). (**A**) UMAP of T cells. (**B**) αβTCR positive and αβTCR negative cells on UMAP. (**C**) TCR module scores calculated on *TRD* vs *TRA/TRB* genes. (**D**) Proportions of αβTCR positive and αβTCR negative cells in putative cell populations. (**E**) Proportions of putative T subtypes in αβTCR positive and αβTCR negative populations. (**F**) TCR gene module scores of Vγ9Vδ2⁺ cells calculated from *TRD* vs *TRA/TRB* genes. (**G**) Vδ2 and αβTCR expression of Vγ9Vδ2⁺ cells. Proportions of captured γδ T cells in panels (**F**) and (**G**) were indicated. (**H**) Putative γδ and αβ T cells on UMAP.

Downloaded from https://academic.oup.com/jleukbio/article/114/6/630/7223408 by Universitaets-Krankenhaus Eppendorf user on 03 February 2026

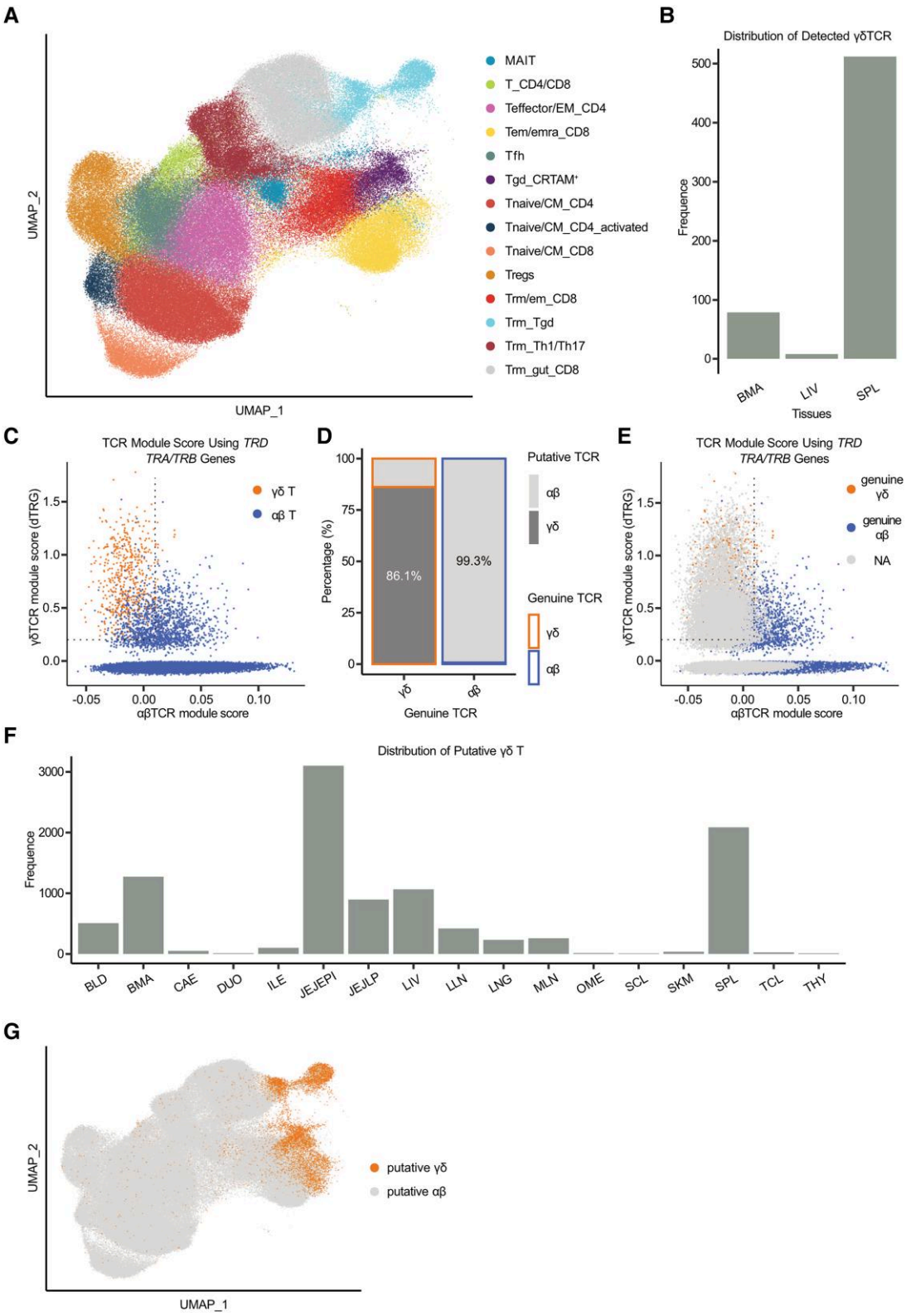


Fig. 4. Evaluation of a γδ T lymphocyte identification strategy on a multiorgan dataset. Reanalysis of the multiorgan CD3⁺ T lymphocytes (183,680 cells) dataset (E-MTAB-11536). (**A**) UMAP of T cells: cluster annotations were taken from the original publication.[22] (**B**) Tissue distribution of detected γδTCR. (**C**) Cells with detected γδ or αβ CDR3s (genuine γδ or αβ TCR) on TCR module scores calculated on *TRD* vs *TRA/TRB* genes. (**D**) Proportions of putative T subtypes in genuine T cell populations. (**E**) All cells on TCR gene module scores. The dashed line in panels (**C**) and (**E**) indicates the same thresholds for low and high TCR module scores. (**F**) Tissue distribution of putative γδ T cells. (**G**) Putative γδ T and αβ T cells on UMAP. BLD = blood; BMA = bone marrow; CAE = cecum; DUO = duodenum; ILE = ileum; JEJEPI = jejunum epithelial; JEJELP = jejunum lamina propria; LIV = liver; LLN = lung-draining lymph nodes; LNG = lungs; MLN = mesenteric lymph nodes; OME = omentum; SCL = sigmoid colon; SKM = skeletal muscle; SPL = spleen; TCL = transverse colon; THY = thymus.

Downloaded from https://academic.oup.com/jleukbio/article/114/6/630/7223408 by Universitaets-Krankenhaus Eppendorf user on 03 February 2026

3.3 Demonstration of γδ T cell identification on a 5′-end scRNA-seq dataset with CITE-seq

To assess the efficacy of our approach for identifying γδ T cells, we reanalyzed a dataset of CD45$^+$ lymphocytes from human liver perfusates prepared with the 5′-end scRNA-seq plus CITE-seq strategy.[20] Within this dataset, 25,254 CD3$^+$ T cells were clustered as CD4$^+$ T cells, CD8$^+$ T cells, MAIT cells, and Vγ9Vδ2$^+$ T cells based on the transcriptome and cellular surface proteins (Fig. 3A and Supplementary Fig. 3A). Cells were classified into αβTCR$^+$ or αβTCR$^-$ groups based on the protein expression (Supplementary Fig. 3B). In addition to Vγ9Vδ2$^+$ T cells, a substantial proportion of CD8$^+$ T cells were observed to lack αβTCR expression (Fig. 3B). αβTCR$^+$ or αβTCR$^-$ cells were separated into 2 distinct populations by γδTCR and αβTCR module scores (Supplementary Table 1), 89.5% of cells in the putative γδ T cells were αβTCR$^-$ cells, while 84.9% of putative αβ T cells were αβTCR$^+$ cells (Fig. 3C–E and Supplementary Fig. 3C and D). Among the Vγ9Vδ2$^+$ T cell cluster, 77.0% of cells were classified as captured γδ T cells by TCR module scores, while the Vδ2 expression from CITE-seq identified 85% of cells as captured γδ T cells (Fig. 3F and G). The distribution of putative γδ T cells was similar to αβTCR-negative cells (Fig. 3B and H), with cells overlapping with CD8$^+$ T cells mainly expressing *TRDV1* or *TRDV3* genes (Supplementary Fig. 3E).

3.4 Assessment of modular TCR analysis for identifying γδ T cells from 3′-end scRNA-seq datasets

Next, we expanded our analysis to a 3′-end scRNA-seq dataset of tumor-infiltrating T cells in primary liver cancer.[21] We found that using *TRD* based γδTCR module score to identify γδ T cells did not yield a better result compared with using *TRDC* expression. Both methods defined a similar number of γδ T cells (Supplementary Fig. 4A–D and Supplementary Table 1). Indeed, the *TRDV* genes were rarely captured in the 3′-end scRNA-seq datasets (Supplementary Fig. 4E).

3.5 Identifying γδ T cells by TCR module score from multiorgan T cell atlas

Finally, to further assess the ability of our solution for identifying γδ T cells from large datasets, we reanalyzed a heterogeneous single-cell atlas comprising a total of 183,680 T cells from 16 different tissues obtained from 12 deceased organ donors.[22] Sixteen T cell subpopulations were defined by Domínguez Conde et al. (Fig. 4A).[22] sc-αβTCR-seq and sc-γδTCR-seq were performed on a small number of samples in this dataset, resulting in 599 genuine γδ T cells (mainly from spleen and bone marrow) and 68,426 genuine αβ T cells (mainly from lung-draining lymph nodes, mesenteric lymph nodes, spleen, and jejunum) (Fig. 4B and Supplementary Fig. 5). TCR module score analysis based on *TRD* and *TRA/TRB* genes was first performed on genuine γδ T cells and αβ T cells to set up the gate for γδ T cells (Supplementary Table 1). A total of 86.1% of genuine γδ T cells were defined as γδ T cells by TCR module scores (Fig. 4C and D). Next, we applied the same gate for all the T cells in the dataset, and 10,110 putative γδ T cells were identified, mainly from lung-draining lymph nodes, mesenteric lymph nodes, spleen, and jejunum (Fig. 4E and F). Notably, apart from the originally defined γδ T cell clusters (Tgd_CRTAM$^+$ and Trm_Tgd), a substantial part of the putative γδ T cells were from originally defined CD8$^+$ memory T cell clusters, highlighting the phenotypic overlapping between γδ T cells and CD8$^+$ αβ T cells (Fig. 4A and G).

4 Discussion

In this study, we propose a solution to efficiently define γδ T cells from scRNA-seq datasets by computing the TCR gene module scores based on *TRD* genes and *TRA/TRB* genes. The γδ T cells in T cell datasets formed a γδTCR score high, αβTCR score low population by the TCR module scores. We found that this modular TCR score analysis for identifying γδ T cells was as efficient as sc-γδTCR-seq. We tested this method on 5 different datasets, including a heterogenous multiorgan cell atlas, and our results showed that the identification of γδ T cells by TCR gene module scores was simple and reliable on 5′-end scRNA-seq datasets.

All the genuine γδ T cells were featured as γδTCR score high and αβTCR score low in our tested datasets. In contrast, some of the genuine αβ T cells display intermediate γδTCR scores. This phenomenon was even more pronounced when *TRG* genes were included in the calculation of γδTCR score. The expression of *TRD/TRG* genes in αβ T cells can be traced back to the intrathymic T cell development. Heterogeneous CD4$^-$CD8$^-$ (double negative [DN]) thymocytes give rise to both αβ and γδ T cell lineages. The lineage commitment of αβ T cells and γδ T cells starts from the DN2 stage when *TRD*, *TRG*, and *TRB* gene loci begin to rearrange concurrently and is completed in the DN3b stage.[24] When a productive β chain is rearranged, it can form a pre-TCR by pairing with an invariant pTα. The resulting pre-TCR serves to pass a checkpoint termed β-selection for αβ lineage development.[25,26] However, rearranged *TRG* gene does not prevent thymocytes from passing β-selection, thus some αβ T cells can still preserve rearranged *TRG* loci and continue to transcribe *TRG* genes.[5,27] Conversely, it is unclear whether the committed γδ thymocytes can have productive TCR-α or β segment rearrangement.[6,28–30]

Some non-Vδ2 γδ T cells share a similar transcriptome profile with cytotoxic CD8$^+$ αβ T cells.[2,17] Indeed, as we observed in our results, γδ T cells and CD8$^+$ αβ T cells frequently clustered together by transcriptome analysis. To this end, we used the TCR module scores to successfully identify genuine γδ T cells.

Our TCR module score method is limited in improving the γδ T cell identification when applied on 3′-end scRNA-seq datasets. Mainstream scRNA-seq methods capture messenger RNA molecules from either the 3′ end or the 5′ end, and the majority of sequencing reads cover around 200 to 300 bp length from the respective end.[31,32] In a rearranged TCR gene, the constant region maps to the 3′ end, while the variable region is closer to the 5′ end. Conceivably, the 5′-end scRNA-seq methods are more sensitive in capturing variable TCR genes,[33] whereas the identification of γδ T cells in 3′-end RNA-seq data is mainly based on the constant TCR genes, and incorporating the variable TCR genes does not significantly improve the resolution.

5 Conclusion

Accurately identifying γδ T cells in scRNA-seq datasets is essential for studying the biology of this important but understudied T cell subset. Our analysis strategy, based on calculating gene module scores for constant and variable TCR genes, demonstrated high sensitivity and stable performance across different tissue datasets and γδ T cell subtypes. The adoption of this method as a standardized tool will facilitate the in-depth reanalysis of γδ T cells from existing scRNA-seq data, thus enabling us to gain insights into the heterogeneity and diversity of γδ T cells in different tissues and disease states.

Acknowledgments

The authors thank the FACS Sorting Core Unit of the University Medical Center Hamburg-Eppendorf (UKE Hamburg) for technical

Downloaded from https://academic.oup.com/jleukbio/article/114/6/630/7223408 by Universitaets-Krankenhaus Eppendorf user on 03 February 2026

assistance. They thank Rixa-Mareike Köhn, UKE Hamburg for proofreading the manuscript. ChatGPT (chat.openai.com) was used for language correction of the first draft.

Author Contributions

Z.S., L.T., and I.P. designed the study. Z.S. analyzed data. L.T. and C.C. contributed to data analysis. L.H., C.S., J.F., and D.S. organized tissue collection. L.H. and D.S. processed samples. Z.S. and L.T. wrote the manuscript. L.T. and I.P. supervised the study and reviewed the manuscript.

Supplementary material

Supplementary materials are available at *Journal of Leukocyte Biology* online.

Funding

This work was supported by the German Research Foundation Grants Research Unit FOR2799 to I.P. (Project Number 395236335), DFG-PR727-13/1 (Project Number 431861465) to I.P., and Research Unit FOR 5068 to C.S. (Project Number 429191104).

Conflict of interest statement: The authors declare that they have no competing interests.

References

1. Gomes T, Teichmann SA, Talavera-Lopez C. Immunology driven by large-scale single-cell sequencing. *Trends Immunol*. 2019:40(11):1011–1021. https://doi.org/10.1016/j.it.2019.09.004
2. Tan L, Fichtner AS, Bruni E, Odak I, Sandrock I, Bubke A, Borchers A, Schultze-Florey C, Koenecke C, Forster R, *et al.* A fetal wave of human type 3 effector gamma delta cells with restricted TCR diversity persists into adulthood. *Sci Immunol*. 2021:6(58):eabf0125. https://doi.org/10.1126/sciimmunol.abf0125
3. Pizzolato G, Kaminski H, Tosolini M, Franchini DM, Pont F, Martins F, Valle C, Labourdette D, Cadot S, Quillet-Mary A, *et al.* Single-cell RNA sequencing unveils the shared and the distinct cytotoxic hallmarks of human TCRVdelta1 and TCRVdelta2 gammadelta T lymphocytes. *Proc Natl Acad Sci U S A*. 2019:116(24):11906–11915. https://doi.org/10.1073/pnas.1818488116
4. Qiu P. Embracing the dropouts in single-cell RNA-seq analysis. *Nat Commun*. 2020:11(1):1169. https://doi.org/10.1038/s41467-020-14976-9
5. Kranz DM, Saito H, Heller M, Takagaki Y, Haas W, Eisen HN, Tonegawa S. Limited diversity of the rearranged T-cell gamma gene. *Nature*. 1985:313(6005):752–755. https://doi.org/10.1038/313752a0
6. Sherwood AM, Desmarais C, Livingston RJ, Andriesen J, Haussler M, Carlson CS, Robins H. Deep sequencing of the human TCR gamma and TCR beta repertoires suggests that TCR beta rearranges after alpha beta and gamma delta T cell commitment. *Sci Transl Med*. 2011:3(90):90ra61. https://doi.org/10.1126/scitranslmed.3002536
7. Sanchez Sanchez G, Papadopoulou M, Azouz A, Tafesse Y, Mishra A, Chan JKY, Fan Y, Verdebout I, Porco S, Libert F, *et al.* Identification of distinct functional thymic programming of fetal and pediatric human γδ thymocytes via single-cell analysis. *Nat Commun*. 2022:13(1):5842. https://doi.org/10.1038/s41467-022-33488-2
8. Wragg KM, Tan HX, Kristensen AB, Nguyen-Robertson CV, Kelleher AD, Parsons MS, Wheatley AK, Berzins SP, Pellicci DG, Kent SJ, *et al.* High CD26 and low CD94 expression identifies an IL-23 responsive V delta 2(+) T cell subset with a MAIT cell-like transcriptional profile. *Cell Rep*. 2020:31(11):107773. https://doi.org/10.1016/j.celrep.2020.107773
9. Dimova T, Brouwer M, Gosselin F, Tassignon J, Leo O, Donner C, Marchant A, Vermijlen D. Effector Vgamma9Vdelta2 T cells dominate the human fetal gammadelta T-cell repertoire. *Proc Natl Acad Sci U S A*. 2015:112(6):E556–E565. https://doi.org/10.1073/pnas.1412058112
10. Prinz I, Silva-Santos B, Pennington DJ. Functional development of gamma delta T cells. *Eur J Immunol*. 2013:43(8):1988–1994. https://doi.org/10.1002/eji.201343759
11. Carding SR, Egan PJ. Gamma delta T cells: functional plasticity and heterogeneity. *Nat Rev Immunol*. 2002:2(5):336–345. https://doi.org/10.1038/nri797
12. Fichtner AS, Ravens S, Prinz I. Human gamma delta TCR repertoires in health and disease. *Cells*. 2020:9(4):800. https://doi.org/10.3390/cells9040800
13. Deseke M, Prinz I. Ligand recognition by the gamma delta TCR and discrimination between homeostasis and stress conditions. *Cell Mol Immunol*. 2020:17(9):914–924. https://doi.org/10.1038/s41423-020-0503-y
14. Davey MS, Willcox CR, Baker AT, Hunter S, Willcox BE. Recasting human V delta 1 lymphocytes in an adaptive role. *Trends Immunol*. 2018:39(6):446–459. https://doi.org/10.1016/j.it.2018.03.003
15. Ravens S, Schultze-Florey C, Raha S, Sandrock I, Drenker M, Oberdorfer L, Reinhardt A, Ravens I, Beck M, Geffers R, *et al.* Human gamma delta T cells are quickly reconstituted after stem-cell transplantation and show adaptive clonal expansion in response to viral infection. *Nat Immunol*. 2017:18(4):393–401. https://doi.org/10.1038/ni.3686
16. Davey MS, Willcox CR, Joyce SP, Ladell K, Kasatskaya SA, McLaren JE, Hunter S, Salim M, Mohammed F, Price DA, *et al.* Clonal selection in the human V delta 1 T cell repertoire indicates gamma delta TCR-dependent adaptive immune surveillance. *Nat Commun*. 2017:8(1):14760. https://doi.org/10.1038/ncomms14760
17. McMurray JL, von Borstel A, Taher TE, Syrimi E, Taylor GS, Sharif M, Rossjohn J, Remmerswaal EBM, Bemelman FJ, Vieira Braga FA, *et al.* Transcriptional profiling of human V delta 1T cells reveals a pathogen-driven adaptive differentiation program. *Cell Rep*. 2022:39(8):110858. https://doi.org/10.1016/j.celrep.2022.110858
18. Roy Chowdhury R, Valainis JR, Dubey M, von Boehmer L, Sola E, Wilhelmy J, Guo J, Kask O, Ohanyan M, Sun M, *et al.* NK-like CD8(+) γδ T cells are expanded in persistent Mycobacterium tuberculosis infection. *Sci Immunol*. 2023:8(81):eade3525. https://doi.org/10.1126/sciimmunol.ade3525
19. Gherardin NA, Waldeck K, Caneborg A, Martelotto LG, Balachander S, Zethoven M, Petrone PM, Pattison A, Wilmott JS, Quiñones-Parra SM, *et al.* Gamma delta T cells in merkel cell carcinomas have a proinflammatory profile prognostic of patient survival. *Cancer Immunol Res*. 2021:9(6):612–623. https://doi.org/10.1158/2326-6066.CIR-20-0817
20. Koh JY, Rha MS, Choi SJ, Lee HS, Han JW, Nam H, Kim DU, Lee JG, Kim MS, Park JY, *et al.* Identification of a distinct NK-like hepatic T-cell population activated by NKG2C in a TCR-independent manner. *J Hepatol*. 2022:77(4):1059–1070. https://doi.org/10.1016/j.jhep.2022.05.020
21. Xue R, Zhang Q, Cao Q, Kong R, Xiang X, Liu H, Feng M, Wang F, Cheng J, Li Z, *et al.* Liver tumour immune microenvironment subtypes and neutrophil heterogeneity. *Nature*. 2022:612(7938):141–147. https://doi.org/10.1038/s41586-022-05400-x
22. Domínguez Conde C, Xu C, Jarvis LB, Rainbow DB, Wells SB, Gomes T, Howlett SK, Suchanek O, Polanski K, King HW, *et al.*

Downloaded from https://academic.oup.com/jleukbio/article/114/6/630/7223408 by Universitaets-Krankenhaus Eppendorf user on 03 February 2026

Cross-tissue immune cell analysis reveals tissue-specific features in humans. *Science*. 2022:376(6594):eabl5197. https://doi.org/10.1126/science.abl5197
23. Hao Y, Hao S, Andersen-Nissen E, Mauck WM 3rd, Zheng S, Butler A, Lee MJ, Wilk AJ, Darby C, Zager M, *et al.* Integrated analysis of multimodal single-cell data. *Cell*. 2021:184(13):3573–3587.e29. https://doi.org/10.1016/j.cell.2021.04.048
24. Rothenberg EV, Moore JE, Yui MA. Launching the T-cell-lineage developmental programme. *Nat Rev Immunol*. 2008:8(1):9–21. https://doi.org/10.1038/nri2232
25. Shinkai Y, Koyasu S, Nakayama K, Murphy KM, Loh DY, Reinherz EL, Alt FW. Restoration of T cell development in RAG-2-deficient mice by functional TCR transgenes. *Science*. 1993:259(5096):822–825. https://doi.org/10.1126/science.8430336
26. Mallick CA, Dudley EC, Viney JL, Owen MJ, Hayday AC. Rearrangement and diversity of t cell receptor beta chain genes in thymocytes: a critical role for the beta chain in development. *Cell*. 1993:73(3):513–519. https://doi.org/10.1016/0092-8674(93)90138-G
27. Ishida I, Verbeek S, Bonneville M, Itohara S, Berns A, Tonegawa S. T-cell receptor gamma delta and gamma transgenic mice suggest a role of a gamma gene silencer in the generation of alpha beta T cells. *Proc Natl Acad Sci U S A*. 1990:87(8):3067–3071. https://doi.org/10.1073/pnas.87.8.3067
28. Sleckman BP, Khor B, Monroe R, Alt FW. Assembly of productive T cell receptor delta variable region genes exhibits allelic inclusion. *J Exp Med*. 1998:188(8):1465–1471. https://doi.org/10.1084/jem.188.8.1465
29. Boucontet L, Sepulveda N, Carneiro J, Pereira P. Mechanisms controlling termination of V-J recombination at the TCRgamma locus: implications for allelic and isotypic exclusion of TCRgamma chains. *J Immunol*. 2005:174(7):3912–3919. https://doi.org/10.4049/jimmunol.174.7.3912
30. Davodeau F, Peyrat MA, Houde I, Hallet MM, De Libero G, Vié H, Bonneville M. Surface expression of two distinct functional antigen receptors on human gamma delta T cells. *Science*. 1993:260(5115):1800–1802. https://doi.org/10.1126/science.8390096
31. Plass M, Solana J, Wolf FA, Ayoub S, Misios A, Glažar P, Obermayer B, Theis FJ, Kocks C, Rajewsky N. Cell type atlas and lineage tree of a whole complex animal by single-cell transcriptomics. *Science*. 2018:360(6391):eaaq1723. https://doi.org/10.1126/science.aaq1723
32. Briggs JA, Weinreb C, Wagner DE, Megason S, Peshkin L, Kirschner MW, Klein AM. The dynamics of gene expression in vertebrate embryogenesis at single-cell resolution. *Science*. 2018:360(6392):eaar5780. https://doi.org/10.1126/science.aar5780
33. Pai JA, Satpathy AT. High-throughput and single-cell T cell receptor sequencing technologies. *Nat Methods*. 2021:18(8):881–892. https://doi.org/10.1038/s41592-021-01201-8

Downloaded from https://academic.oup.com/jleukbio/article/114/6/630/7223408 by Universitaets-Krankenhaus Eppendorf user on 03 February 2026

Fig. S1

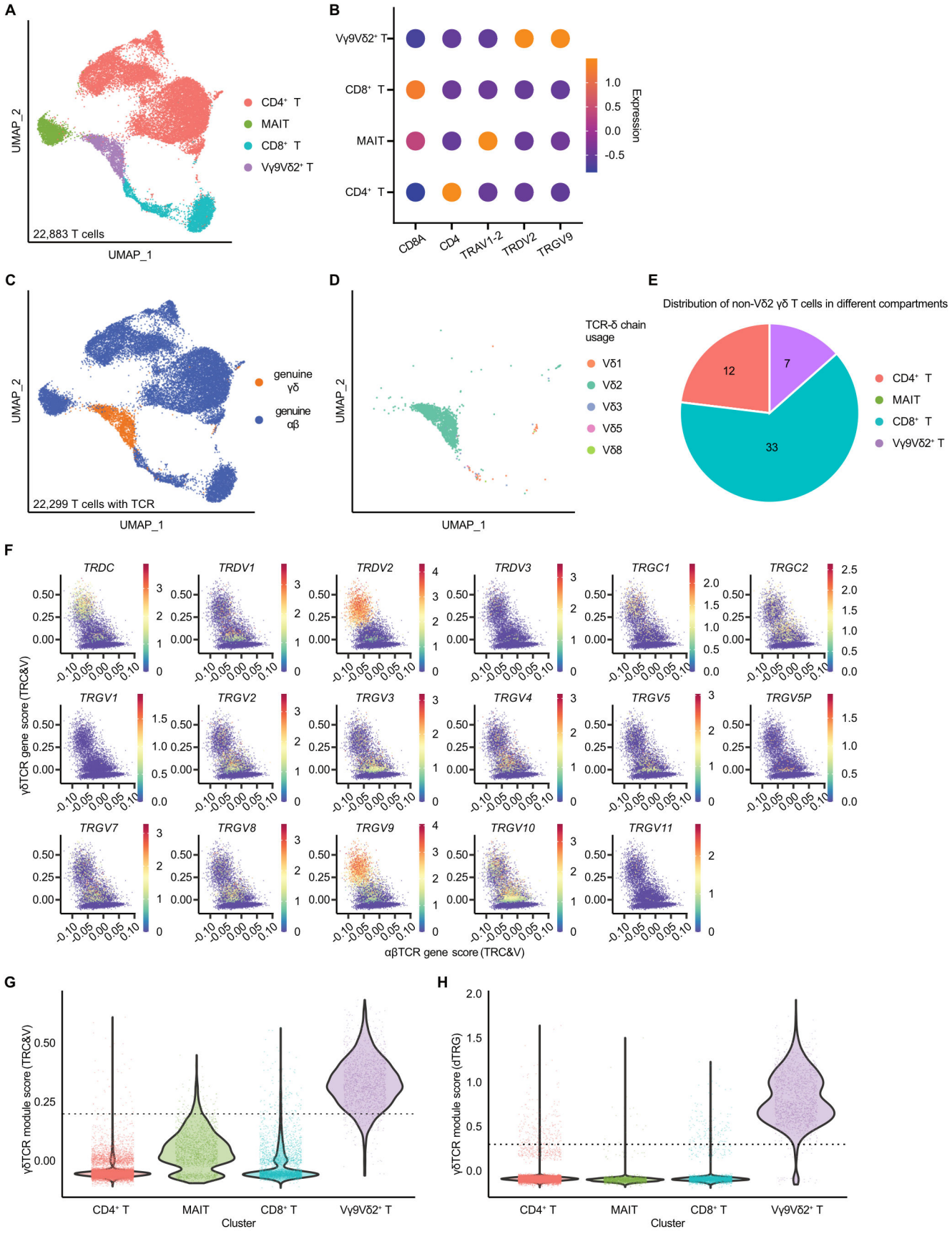

A
UMAP_2
UMAP_1
22,883 T cells
CD4⁺ T
MAIT
CD8⁺ T
Vγ9Vδ2⁺ T
B
Vγ9Vδ2⁺ T
CD8⁺ T
MAIT
CD4⁺ T
CD8A
CD4
TRAV1-2
TRDV2
TRGV9
Expression
1.0
0.5
0.0
-0.5
C
UMAP_2
UMAP_1
22,299 T cells with TCR
genuine γδ
genuine αβ
D
UMAP_2
UMAP_1
TCR-δ chain usage
Vδ1
Vδ2
Vδ3
Vδ5
Vδ8
E
Distribution of non-Vδ2 γδ T cells in different compartments
12
7
33
CD4⁺ T
MAIT
CD8⁺ T
Vγ9Vδ2⁺ T
F
TRDC
TRDV1
TRDV2
TRDV3
TRGC1
TRGC2
TRGV1
TRGV2
TRGV3
TRGV4
TRGV5
TRGV5P
TRGV7
TRGV8
TRGV9
TRGV10
TRGV11
γδTCR gene score (TRC&V)
αβTCR gene score (TRC&V)
G
γδTCR module score (TRC&V)
CD4⁺ T
MAIT
CD8⁺ T
Vγ9Vδ2⁺ T
Cluster
H
γδTCR module score (dTRG)
CD4⁺ T
MAIT
CD8⁺ T
Vγ9Vδ2⁺ T
Cluster

Fig. S2

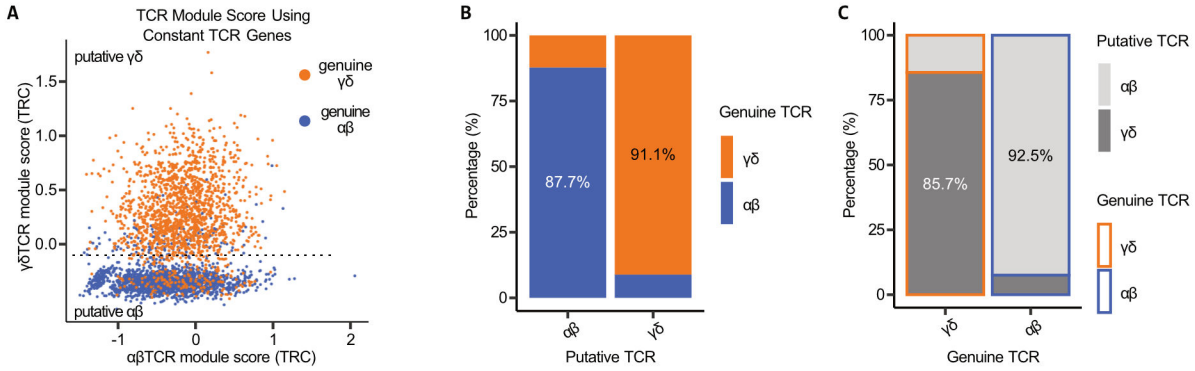

A
TCR Module Score Using
Constant TCR Genes
putative γδ
genuine
γδ
genuine
αβ
putative αβ
γδTCR module score (TRC)
αβTCR module score (TRC)
B
Percentage (%)
87.7%
91.1%
Genuine TCR
γδ
αβ
αβ
γδ
Putative TCR
C
Percentage (%)
85.7%
92.5%
Putative TCR
αβ
γδ
Genuine TCR
γδ
αβ
γδ
αβ
Genuine TCR

Fig. S3

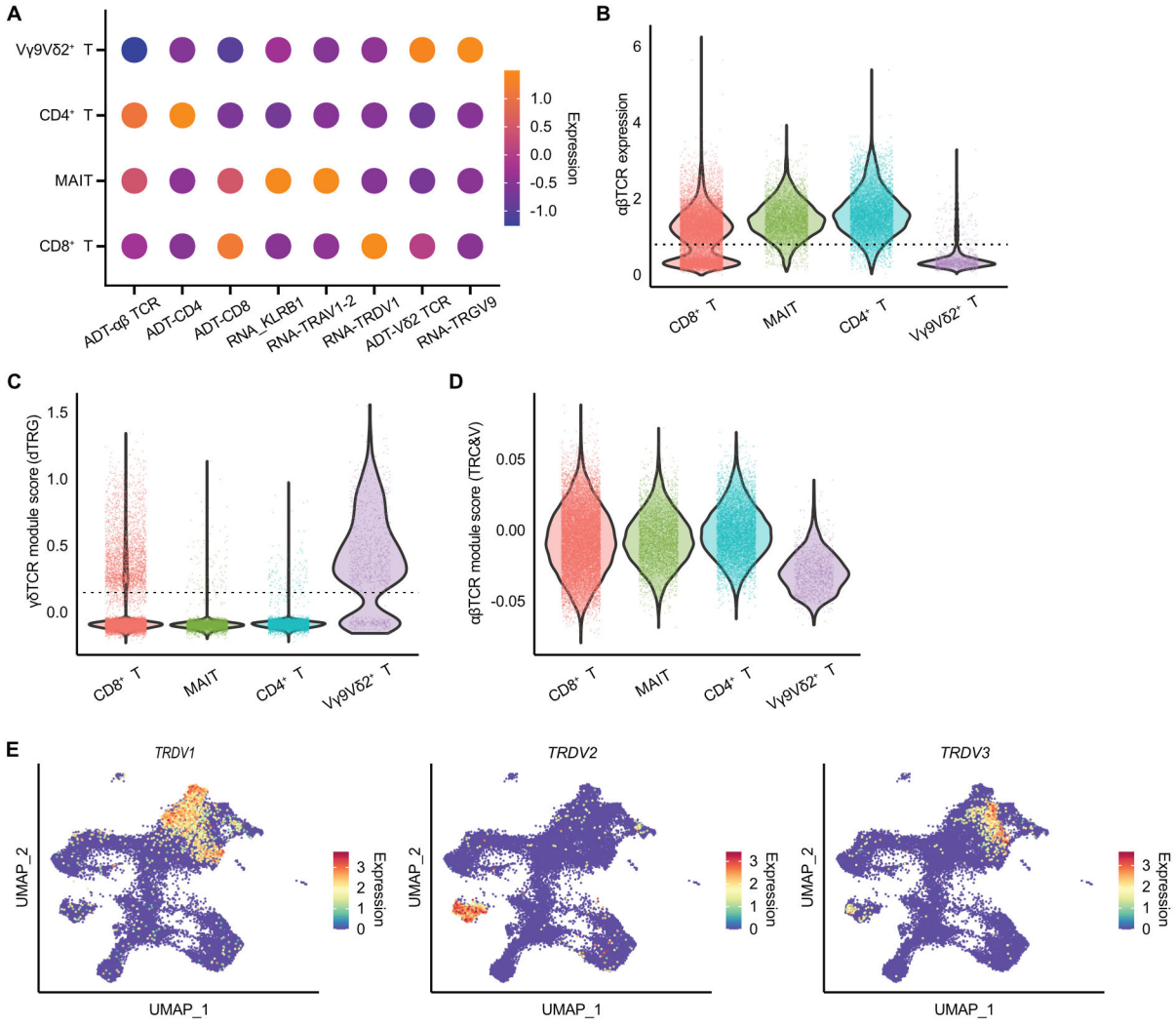

A
Vγ9Vδ2+ T
CD4+ T
MAIT
CD8+ T
ADT-αβ TCR
ADT-CD4
ADT-CD8
RNA_KLRB1
RNA-TRAV1-2
RNA-TRDV1
ADT-Vδ2 TCR
RNA-TRGV9
Expression
1.0
0.5
0.0
-0.5
-1.0
B
qβTCR expression
CD8+ T
MAIT
CD4+ T
Vγ9Vδ2+ T
C
γδTCR module score (dTRG)
D
qβTCR module score (TRC&V)
E
TRDV1
TRDV2
TRDV3
UMAP_1
UMAP_2
Expression

Fig. S4

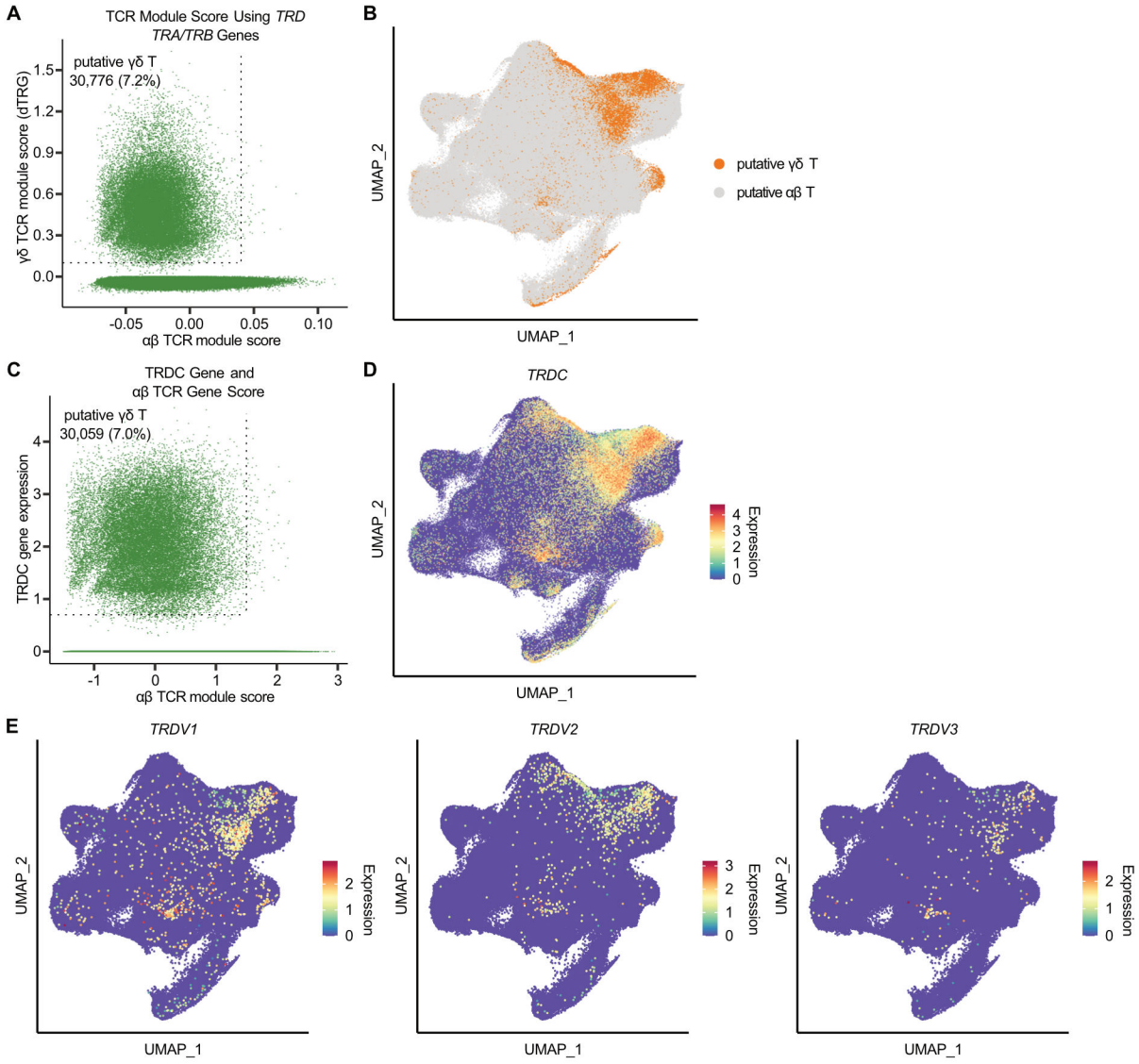
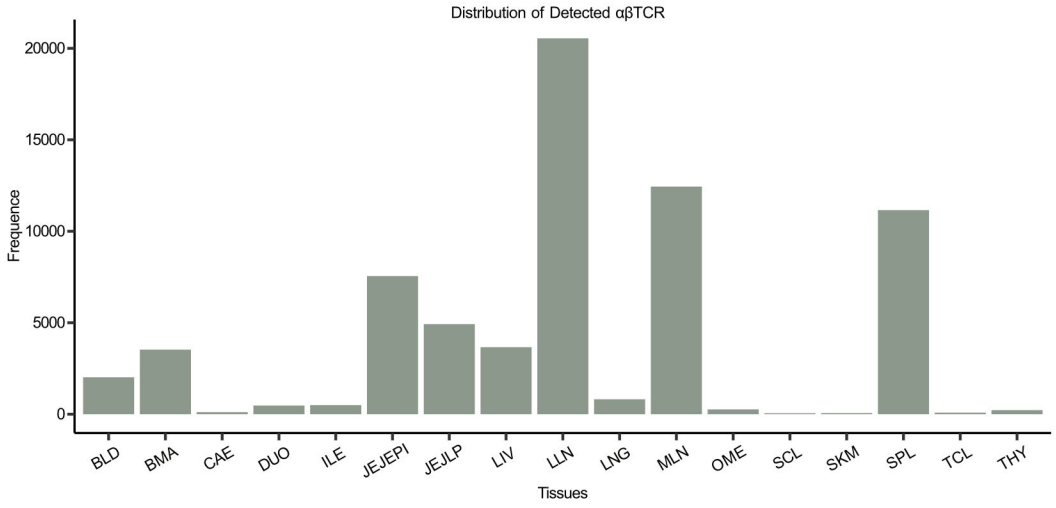

A
TCR Module Score Using TRD TRA/TRB Genes
putative γδ T
30,776 (7.2%)
γδ TCR module score (dTRG)
αβ TCR module score
B
UMAP_2
UMAP_1
putative γδ T
putative αβ T
C
TRDC Gene and αβ TCR Gene Score
putative γδ T
30,059 (7.0%)
TRDC gene expression
αβ TCR module score
D
TRDC
UMAP_2
UMAP_1
Expression
E
TRDV1
TRDV2
TRDV3
UMAP_2
UMAP_1
Expression

Fig. S5


Distribution of Detected αβTCR
Frequence
20000
15000
10000
5000
0
BLD
BMA
CAE
DUO
ILE
JEJEPI
JEJLP
LIV
LLN
LNG
MLN
OME
SCL
SKM
SPL
TCL
THY
Tissues

Supplementary figure legends

Supplementary Fig. S1 Overview of the scRNA-seq dataset on PBMC CD3$^+$ T cells

A UMAP of T cells in Fig. 1. Cells are colored by subtypes. **B** Marker gene expression of cell populations in **A**. **C** γδ and αβ T cell on UMAP. **D** TCR δ chain usage of γδ T cells. Cells are colored by indicated TCR δ chain. **E** Number of non-Vγ9Vδ2 γδ T cells distributed in each clusters. **F** Gene expression of indicated γδTCR genes. **G,H** Violin plots showing the γδTCR and αβTCR score for each clusters. The dashed line indicates the cutoff for annotating putative γδ T cells in **Fig. 1**.

Supplementary Fig. S2 TCR gene module score on constant TCR genes

A-C T cells in **Fig. 2** on TCR module scores calculated based on the constant TCR genes. Dashed line in **A** is the cutoff for annotating putative γδ T cells.

Supplementary Fig. S3 Overview of the 5' end scRNA-seq dataset on human liver perfusates CD3$^+$ T lymphocytes

A Marker gene and protein expression on cell populations in **Fig. 3**. **B-D** Violin plots showing the expression αβTCR protein, γδTCR module score, and αβTCR module score of cell populations. Dashed line indicates the cutoff for annotating cell type in **Fig. 3**. **E** *TRDV1, TRDV2, TRDV3* expression on UMAP.

Supplementary Fig. S4 Overview of the 3' end scRNA-seq dataset on primary liver cancer infiltrated CD3$^+$ T lymphocytes

A T cells in **Fig. 4** on TCR module scores calculated based on the TRC and TRV genes. **B** Putative γδ T cells on UMAP. **C** T cells in **A** on TCR module scores

calculated based on the TRC genes. **D-E** *TRDC, TRDV1, TRDV2, TRDV3* gene expression on UMAP.

Supplementary Fig. S5 Tissue distribution of detected αβTCR.

Table.S1: Gene lists used for calculation of αβTCR module score and γδTCR module score

Gene lists for **Fig. 1B**

αβTCR module score (TRC)

TRBC1 *TRBC2* *TRAC*

γδTCR module score (TRC)

TRGC1 *TRGC2* *TRDC*

Gene lists for **Fig. 1E**

αβTCR module score (TRC&V)

TRBV1	*TRBV6-5*	*TRBV15*	*TRAV4*	*TRAV17*	*TRAV39*
TRBV2	*TRBV7-4*	*TRBV16*	*TRAV5*	*TRAV18*	*TRAV40*
TRBV3-1	*TRBV5-4*	*TRBV18*	*TRAV6*	*TRAV19*	*TRAV41*
TRBV4-1	*TRBV6-6*	*TRBV19*	*TRAV8-1*	*TRAV20*	*TRAC*
TRBV5-1	*TRBV7-5*	*TRBV20-1*	*TRAV9-1*	*TRAV21*	*TRAV11*
TRBV6-1	*TRBV5-5*	*TRBV21-1*	*TRAV10*	*TRAV22*	*TRBV22-1*
TRBV7-1	*TRBV6-7*	*TRBV23-1*	*TRAV12-1*	*TRAV23DV6*	*TRAV7*
TRBV4-2	*TRBV7-6*	*TRBV24-1*	*TRAV8-2*	*TRAV24*	*TRAV33*
TRBV6-2	*TRBV5-6*	*TRBV25-1*	*TRAV8-3*	*TRAV25*	
TRBV7-2	*TRBV6-8*	*TRBV27*	*TRAV13-1*	*TRAV26-1*	
TRBV6-4	*TRBV7-7*	*TRBV28*	*TRAV12-2*	*TRAV27*	
TRBV7-3	*TRBV5-7*	*TRBV29-1*	*TRAV8-4*	*TRAV29DV5*	
TRBV5-3	*TRBV7-9*	*TRBC1*	*TRAV8-5*	*TRAV30*	
TRBV9	*TRBV13*	*TRBC2*	*TRAV13-2*	*TRAV26-2*	
TRBV10-1	*TRBV10-3*	*TRBV30*	*TRAV14DV4*	*TRAV34*	
TRBV11-1	*TRBV11-3*	*TRBV20OR9-2*	*TRAV9-2*	*TRAV35*	
TRBV12-1	*TRBV12-3*	*TRAV1-1*	*TRAV15*	*TRAV36DV7*	
TRBV10-2	*TRBV12-4*	*TRAV1-2*	*TRAV12-3*	*TRAV37*	
TRBV11-2	*TRBV12-5*	*TRAV2*	*TRAV8-6*	*TRAV38-1*	
TRBV12-2	*TRBV14*	*TRAV3*	*TRAV16*	*TRAV38-2DV8*	

γδTCR module score (TRC&V)

TRGC2	*TRGC1*	*TRGV11*	*TRGV10*	*TRGV9*	*TRGVA*
TRGV8	*TRGV7*	*TRGV5P*	*TRGV5*	*TRGV4*	*TRGV3*
TRGV2	*TRGV1*	*TRDV1*	*TRDV2*	*TRDC*	*TRDV3*
TRGV6					

Gene list for **Fig. 1H**

αβTCR module score (TRC&V)

TRBV1	*TRBV6-5*	*TRBV15*	*TRAV4*	*TRAV17*	*TRAV39*
TRBV2	*TRBV7-4*	*TRBV16*	*TRAV5*	*TRAV18*	*TRAV40*
TRBV3-1	*TRBV5-4*	*TRBV18*	*TRAV6*	*TRAV19*	*TRAV41*
TRBV4-1	*TRBV6-6*	*TRBV19*	*TRAV8-1*	*TRAV20*	*TRAC*
TRBV5-1	*TRBV7-5*	*TRBV20-1*	*TRAV9-1*	*TRAV21*	*TRAV11*
TRBV6-1	*TRBV5-5*	*TRBV21-1*	*TRAV10*	*TRAV22*	*TRBV22-1*
TRBV7-1	*TRBV6-7*	*TRBV23-1*	*TRAV12-1*	*TRAV23DV6*	*TRAV7*
TRBV4-2	*TRBV7-6*	*TRBV24-1*	*TRAV8-2*	*TRAV24*	*TRAV33*
TRBV6-2	*TRBV5-6*	*TRBV25-1*	*TRAV8-3*	*TRAV25*	
TRBV7-2	*TRBV6-8*	*TRBV27*	*TRAV13-1*	*TRAV26-1*	
TRBV6-4	*TRBV7-7*	*TRBV28*	*TRAV12-2*	*TRAV27*	
TRBV7-3	*TRBV5-7*	*TRBV29-1*	*TRAV8-4*	*TRAV29DV5*	

TRBV5-3	*TRBV7-9*	*TRBC1*	*TRAV8-5*	*TRAV30*
TRBV9	*TRBV13*	*TRBC2*	*TRAV13-2*	*TRAV26-2*
TRBV10-1	*TRBV10-3*	*TRBV30*	*TRAV14DV4*	*TRAV34*
TRBV11-1	*TRBV11-3*	*TRBV20OR9-2*	*TRAV9-2*	*TRAV35*
TRBV12-1	*TRBV12-3*	*TRAV1-1*	*TRAV15*	*TRAV36DV7*
TRBV10-2	*TRBV12-4*	*TRAV1-2*	*TRAV12-3*	*TRAV37*
TRBV11-2	*TRBV12-5*	*TRAV2*	*TRAV8-6*	*TRAV38-1*
TRBV12-2	*TRBV14*	*TRAV3*	*TRAV16*	*TRAV38-2DV8*

γδTCR module score (dTRG)

TRDV1	*TRDV2*	*TRDC*	*TRDV3*

Gene lists for **Fig. S2A**

αβTCR module score (TRC)

TRBC1	*TRBC2*	*TRAC*

γδTCR module score (TRC)

TRGC2	*TRGC1*	*TRDC*

Gene lists for **Fig. 2C**

αβTCR module score (TRC&V)

TRBV2	*TRBV5-6*	*TRBV29-1*	*TRAV13-2*	*TRAV34*
TRBV3-1	*TRBV7-7*	*TRBC1*	*TRAV14DV4*	*TRAV35*
TRBV4-1	*TRBV7-9*	*TRBC2*	*TRAV9-2*	*TRAV36DV7*
TRBV5-1	*TRBV13*	*TRBV30*	*TRAV12-3*	*TRAV38-1*
TRBV6-1	*TRBV10-3*	*TRAV1-1*	*TRAV8-6*	*TRAV38-2DV8*
TRBV4-2	*TRBV11-3*	*TRAV1-2*	*TRAV16*	*TRAV39*
TRBV6-2	*TRBV12-3*	*TRAV2*	*TRAV17*	*TRAV41*
TRBV7-2	*TRBV12-4*	*TRAV3*	*TRAV18*	*TRAC*
TRBV6-4	*TRBV12-5*	*TRAV4*	*TRAV19*	*TRBV5-3*
TRBV7-3	*TRBV14*	*TRAV5*	*TRAV20*	*TRBV6-8*
TRBV9	*TRBV15*	*TRAV6*	*TRAV21*	*TRAV40*
TRBV11-1	*TRBV18*	*TRAV8-1*	*TRAV22*	
TRBV11-2	*TRBV19*	*TRAV10*	*TRAV23DV6*	
TRBV12-2	*TRBV20-1*	*TRAV12-1*	*TRAV24*	
TRBV6-5	*TRBV21-1*	*TRAV8-2*	*TRAV25*	
TRBV7-4	*TRBV23-1*	*TRAV8-3*	*TRAV26-1*	
TRBV5-4	*TRBV24-1*	*TRAV13-1*	*TRAV27*	
TRBV6-6	*TRBV25-1*	*TRAV12-2*	*TRAV29DV5*	
TRBV5-5	*TRBV27*	*TRAV8-4*	*TRAV30*	
TRBV7-6	*TRBV28*	*TRAV8-5*	*TRAV26-2*	

γδTCR module score (dTRG)

TRDV1	*TRDV2*	*TRDC*	*TRDV3*

Gene lists for **Fig.3C**

αβTCR module score (TRC&V)

TRBV1	*TRBV10-2*	*TRBV12-4*	*TRBC1*	*TRAV9-1*	*TRAV20*	*TRAV38-1*
TRBV2	*TRBV11-2*	*TRBV12-5*	*TRBC2*	*TRAV10*	*TRAV21*	*TRAV38-2DV8*
TRBV3-1	*TRBV12-2*	*TRBV14*	*TRBV30*	*TRAV11*	*TRAV22*	*TRAV39*
TRBV4-1	*TRBV6-5*	*TRBV15*	*TRBV20OR9-2*	*TRAV12-1*	*TRAV23DV6*	*TRAV40*
TRBV5-1	*TRBV7-4*	*TRBV16*	*TRBV21OR9-2*	*TRAV8-2*	*TRAV24*	*TRAV41*
TRBV6-1	*TRBV5-4*	*TRBV17*	*TRBV22OR9-2*	*TRAV8-3*	*TRAV25*	*TRAC*

TRBV7-1	*TRBV6-6*	*TRBV18*	*TRBV23OR9-2*	*TRAV13-1*	*TRAV26-1*
TRBV4-2	*TRBV7-5*	*TRBV19*	*TRBV24OR9-2*	*TRAV12-2*	*TRAV8-7*
TRBV6-2	*TRBV5-5*	*TRBV20-1*	*TRBV25OR9-2*	*TRAV8-4*	*TRAV27*
TRBV7-2	*TRBV6-7*	*TRBV21-1*	*TRBV26OR9-2*	*TRAV8-5*	*TRAV28*
TRBV8-1	*TRBV7-6*	*TRBV22-1*	*TRBV29OR9-2*	*TRAV13-2*	*TRAV29DV5*
TRBV5-2	*TRBV5-6*	*TRBV23-1*	*TRAV1-1*	*TRAV14DV4*	*TRAV30*
TRBV6-4	*TRBV6-8*	*TRBV24-1*	*TRAV1-2*	*TRAV9-2*	*TRAV31*
TRBV7-3	*TRBV7-7*	*TRBV25-1*	*TRAV2*	*TRAV15*	*TRAV32*
TRBV8-2	*TRBV5-7*	*TRBVA*	*TRAV3*	*TRAV12-3*	*TRAV33*
TRBV5-3	*TRBV7-9*	*TRBV26*	*TRAV4*	*TRAV8-6*	*TRAV26-2*
TRBV9	*TRBV13*	*TRBVB*	*TRAV5*	*TRAV16*	*TRAV34*
TRBV10-1	*TRBV10-3*	*TRBV27*	*TRAV6*	*TRAV17*	*TRAV35*
TRBV11-1	*TRBV11-3*	*TRBV28*	*TRAV7*	*TRAV18*	*TRAV36DV7*
TRBV12-1	*TRBV12-3*	*TRBV29-1*	*TRAV8-1*	*TRAV19*	*TRAV37*

γδTCR module score (dTRG)

TRDV1	*TRDV2*	*TRDC*	*TRDV3*

Gene lists for **Fig. S4A**

αβTCR module score (TRC&V)

TRBV2	*TRBV5-5*	*TRBV20-1*	*TRAV9-1*	*TRAV23DV6*
TRBV3-1	*TRBV6-7*	*TRBV23-1*	*TRAV10*	*TRAV24*
TRBV4-1	*TRBV7-6*	*TRBV24-1*	*TRAV12-1*	*TRAV25*
TRBV5-1	*TRBV5-6*	*TRBV25-1*	*TRAV8-2*	*TRAV26-1*
TRBV6-1	*TRBV6-8*	*TRBV27*	*TRAV8-3*	*TRAV8-7*
TRBV7-1	*TRBV7-7*	*TRBV28*	*TRAV13-1*	*TRAV27*
TRBV4-2	*TRBV5-7*	*TRBV29-1*	*TRAV12-2*	*TRAV29DV5*
TRBV6-2	*TRBV7-9*	*TRBC1*	*TRAV8-4*	*TRAV30*
TRBV7-2	*TRBV13*	*TRBC2*	*TRAV13-2*	*TRAV26-2*
TRBV6-4	*TRBV10-3*	*TRBV30*	*TRAV14DV4*	*TRAV34*
TRBV7-3	*TRBV11-3*	*TRBV20OR9-2*	*TRAV9-2*	*TRAV36DV7*
TRBV5-3	*TRBV12-3*	*TRAV1-1*	*TRAV12-3*	*TRAV38-1*
TRBV9	*TRBV12-4*	*TRAV1-2*	*TRAV8-6*	*TRAV38-2DV8*
TRBV10-1	*TRBV12-5*	*TRAV2*	*TRAV16*	*TRAV39*
TRBV11-1	*TRBV14*	*TRAV3*	*TRAV17*	*TRAV40*
TRBV10-2	*TRBV15*	*TRAV4*	*TRAV18*	*TRAV41*
TRBV6-5	*TRBV16*	*TRAV5*	*TRAV19*	*TRAC*
TRBV7-4	*TRBV17*	*TRAV6*	*TRAV20*	
TRBV5-4	*TRBV18*	*TRAV7*	*TRAV21*	
TRBV6-6	*TRBV19*	*TRAV8-1*	*TRAV22*	

γδTCR module score (dTRG)

TRDV1	*TRDV2*	*TRDC*	*TRDV3*

Gene lists for **Fig. 4C**

αβTCR module score (TRC&V)

TRBV1	*TRBV10-2*	*TRBV12-4*	*TRBC1*	*TRAV9-1*	*TRAV20*	TRAV38-1
TRBV2	*TRBV11-2*	*TRBV12-5*	*TRBC2*	*TRAV10*	*TRAV21*	TRAV38-2DV8
TRBV3-1	*TRBV12-2*	*TRBV14*	*TRBV30*	*TRAV11*	*TRAV22*	TRAV39
TRBV4-1	*TRBV6-5*	*TRBV15*	*TRBV20OR9-2*	*TRAV12-1*	*TRAV23DV6*	TRAV40
TRBV5-1	*TRBV7-4*	*TRBV16*	*TRBV21OR9-2*	*TRAV8-2*	*TRAV24*	TRAV41
TRBV6-1	*TRBV5-4*	*TRBV17*	*TRBV22OR9-2*	*TRAV8-3*	*TRAV25*	TRAC

TRBV7-1	*TRBV6-6*	*TRBV18*	*TRBV23OR9-2*	*TRAV13-1*	*TRAV26-1*
TRBV4-2	*TRBV7-5*	*TRBV19*	*TRBV24OR9-2*	*TRAV12-2*	*TRAV8-7*
TRBV6-2	*TRBV5-5*	*TRBV20-1*	*TRBV25OR9-2*	*TRAV8-4*	*TRAV27*
TRBV7-2	*TRBV6-7*	*TRBV21-1*	*TRBV26OR9-2*	*TRAV8-5*	*TRAV28*
TRBV8-1	*TRBV7-6*	*TRBV22-1*	*TRBV29OR9-2*	*TRAV13-2*	*TRAV29DV5*
TRBV5-2	*TRBV5-6*	*TRBV23-1*	*TRAV1-1*	*TRAV14DV4*	*TRAV30*
TRBV6-4	*TRBV6-8*	*TRBV24-1*	*TRAV1-2*	*TRAV9-2*	*TRAV31*
TRBV7-3	*TRBV7-7*	*TRBV25-1*	*TRAV2*	*TRAV15*	*TRAV32*
TRBV8-2	*TRBV5-7*	*TRBVA*	*TRAV3*	*TRAV12-3*	*TRAV33*
TRBV5-3	*TRBV7-9*	*TRBV26*	*TRAV4*	*TRAV8-6*	*TRAV26-2*
TRBV9	*TRBV13*	*TRBVB*	*TRAV5*	*TRAV16*	*TRAV34*
TRBV10-1	*TRBV10-3*	*TRBV27*	*TRAV6*	*TRAV17*	*TRAV35*
TRBV11-1	*TRBV11-3*	*TRBV28*	*TRAV7*	*TRAV18*	*TRAV36DV7*
TRBV12-1	*TRBV12-3*	*TRBV29-1*	*TRAV8-1*	*TRAV19*	*TRAV37*

γδTCR module score (dTRG)

TRDV1	*TRDV2*	*TRDC*	*TRDV3*

Chapter 3: Publication in *Biomarker Research*, December 2025

Mega-scale single-cell profiling reveals novel biomarkers associated with acute GvHD after allogeneic hematopoietic stem cell transplantation

Specific contributions:

The following research article has been published in *Biomarker Research*. I am the first author of the publication. I performed the single-cell library preparation, conducted the computational analyses, generated the figures, drafted the manuscript, and contributed to the conceptual development of the study.

I, Immo Prinz, agree with the above statements as the direct supervisor.

Signature

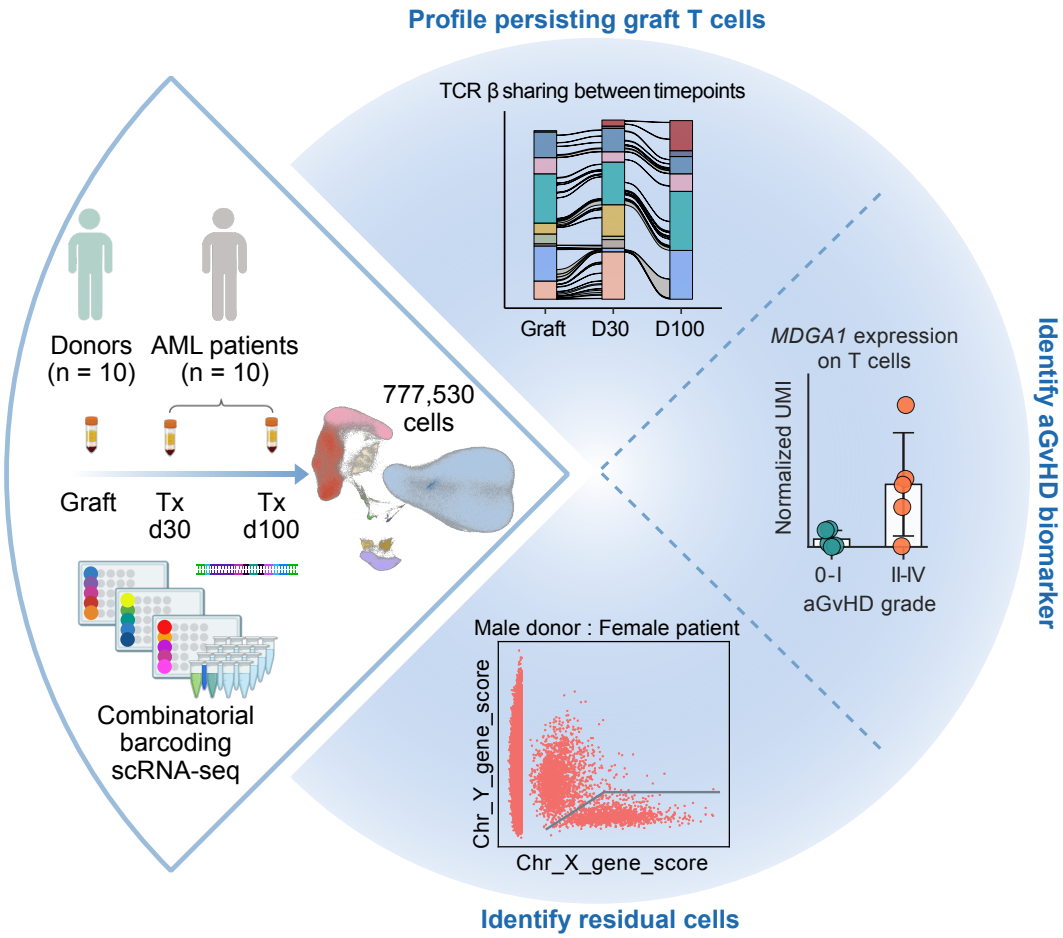
Universitätsklinikum Hamburg-Eppendorf
Hamburg Center for Translational Immunology (HCTI)
Prof. Dr. Immo Prinz
Institute of Systems Immunology
Martinistraße 52 • 20246 Hamburg • Germany
Tel.: +49 40 7410 55028 • Email: i.prinz@uke.de

Date & Place 30.03.2026, Hamburg

Graphic Abstract

Mega-scale longitudinal single-cell profiling reveals novel peripheral biomarkers associated with allogeneic stem cell transplantation outcomes

Song et al.



Song *et al. Biomarker Research* (2025) 13:155
https://doi.org/10.1186/s40364-025-00868-x

Biomarker Research

RESEARCH Open Access

Mega-scale single-cell profiling reveals novel biomarkers associated with acute GvHD after allogeneic hematopoietic stem cell transplantation

Zheng Song[1,2†], Evgeny Klyuchnikov[3†], Anita Badbaran[3], Likai Tan[4,5], Regine J. Dress[1,2], Emilia Czajkowski[1,2], Simeon Weßler[1,2], Radwan Massoud[3], Christine Wolschke[3], Anja Schimrock[6], Yu Zhang[1,2], Cedric Ly[2,7], Nico Gagelmann[3], Kristin Rathje[3], Boris Fehse[3], Stefan Bonn[2,7], Sarina Ravens[6], Nicola Gagliani[2,8,9], Christian F. Krebs[2,10,11], Ulf Panzer[2,10,11], Francis Ayuk[3], Nicolaus Kröger[3†] and Immo Prinz[1,2,6*†]

Abstract

Background Alloreactive T cells mediate graft-versus-leukemia (GvL) reactions and acute graft-versus-host disease (aGvHD) in AML patients following allogeneic hematopoietic stem cell transplantation.

Methods To investigate biomarkers that identify alloreactive T cells associated with either beneficial GvL or detrimental aGvHD, we collected graft samples and two post-transplant follow-up blood samples (day 30 and day 100) of ten AML patients undergoing hematopoietic stem cell transplantation and profiled over 777,000 $CD45^+$ leukocytes in total by combinatorial barcoding-based mega-scale single-cell RNA sequencing.

Results Using immune receptor sequences as intrinsic clonal barcodes, we observed that especially $CD8^+$ graft-derived T cells persisted and displayed enhanced proliferation, clonal expansion, and likely alloreactivity. Notably, patient-derived peripheral leukocytes that survived the conditioning, as identified by sex-chromosome-related genes, were primarily $CD4^+$ T helper cells. MDGA1 expression on T cells and NK cells emerged as a novel biomarker potentially associated with aGvHD. Additionally, we observed a significant deficiency of ADGRG1 expression, a marker of alloreactive cytotoxic T cells, by αβ and γδ T cells from relapsed patients.

Conclusions In conclusion, mega-scale single-cell monitoring of graft and hematopoietic immune cell reconstitution allowed us to demonstrate that MDGA1 and ADGRG1 may function as complementary biomarkers expressed by distinct circulating T cells that are associated with divergent outcomes in AML patients, enabling precise risk stratification of alloHSCT outcomes and presenting potential therapeutic targets.

†Zheng Song and Evgeny Klyuchnikov contributed equally to this work.

†Nicolaus Kröger and Immo Prinz are joint senior authors.

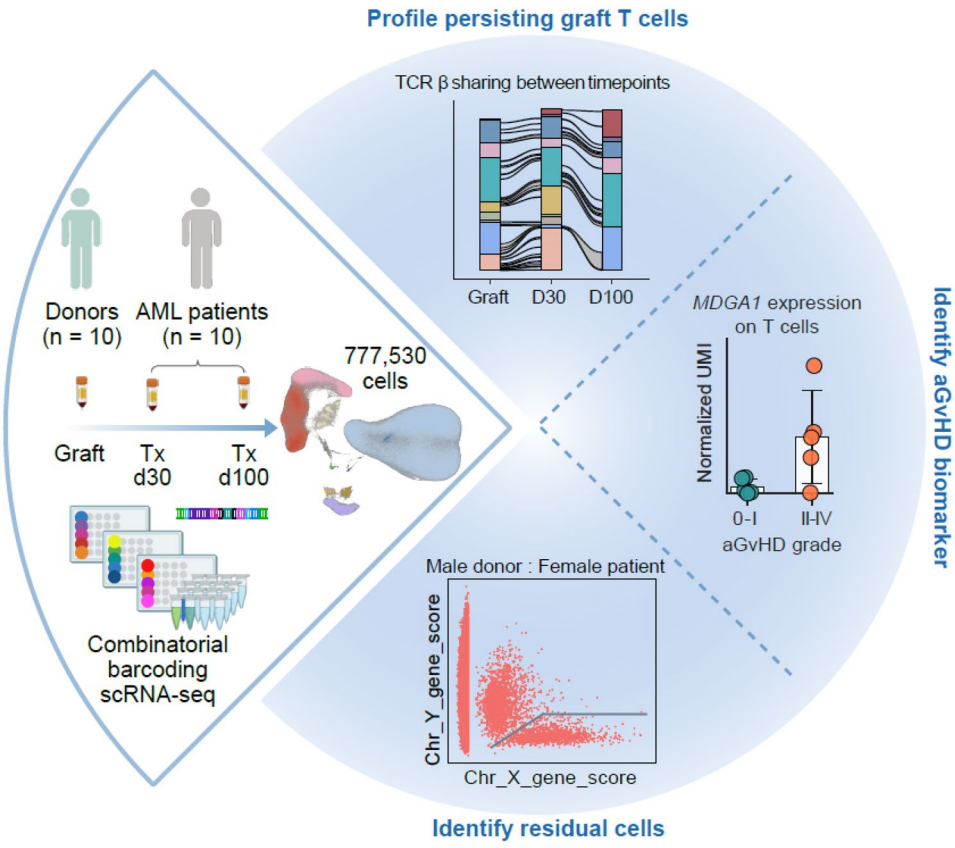
*Correspondence:
Immo Prinz
i.prinz@uke.de

Full list of author information is available at the end of the article

© The Author(s) 2025. **Open Access** This article is licensed under a Creative Commons Attribution 4.0 International License, which permits use, sharing, adaptation, distribution and reproduction in any medium or format, as long as you give appropriate credit to the original author(s) and the source, provide a link to the Creative Commons licence, and indicate if changes were made. The images or other third party material in this article are included in the article's Creative Commons licence, unless indicated otherwise in a credit line to the material. If material is not included in the article's Creative Commons licence and your intended use is not permitted by statutory regulation or exceeds the permitted use, you will need to obtain permission directly from the copyright holder. To view a copy of this licence, visit http://creativecommons.org/licenses/by/4.0/. The Creative Commons Public Domain Dedication waiver (http://creativecommons.org/publicdomain/zero/1.0/) applies to the data made available in this article, unless otherwise stated in a credit line to the data.

Keywords Mega-scale scRnAseq, AML, alloHSCT, αβ and γδ T cell persistence, aGvHD, GvL

Graphical Abstract



Background

Allogeneic hematopoietic stem cell transplantation (alloHSCT) remains the only curative therapy in acute myeloid leukemia (AML). [1] In alloHSCT, the elimination of residual leukemia cells surviving the preparative regimen is primarily driven by engrafted alloreactive lymphocytes, especially by αβ T cells through the GvL effect. [2, 3] However, alloreactive T cells responding to alloantigens and/or minor histocompatibility antigens on recipient cells are also involved in the pathogenesis of graft-versus-host disease (GvHD). [4, 5] Based on clinical symptoms, GvHD is classified as acute GvHD (aGvHD) or chronic GvHD, with aGvHD characterized by severe inflammation typically affecting the gastrointestinal tract, skin, and liver[6–8].

The failure of graft-versus-leukemia (GvL) reactivity leads to relapse (REL) which is the main cause of post-alloHSCT mortality. [9] To overcome this, clinical strategies aim at augmenting GvL while minimizing GvHD through graft composition modification. [10] However, there is a positive correlation between GvL and GvHD in AML patients. [11–13] Notably, depleting alloreactive αβ T cells from graft before infusion has shown significant improvement of the chronic GvHD-free, relapse free survival probability in pediatric leukemia patients. [14, 15] This benefit is partly attributed to natural killer (NK) cells and γδ T cells, which exert potent antileukemic effects in a major histocompatibility complex (MHC)-independent way [16–18].

Despite advancements in graft engineering, some AML patients undergoing alloHSCT treatment still relapse or develop aGvHD, highlighting the need for identifying robust biomarkers for rapid diagnosis and early interventions of alloHSCT-associated GvL and aGvHD. Recently, using single-cell RNA sequencing (scRNA-seq), *ADGRG1* (GPR56) and *ZNF683* (HOBIT) were identified as biomarkers of alloreactive $CD8^+$ cytotoxic T lymphocytes linked to effective antileukemia response, that were significantly enriched in the bone marrow of patients achieving complete remission (CR) following alloHSCT. [19–21] However, whether the predictive value of these biomarkers extends to expression by other cytotoxic T cells, such as γδ T cells, in peripheral blood remains unexplored.

Furthermore, a recent CyTOF-based study revealed that $CD11b^+$ $CD163^+$ monocytes and $CXCR3^+$ T cells appear in the blood and accumulate in the skin and gastrointestinal (GI) tract at the onset of aGvHD [22, 23], highlighting the power of high-throughput technologies in advancing biomarker discovery. Recent advances in scRNA-seq now enable large-scale, transcriptome-wide identification of novel aGvHD biomarkers across all immune cell populations in peripheral blood and biopsy samples [19–21, 24].

Methods

Clinical cohort and patient samples

Ten adult (>18y) patients with AML in complete remission who underwent alloHSCT with peripheral blood stem cell grafts (matched unrelated, $n=8$; matched related, $n=2$) in the Department for Stem Cell Transplantation of University Cancer Center Hamburg-Eppendorf from December 2021 to May 2022 were included in this study (Table 1). The study was approved by ethics commission of the Medical Chamber of Hamburg and was performed according to the approved study protocol (version 1.1 from 01.11.2021). Written informed consent was obtained from all participants. The majority of patients received myeloablative conditioning ($n=7$) with ATG-based immunoablation ($n=9$). After a median follow-up of 20 months (18–22), three patients died (relapse, $n=2$; NRM, $n=1$). The relapses occurred on days +149 and +622. Five patients developed acute GvHD (II-IV) at a median of 57 days (19–136). The eight patients remained alive in complete remission at the last follow-up.

Peripheral blood stem cell graft samples were collected at the time of transplantation and were cryopreserved on the next day. The PBMC samples of recipients were collected at day +30 (D30) and day +100 (D100) and were cryopreserved on the same or the following day. Mononuclear cells were isolated using a Ficoll gradient and cryopreserved in DMSO until they were used for single cell analysis.

scRNA-seq library preparation and sequencing

All $DAPI^-$ (Thermo Fisher Scientific Cat# D1306) (RRID:AB_2629482) live cells were sorted from frozen PBMC samples at the flow cytometry core facility of University Medical Center Hamburg-Eppendorf (RRID:SCR_017156). The sorted cells were fixed and permeabilized using Evercode™ Cell Fixation v2 (Parse Biosciences, Cat. ECF2001) following the manufacturer's protocol. Fixed cells were stored at −80 °C. All samples were then processed together to prepare single-cell libraries using one Evercode™ WT Mega v2 Kit (Parse

Table 1 A. Clinical characteristics of patients. MUD: Match unrelated donor; MRD: Match related donor; MAC: Myeloablative conditioning; RIC: Reduced-intensity conditioning; BU: Busulfan; Flu: Fludarabine; pCy: Post-transplant cyclophosphamide; TT: Thiotepa; ATG: Anti-thymocyte globulin; Treo: Treosulfan; TBI: Total body irradiation; NRM: Non-relapse mortality. B. Sample information. Available samples for the single-cell experiment are indicated

Patient	Age/sex	ELN 2022	Donor	Conditioning	Protocol	aGvHD (II-IV)	cGvHD	Relapse	NRM	Death
A										
REL_1	36/f	intermediate	MUD	MAC	Bu/Flu/pCy	no	0	yes	no	yes
REL_2	68/m	adverse	MUD	RIC	TT/Bu/ATG	yes	0	yes	no	no
CR_1	47/f	intermediate	MUD	MAC	TT/Bu/ATG	yes	moderate	no	no	no
CR_2	56/m	intermediate	MUD	RIC	TT/Bu/ATG	yes	severe	no	no	no
CR_3	38/m	favorable	MRD	MAC	TT/Bu/ATG	no	0	no	no	no
CR_4	52/f	intermediate	MUD	RIC	Treo/Flu/ATG	yes	0	no	yes	yes
CR_5	67/f	intermediate	MUD	MAC	TT/Bu/ATG	yes	0	no	yes	yes
CR_6	68/m	favorable	MUD	MAC	TBI/Flu/ATG	no	moderate	no	no	no
CR_7	68/f	intermediate	MUD	MAC	TBI/Flu/ATG	no	0	no	no	no
CR_8	30/f	favorable	MRD	MAC	TT/Bu/ATG	no	0	no	no	no

B			
Patient	Graft sample	D30 sample	D100 sample
REL_1	no	yes	yes
REL_2	yes	yes	yes
CR_1	yes	yes	yes
CR_2	yes	yes	yes
CR_3	yes	yes	yes
CR_4	yes	yes	no
CR_5	yes	yes	no
CR_6	yes	yes	no
CR_7	yes	yes	yes
CR_8	yes	yes	no

Biosciences, Cat. ECW02050), according to the manufacturer's instructions. Fifteen sub-libraries were sequenced on the Illumina NovaSeq 6000 S4 flow cell platform (RRID:SCR_016387) using PE150 chemistry with a sequencing depth of 25,000 reads per cell.

Preprocessing and dimensional reduction of scRNA-seq data

Raw fastq data were aligned to human genome assembly GRCh38 (hg38, Annotation release 109) and quantified using split-pipe software suite (Parse Biosciences, v1.1.1). The filtered feature-barcode matrices containing only cellular barcodes (Valid cell barcodes: 777 920; Median transcripts/cell: 5 931; Median genes/cell: 2 511) were used for further analysis. Single cell gene expression matrices were analyzed using Seurat (5.1.0, RRID:SCR_016341) [25]. To maximize cell retention, a relative broad threshold was first set to clean the data with n_genes < 8 500, n_transcripts < 60 000, and percent_mito < 25%. After normalization, we sketched 10 000 cells of each donor and performed integration on the sketched cells using Harmony algorithm [26] based on donors. Dimensional reduction of the integrated sketched matrix was performed using Uniform Manifold Approximation and Projection (UMAP, RRID:SCR_018217) [27] with the first 14 principal components. Clustering was done by constructing a k-nearest neighbors graph and identifying groups of cells using the original Louvain algorithm [28] with resolution of 2.0. Clusters were annotated based on the expression of canonical marker genes and three populations representing doublets (doublets number: 26,111, doublets ratio: 3.36%) were annotated.

Major immune cell populations—including T cells, NK cells, B cells, monocytes, and dendritic cells—were subset and analyzed using Scanpy (v1.10.3, RRID:SCR_018139) [29, 30]. For each subset, preprocessing was performed using stringent quality control thresholds: n_genes < 5 000, n_transcripts < 15 000, and percent_mito < 10%. Putative doublets were identified and removed using the Scrublet algorithm (RRID:SCR_018098) [31]. For each sample, the top 3000 highly variable genes (HVGs) were identified. Hemoglobin genes, unannotated genes, mitochondrial genes, heat shock proteins, and ribosomal genes were excluded from HVGs. Integration was performed based on samples using Harmony algorithm (RRID:SCR_022206) [26]. Clustering was performed by constructing a k-nearest neighbors graph (k = 10) using the first 40 principal components from Harmony-corrected embeddings. Cell clusters were identified using the Leiden algorithm [32] with a resolution of 0.6. A PAGA [33] graph was computed to infer connectivity between clusters, and UMAP [27] embedding was initialized using the PAGA positions for better preservation of global topology. Clusters were annotated based on the expression of canonical marker genes and by referencing previously published gene modules [34].

γδ T cells were distinguished from αβ T cells based on their transcriptomic profiles using an in-house developed algorithm [35] and were annotated using reference gene modules [36].

Immune repertoire reconstitution and analysis

Immune repertoire was reconstituted from transcriptome using TRUST4 algorithm (RRID:SCR_026162) [37]. Briefly, TRUST4 performed de novo assembly of V, J, and C gene segments, including the hypervariable complementarity-determining region 3 (CDR3), to generate consensus contigs of BCR/TCR sequences. These contigs were then realigned to IMGT reference gene sequences to annotate V(D)J gene usage and CDR3 features. Only functional BCR/TCR with valid cell barcodes were retained for downstream analysis. CDR3 amino acid sequences were used to define unique clonotypes. Top three clonally expanded TCR β chain were employed to perform clone-matched analysis.

Differentially expressed genes and enrichment analysis

To mitigate the 'drop-out' effect associated with lowly expressed genes in single-cell data, functional analyses of $CD8^+$ T cells were performed at the pseudo-bulk level rather than at the single-cell level. Specifically, $CD8^+$ T cells from each sample (graft and follow-up) were aggregated by summing gene-level counts to create pseudo-bulk expression profiles. Differential expression analysis (DEA) was conducted using DESeq2 (RRID:SCR_015687) [38], and functional enrichment was assessed using the Over Representation Analysis (ORA) method implemented in decoupleR (RRID:SCR_027127) [39]. Gene set activity was inferred using the Hallmark gene sets from the Molecular Signatures Database (MSigDB) (RRID:SCR_016863) [40].

Donor-recipient cell demultiplexing based on sex-specific gene expression

To distinguish recipient-derived cells in sex-mismatched post-transplant samples, demultiplexing was performed based on the expression of sex-specific genes. Expression of Y chromosome–linked genes (*UTY*, *DDX3Y*, *USP9Y*, *RPS4Y1*, *RPS4Y2*, *EIF1AY*, *KDM5D*, *PRY*, *PRY2*, *DAZ1*, *DAZ2*, *DAZ4*, *ZFY*, *AMELY*, *TBL1Y*, *PCDH11Y*) and X chromosome–linked genes (*XIST*, *TSIX*) was used to compute gene expression scores (Chr_Y_gene_score and Chr_X_gene_score) using the scanpy.tl.score_genes function from the Scanpy package. Female patient-derived (recipient) cells were identified based on low Chr_Y_gene_score and high Chr_X_gene_score.

Quantitative PCR to measure MDGA1 expression in T cells

Total RNA was extracted from sorted T cells obtained from three patients without aGvHD and four patients with aGvHD before treatment using the RNeasy Mini Kit (Qiagen, Cat. 74,106) according to the manufacturer's instructions. RNA concentration and purity were assessed using a Qubit RNA BR Assay Kit (Invitrogen, Cat. Q10210). Complementary DNA (cDNA) was synthesized from 30 ng of total RNA using the SMARTScribe Reverse Transcriptase (Takara, Cat. 639,536). Quantitative PCR (qPCR) was performed on a QuantStudio 3 Real-Time PCR System (Applied Biosystems) using PowerUp SYBR Green PCR Master Mix (Thermo Fisher Scientific, Cat. A25742). Gene-specific primers were designed to amplify MDGA1 and the housekeeping gene GAPDH as an internal control. Each reaction was run in triplicate in a total volume of 10 µL under standard cycling conditions: 95 °C for 10 min, followed by 40 cycles of 95 °C for 15 s and 60 °C for 1 min. Ct values were obtained using the QuantStudio software (v1.7). Relative MDGA1 expression was calculated using the 2^{-} ΔΔCt method, with GAPDH serving as the reference gene and the non-aGvHD group as the reference group. The sequences of qPCR primers are MDGA1_F: CATCCTG ACCGATCTCCGTG, MDGA1_R: GTAGTGGATGATG CGGGAGG, GAPDH_F: TCAAGGCTGAGAACGGGA AG, and GAPDH_R: CGCCCCACTTGATTTTGGAG.

Reanalysis of public datasets

For MS [41] dataset, processed AnnData objects were obtained from the original publications.

For the cytokine treated PBMC dataset [42], we obtained the AnnData object of all PBMCs and subset T cells. After log-normalization, the proportion of *MDGA1*$^{+}$ cells was calculated for each sample. Fold change was computed relative to the PBS-treated baseline within each donor, and $\log_2$ fold change ($\log_2$FC) values were transformed accordingly. Paired statistical comparisons between cytokine-treated and PBS-treated samples from the same donor were performed using two-tailed paired t-tests. To visualize the results, volcano plots were generated by plotting $\log_2$FC against $-\log_{10}$(p-value). Points were color-coded based on statistical significance ($p < 0.05$) and direction of change.

For the alloHSCT transplantation [43] dataset, raw matrix was obtained from the original publications and processed with the code from the authors. *ADGRG1* feature was calculated based on the top 20 upregulated genes of ADGRG1^{+} T cells (*ADGRG1*, *GZMB*, *FGFBP2*, *CX3CR1*, *GZMH*, *EFHD2*, *GNLY*, *NKG7*, *SPON2*, *CLIC3*, *PRF1*, *FCGR3A*, *ZEB2*, *KLRD1*, *TRGC2*, *S1PR5*, *CST7*, *SSBP3*, *TTC38*, *PLEK*) [21] using the *scanpy.tl.score_genes* function from the Scanpy package.

Statistical analysis

Statistical analyses were performed using using Python (v3.9.18) with the scipy package (v1.12.0) for independent and paired t-tests (ttest_ind, ttest_rel), and Mann-Whitney U test (mannwhitneyu). In Supplementary figures S3–S4, paired t-tests were conducted between selected timepoints (e.g., Graft vs. D30, D30 vs. D100, Graft vs. D100) for donors with matched samples. To control for multiple testing, Bonferroni correction was applied to adjust p-values. In Fig. 3F-G and Fig. 5A-C, two-tailed paired Student's t-tests were performed to calculate p-values. In Fig. 4A-C, Fig. 4E-F, Fig. 4H-I, Fig. 6F-H, two-tailed Student's t-tests were performed to calculate p-values.

Results

Longitudinal single-cell immune profiling of AML patients undergoing alloHSCT

To profile the immune reconstitution dynamics in AML patients post-alloHSCT, we collected 25 samples from ten patients at three timepoints: prior to graft infusion (Graft, $n = 9$), 30 days post-transplantation (D30, PBMC, $n = 10$), and 100 days post-transplantation (D100, PBMC, $n = 6$) (Table 1). During the observation period, two patients experienced relapse and five developed aGvHD (Table 1). In total, approximately ten million live immune cells were sorted and used to generate scRNA-seq libraries in a single experiment to minimize potential batch effects (Fig. 1A). After quality control, over 770,000 cells from the 25 samples were classified into eight major hematopoietic cell populations and three doublet clusters, with a median of 29,000 cells per sample (Fig. 1B; Fig. S1A-D). Following an additional round of fine-tuned quality control and doublet removal, 45 immune subtypes of αβ T cells, γδ T cells, NK cells, B cells, monocytes, and dendritic cells (DCs) were annotated based on their canonical marker genes (Fig. 1C; Fig. S2A-F).

We next examined the hematopoietic reconstitution patterns after alloHSCT. Within the lymphocyte compartment, quantitative analysis showed a gradual increase of the T cell proportions and a rapid rise in NK cell proportions especially CD56 bright populations at D30, while B cells nearly disappeared at D30 and were only slowly reconstituted at D100 (Fig. S3A, S4A-G). Monocytes accounted for a substantial proportion of the graft samples and show a trend to decrease post-alloHSCT (Fig. S3B, S4H). The overall DC proportion did not change except for an increase of preDC from D30 to D100 and a decrease of cDC1 on D30 (Fig. S3B, S4I-J). Interestingly, the hematopoietic stem cell (HSC) compartment and a population characterized by expression of *MKI67* remained constant at all timepoints (Fig. S3C-D). These findings provide a comprehensive, carefully annotated high resolution landscape of graft and immune

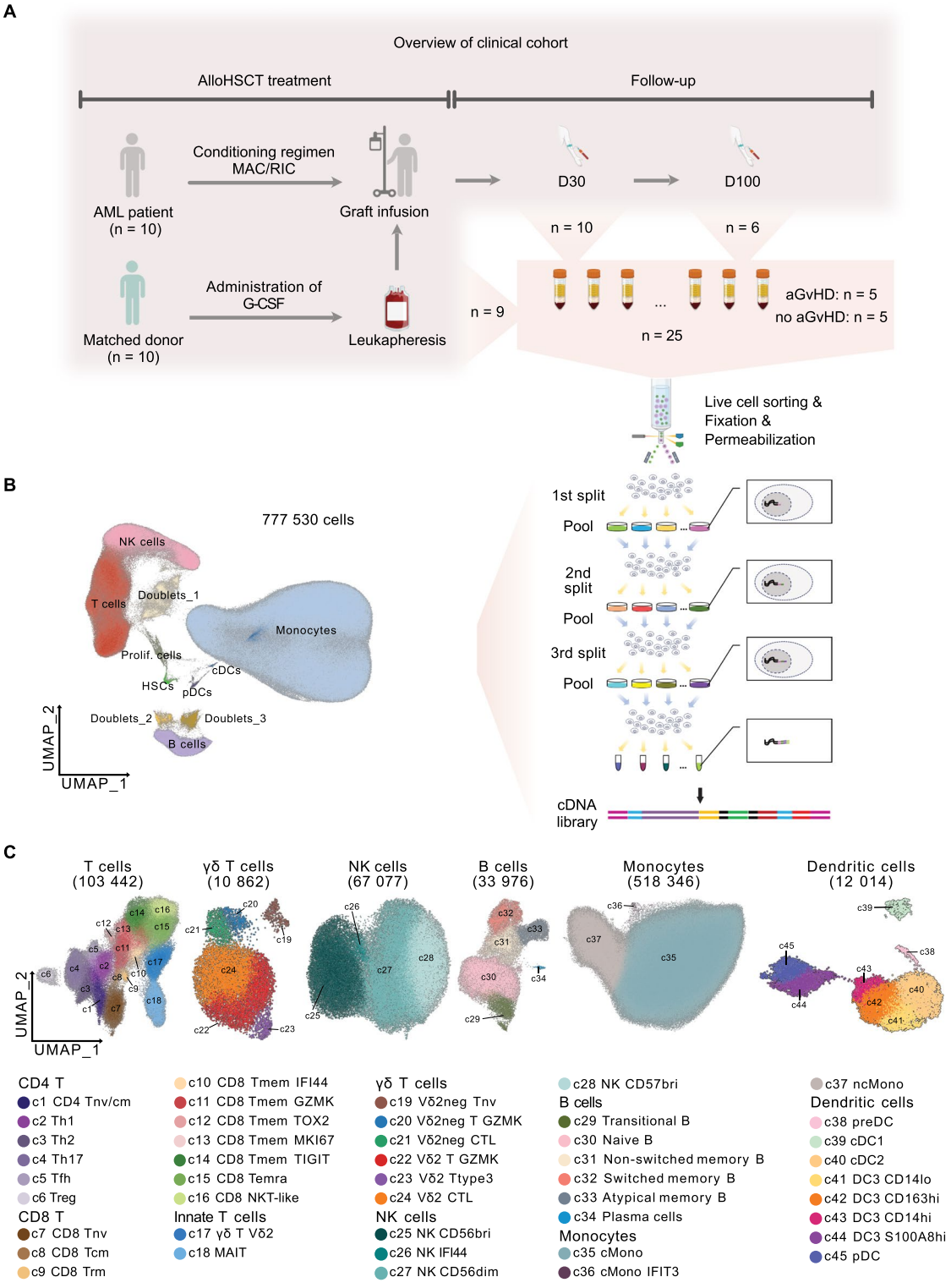


Fig. 1 Experimental design and annotation of immune cells. (**A**) Schematic experimental workflow. The number of patients and samples for each time-point are denoted. AML, acute myeloid leukemia; MAC, myeloablative conditioning; RIC, reduced intensity conditioning; aGvHD, acute graft-versus-host-disease; G-CSF, granulocytes colony stimulating factor. (**B**) Uniform Manifold Approximation and Projection (umap) of 777,530 PBMC transcriptomes (including doublets). Each dot represents a cell or a doublet and is colored based on the cell type. Prolif. cells, proliferating cells; HSCs, hemopoietic stem cells. (**C**) UMAP of T cells, γδ T cells, NK cells, B cells, monocytes, and dendritic cells (DCs) with post-QC cell number indicated. Cells are colored by subtypes and the cluster ID are shown

reconstitution in AML patients following alloHSCT treatment.

Graft-derived αβ T cells and γδ T cells persist in the host environment with activated transcriptional profiles consistent with alloreactivity

The sustained presence of engrafted immune cells in peripheral blood is a key indicator of successful hematopoietic chimerism. To track the graft-derived immune cells over time, the highly variable sequences of immune receptor genes were used as intrinsic molecular identifiers for individual T and B cell clones. We employed the TRUST4 algorithm [37] to reconstruct the αβ/γδ T cell and B cell receptor (TCR/BCR) repertoires from the transcriptomic data (Fig. S5A-C). The CDR3s of TCR β chain, TCR δ chain, and BCR heavy chain, which were distinct among individuals, were used to trace the graft-derived αβ T cells, γδ T cells, and B cells respectively (Fig. S5D-G). We consistently identified multiple shared TCR β and TCR δ clones, but no overlapping immunoglobulin heavy chain (IGH) clones in paired graft and post-alloHSCT samples from the same patients (Fig. 2A–C). These findings indicate that donor-derived αβ and γδ T cell clones persisted in the host circulation after transplantation. At the same time, no persistent donor B cell clones were detected, which is consistent with previous studies. [43–45] The presence of shared TCR clones between graft and post-transplant time points confirmed successful long-term survival of donor T cells.

The most prominent persisting engrafted T cell clones were $CD8^+$ T cells. To further characterize their phenotype and differentiation in the host environment, we monitored their clonal expansion and differential gene expression post-alloHSCT. Clone-matched analysis of the top three most expanded TCR β clones revealed expansion and phenotypic conversion of $CD8^+$ T cell clones to proliferating $CD8^+$ memory or terminally differentiated Temra T cells after alloHSCT (Fig. 2D; Fig. S5H-J). Concurrently, genes upregulated in post-alloHSCT $CD8^+$ T cells were significantly enriched in cell cycle–related and metabolic pathways, indicating an antigen-experienced, activated status of these graft-derived T cells (Fig. 2E–G). Taken together, these results suggest that persistent donor T cells receive ongoing TCR-mediated signals within the host immune environment and are potentially alloreactive. However, homeostatic proliferation and responses to viral reactivation may also contribute to activation of persisting donor T cells.

Some host-derived T cells survive conditioning and alloHSCT treatment

Measurable (minimal) residual disease (MRD) is a strong indicator of the risk of relapse of AML patients after alloHSCT treatment. We thus employed the single nucleotide polymorphism-based demultiplexing algorithm-souporcell [46] to find potential host-derived MRD, however we did not detect re-appearing leukemia cells using this tool. However, we could successfully use sex-chromosome-related genes to distinguish the cell origin in female patients who received the male-derived grafts (Fig. 3A). Compared with the cells from male patients who received male grafts, we observed a distinct cell population comprising 1,087 cells characterized with high chromosome X gene score and low chromosome Y gene score (Fig. 3A–C). Notably, 98.4% (1,070 of 1,087 cells) of these cells originated from post-transplantation samples, which served as an internal control validating our method to detect residual host leukocytes (Fig. S6A). After excluding the 17 graft-derived cells as false-positive the remaining 1,064 cells were classified as residual host cells for downstream analysis (Fig. 3C; Fig. S6B). Across all samples, residual host cells predominantly consisted of T cells (Fig. 3D; Fig. S6C). Within these residual T cell populations, we observed a dominant proportion of $CD4^+$ T cells relative to $CD8^+$ T cells—opposite to the distribution seen in donor-derived T cells (Fig. 3E–F). In particular, terminally differentiated and proliferative $CD8^+$ T cell subsets were missing within the host-derived compartment (Fig. 3G). Collectively, high-throughput scRNA-seq analysis reliably identified residual female host cells in the peripheral blood following male-to-female alloHSCT, revealing that the T cell composition of host-derived cells was distinctly different from that of engrafted donor T cells.

MDGA1 marks aGvHD-associated T cells

AlloHSCT-associated aGvHD is a systemic inflammatory syndrome triggered by tissue damage from the conditioning regimen and subsequently sustained by donor-derived T cells [47]. First, we systematically compared the abundance of distinct T cell subset between two aGvHD outcomes and observed a relative decrease inTreg cells, naive $CD8^+$ cells, and $CD8^+$ Tmem $TIGIT^+$ populations in aGvHD patients at D30 (Fig. 4A–B). The latter population is characterized by upregulation of exhaustion markers *TIGIT* and *TOX* with reduced cytotoxic gene expression like *GZMB*, *PRF1*, and *CX3CR1* while maintaining the expression of memory markers including *TCF7*, and *SELL* (Fig. S2A). These $CD8^+$ $TIGIT^+$ Tmem cells have been described as an exhausted yet persistent subset that may play a regulatory role during chronic antigen exposure. Their relative depletion may contribute to unchecked immune activation in aGvHD, although this remains speculative and warrants functional validation. Meanwhile, we observed a larger population of naïve $CD8^+$ Tnv in aGvHD patients at D30, although the difference was not statistically significant (Fig. 4C). Next, we investigated whether in contrast to the subtle

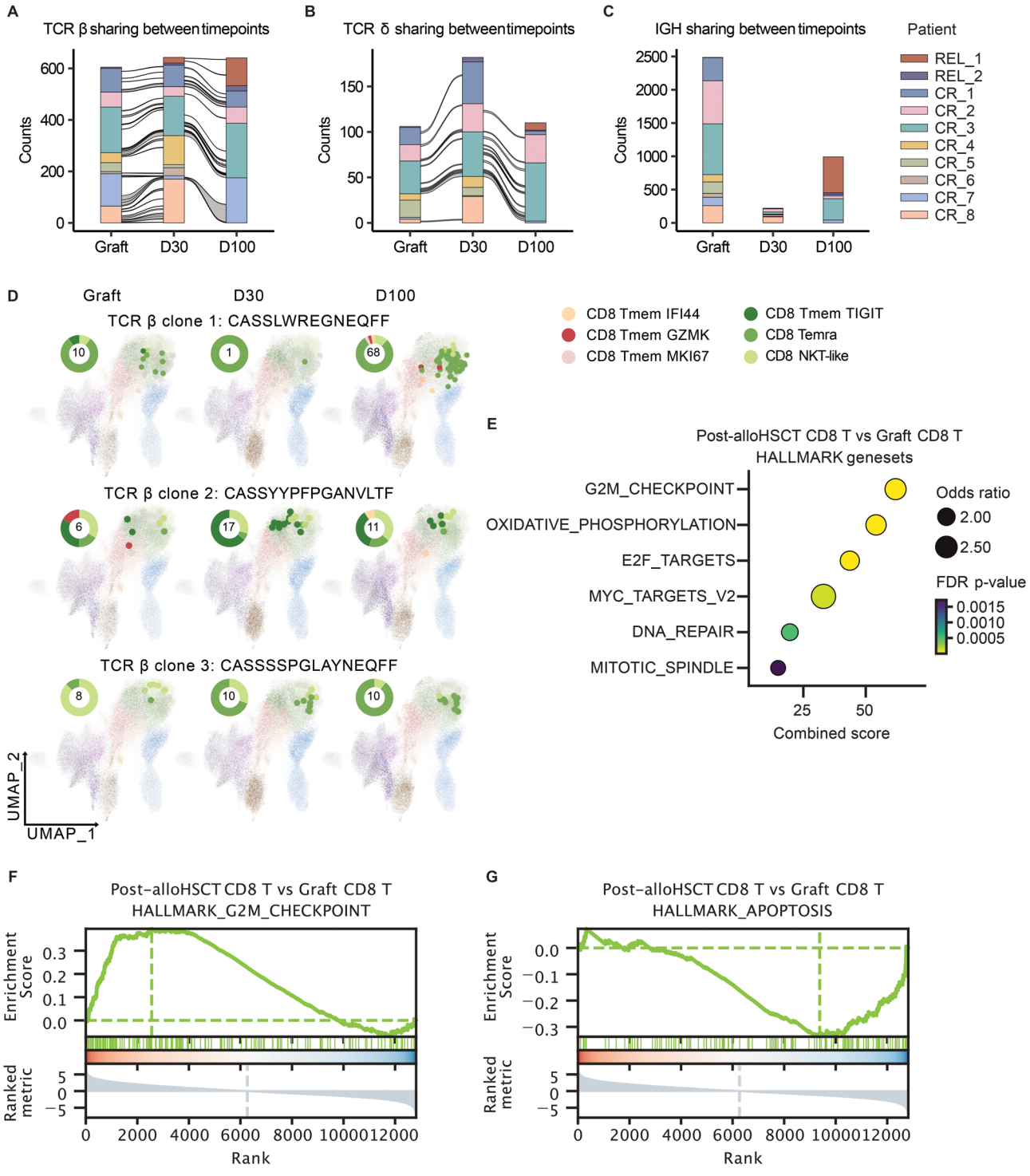


Fig. 2 Comparison of immune repertoire overlap and differentially expressed genes of CD8$^+$ T cells between graft and follow-up samples. (**A-C**) the Complementary Determined Region 3 sequences (CDR3s) of T Cell Receptor (TCR) beta chain (**A**), TCR delta chain (**B**), and **B** Cell Receptor (BCR) heavy chain (**C**) are used to show the overlap of immune repertoire between different timepoints. (**D**) the three hyperexpanded TCR beta clones are shown on the T cell umap at three timepoints. Cells are colored by T cell subtypes. Pie plots on the shoulder are colored by the subtypes of T cells with indicated clones. The number shows the total T cell number with indicated clones at indicated timepoint.(**E**) Pathway analysis of differentially expressed genes of CD8$^+$ T cells. (**F-G**) Enrichment of cell cycle and apoptosis gene signatures on CD8$^+$ T cells

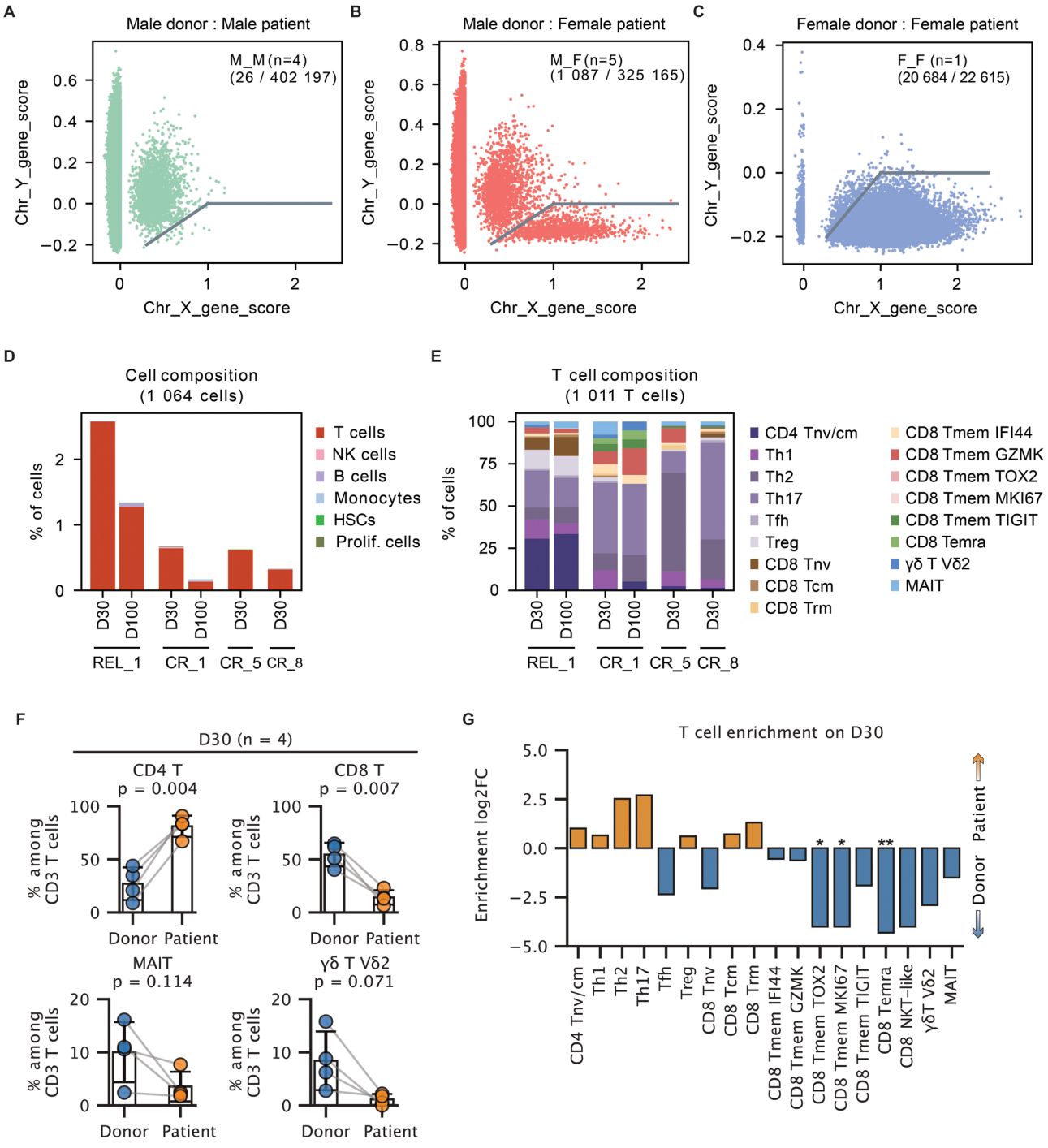


Fig. 3 Characteristics of residual host cells in peripheral blood. (**A-C**) Chromosome X and chromosome Y related gene scores of all cells (doublets excluded) from 4 male-to-male transplantation (**A**), 5 female-to-male transplantation (**B**) patients and 1 female-to-female transplantation (**C**) patients. The female cells are gated. (**D**) Cell composition of major immune cell types from female patients gated in (**B**). Total cell counts per type are indicated. (**E**) T cell subtype composition from female patients gated in (**B**). Total cell counts per subtype are indicated. (**F**) Comparison of T cell population between donor- and patient-derived cells (patient-derived cells were gated in **B**, **D**, **E**). P-values were calculated using a two-sided paired Student's t-test. (**G**) Differential abundance of T cell subtypes between four paired donor and patient (as indicated in **F**) at Day 30. Bars represent log2 Fold changes, with colors indicating cell origin. P-values were calculated using a two-sided paired Student's t-test. $p < 0.05$ (*); $P < 0.01$ (**)

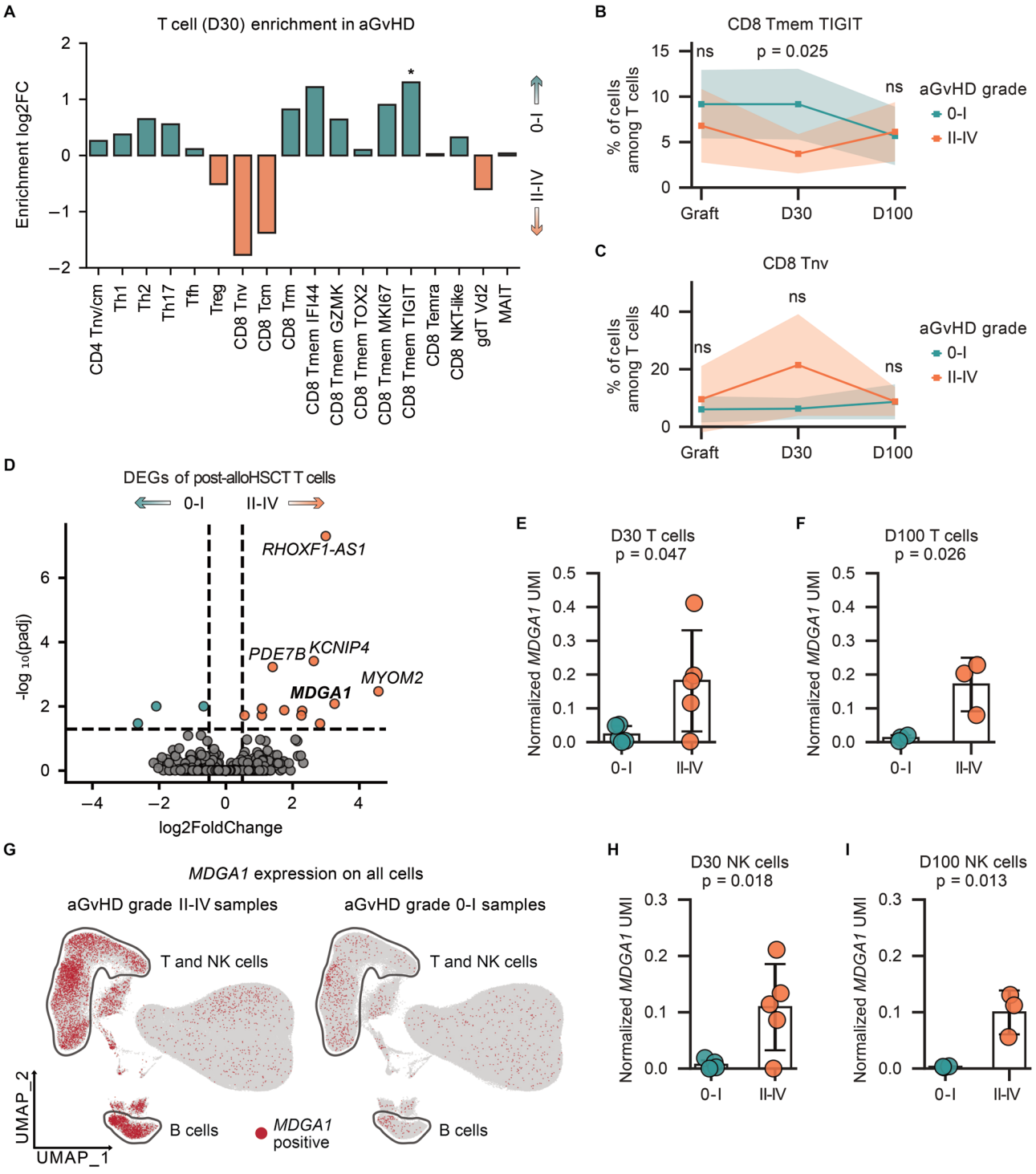


Fig. 4 Identification of *MDGA1*$^{+}$ T cells as a biomarker associated with aGvHD. (**A**) Differential abundance of T cell subtypes between different aGvHD outcomes at Day 30. Bars represent log2 Fold changes, with colors indicating aGvHD outcomes. P-values were calculated using a two-sided Student's t-test. $p < 0.05$ (*). (**B-C**) Comparison of CD8 Tmem TIGIT (**B**) and CD8 Tnv (**C**) cells between different aGvHD outcomes over three timepoints. Lines are colored by aGvHD outcomes. P-values were calculated using a two-sided Student's t-test. Not significant (ns). (**D**) Differentially expressed genes of post-alloHSCT T cells between different aGvHD outcomes. Dots are colored by aGvHD outcomes. (**E-F**) Comparison of normalized *MDGA1* UMIs of T cells between different aGvHD outcome at D30 (**E**) and D100 (**F**). Each dot represents one patient. P-values were calculated using a two-sided Student's t-test. (**G**) Distribution of *MDGA1*-positive cells on the UMPA of all cells from aGvHD grade II-IV (left) and 0-I (right) samples. T and NK cells, B cells are indicated. (**H-I**) Comparison of normalized *MDGA1* UMIs of NK cells between different aGvhd outcome at D30 (**H**) and D100 (**I**). Each dot represents one patient. P-values were calculated using a two-sided Student's t-test. P-values were calculated using a two-sided Student's t-test

differences in cell population frequencies between different outcomes, aGvHD-driven systemic inflammation may exert a broader impact on the entire T cell compartment. To further identify potential cellular biomarkers, we directly compared the differentially expressed genes (DEG) of T cells and identified several upregulated genes in the aGvHD group, such as *PDE7B*, *MYOM2*, *KCNIP4*, and *MDGA1* (Fig. 4D). Of those genes, only *MDGA1* showed consistent and significant upregulation in all post-alloHSCT samples from aGvHD patients without individual dominance (Fig. 4E–F). MDGA1 encodes a glycosylphosphatidylinositol (GPI)-anchored cell surface glycoprotein, of which the function of in the immune system is currently unknown. We found that MDGA1 was exclusively expressed by lymphocytes including T cells and B cells, but barely by myeloid cells (Fig. 4G). Notably, *MDGA1* expression on NK cells was also significantly upregulated in aGvHD patients (Fig. 4H–I). Together, these data suggest that *MDGA1* expression by lymphocytes may be a candidate novel biomarker of aGvHD-associated inflammation. Nevertheless, although none of the patients included in this cohort experienced significant viral reactivation of CMV, EBV, HHV6, HSV or bacterial infection within the observation period, it is conceivable that responses to other pathogens may contribute to induce MDGA1 expression.

MDGA1 expression is induced by proinflammatory cytokines

Next, we hypothesized that *MDGA1* expression at the onset of aGvHD would be regulated by inflammatory cytokines. To validate this, we reanalyzed a publicly available scRNA-seq dataset which contains 10 million PBMCs from twelve healthy female and male donors treated with 90 different cytokines for 24 hours [42]. By systematically comparing the frequencies of *MDGA1* positive T in cytokine treated samples with PBS treated samples, we observed that treatment with pro-inflammatory cytokines such as IL-12, interferons, and TL1A consistently induced the expression of *MDGA1* on $CD4^+$, $CD8^+$, and NK cells. Conversely, anti-inflammatory cytokines such as IL-4, IL-1Ra, IL-10, and TGF-beta1 significantly downregulated the expression of *MDGA1* expression on T cells (Fig. 5A–B, Fig. S7A-B). Furthermore, we sought to validate the upregulation of *MDGA1* expression in T cells of aGvHD patients in an exploratory in vitro assay. Quantitative real time PCR analysis of sorted $CD3^+$ cells showed indeed higher expression in T cells derived from alloHSCT-associated aGvHD (Fig. S8). To additionally validate *MDGA1* expression as a biomarker for other inflammatory diseases, we analyzed a large publicly available single-cell dataset of PBMCs from multiple sclerosis (MS) patients [41]. Consistently with our data, we noticed an increased expression of *MDGA1* on T cells in MS as compared to control samples (Fig. 5D). Together, these results support the hypothesis that inflammatory cytokines induce *MDGA1* expression on peripheral lymphocytes during aGvHD, with some patients exhibiting early upregulation prior to clinical onset, suggesting—though not definitively proving—a potential role in the preclinical phase of GvHD.

ADGRG1 marks GvL-associated cytotoxic T cells

Given recent evidences identifying *ADGRG1* (GPR56) and *ZNF683* (HOBIT) as biomarkers of alloreactive cytotoxic T lymphocytes mediating GvL in the bone marrow [19, 21], we investigated whether these markers were similarly informative in peripheral blood. We firstly compared the expression patterns of *ADGRG1* and *ZNF683* with those of classical cytotoxic genes in peripheral blood $CD3^+$ T cells and observed that *ADGRG1* consistently marked cytotoxic αβ T and γδ T cells (Fig. 6A–E, Fig. S9A-E). These findings indicate that *ADGRG1* functions as a shared marker for both cytotoxic αβ T and γδ T cells in the peripheral blood of AML patients.

To explore if *ADGRG1* expression on the peripheral T cells is associated with the remission status, we calculated the gene module score of *ADGRG1* using the top 20 upregulated genes of $ADGRG1^+$ T cells identified in the bone marrow of AML patients. [21] To overcome the limited number of relapse patients in our cohort ($n = 2$), we incorporated a publicly available scRNA-seq dataset analyzing the graft and PBMCs at day 100 after alloHSCT. [43] That study by Obermayer et al. included single cell analysis of five alloHSCT patients treated for heterogenous underlying leukemia diseases, see supplementary table S3. Combined exploratory validation analysis suggested that the *ADGRG1* gene feature of $CD8^+$ αβ T and γδ T was significantly reduced in patients who relapsed later (Fig. 6F). However, the *ADGRG1* gene feature of $CD8^+$ αβ T and γδ T are not associated with aGvHD (Fig. 6G–H). These data are consistent with a recent report on bone marrow T cell signatures [21] and collectively suggest that *ADGRG1* expression of circulating cytotoxic T cells also is a potential biomarker of effective GvL responses in AML patients following alloHSCT.

Discussion

AlloHSCT remains the standard of care for AML patients, but the lack of robust biomarkers for rapid diagnosis of complications, including GvHD, and risk stratification limits timely intervention and affects the optimization of clinical outcomes. In this study, we used a cutting-edge ultra-high throughput scRNA-seq strategy to profile the reconstituted immune system at single-cell resolution in AML patients. This allowed us to dynamically and longitudinally track the entire engrafted immune cell landscape and explore the association of

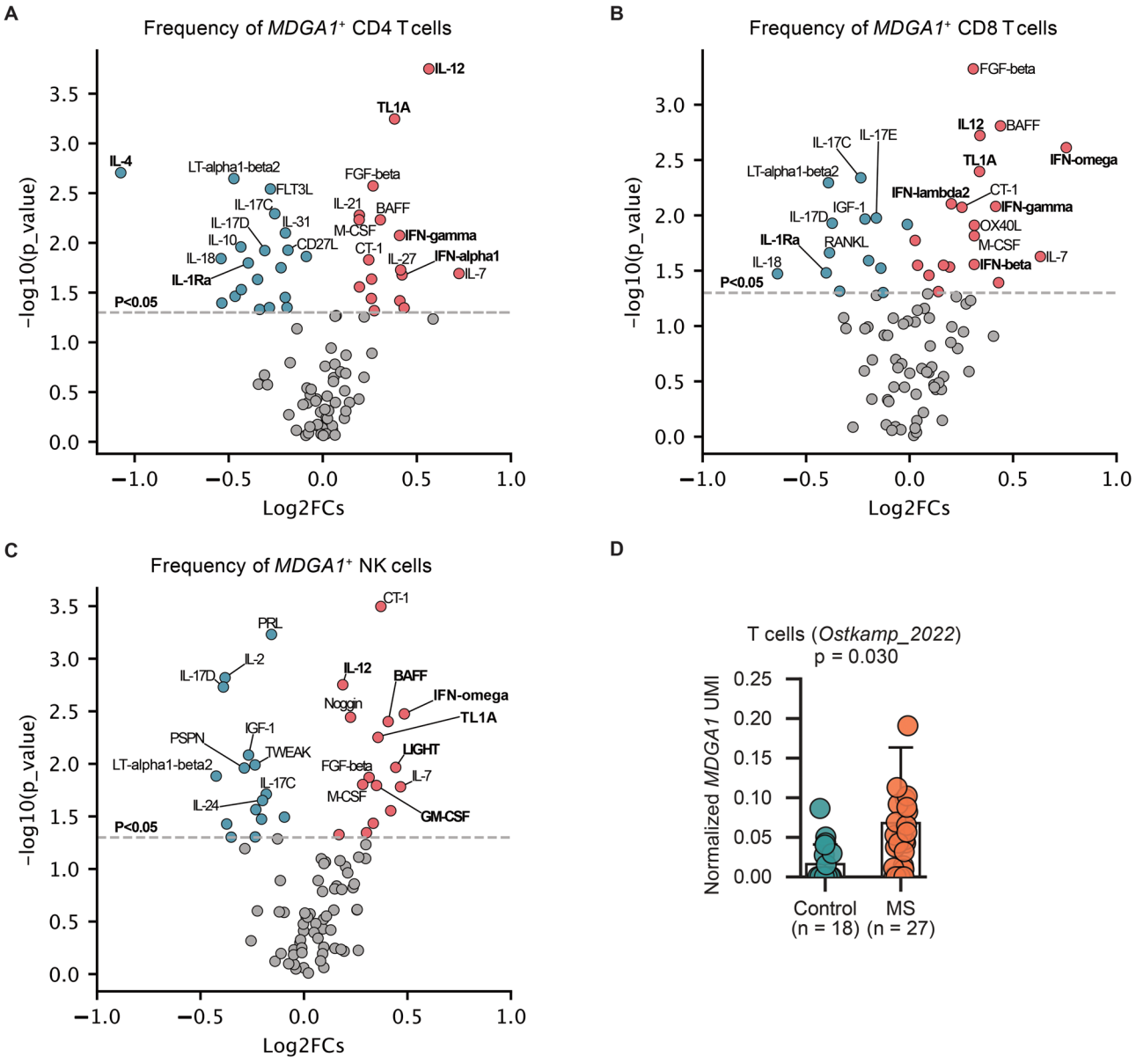


Fig. 5 Screen cytokines for regulating *MDGA1* expression. (**A-C**) Volcano plot showing significant changes in *MDGA1*-positive CD4$^+$ T cells (**A**), CD8$^+$ T cells (**B**), and NK cells (**C**) of samples treated with indicated cytokines compared with PBS-treated controls. The gray dashed line represents a significance threshold of $p = 0.05$. P-values were calculated using a two-sided paired Student's t-test. (**D**) Comparison of normalized *MDGA1* UMIs of T cells in PBMC between healthy donors and patients with multiple sclerosis. Each dot represents one patient. P-values were calculated using a two-sided Student's t-test

immune cell phenotypes with clinical outcomes, thereby enabling transcriptome-wide identification of novel biomarkers of alloHSCT-associated GvL and aGvHD.

The advancement of combinatorial scRNA-seq enabled us to exponentially increase the data size without introducing technical batch effects, which is one of biggest challenges for scRNA-seq analysis. [48–52] We profiled the transcriptome of over 777,000 cells from 25 samples of ten patients in one single experiment. Based on these high-quality data, we confidently identified rare residual host-derived T cells using sex-chromosome-related genes. These host-derived T cells exhibited a markedly different phenotype compared to engrafted donor T cells with a lack of terminal differentiated CD8 T cells, which may underlie their impaired anti-leukemia activity.

Using the T cell receptor sequences as cell-intrinsic molecular identifiers, we observed multiple persistent αβ T and γδ T cell clones post-alloHSCT, which displayed alloreactivity characterized by clonal expansion and increased activity of the cell cycle pathway. Engrafted B cells were not found post-alloHSCT, which is consistent with a previous study that chemotherapy during the

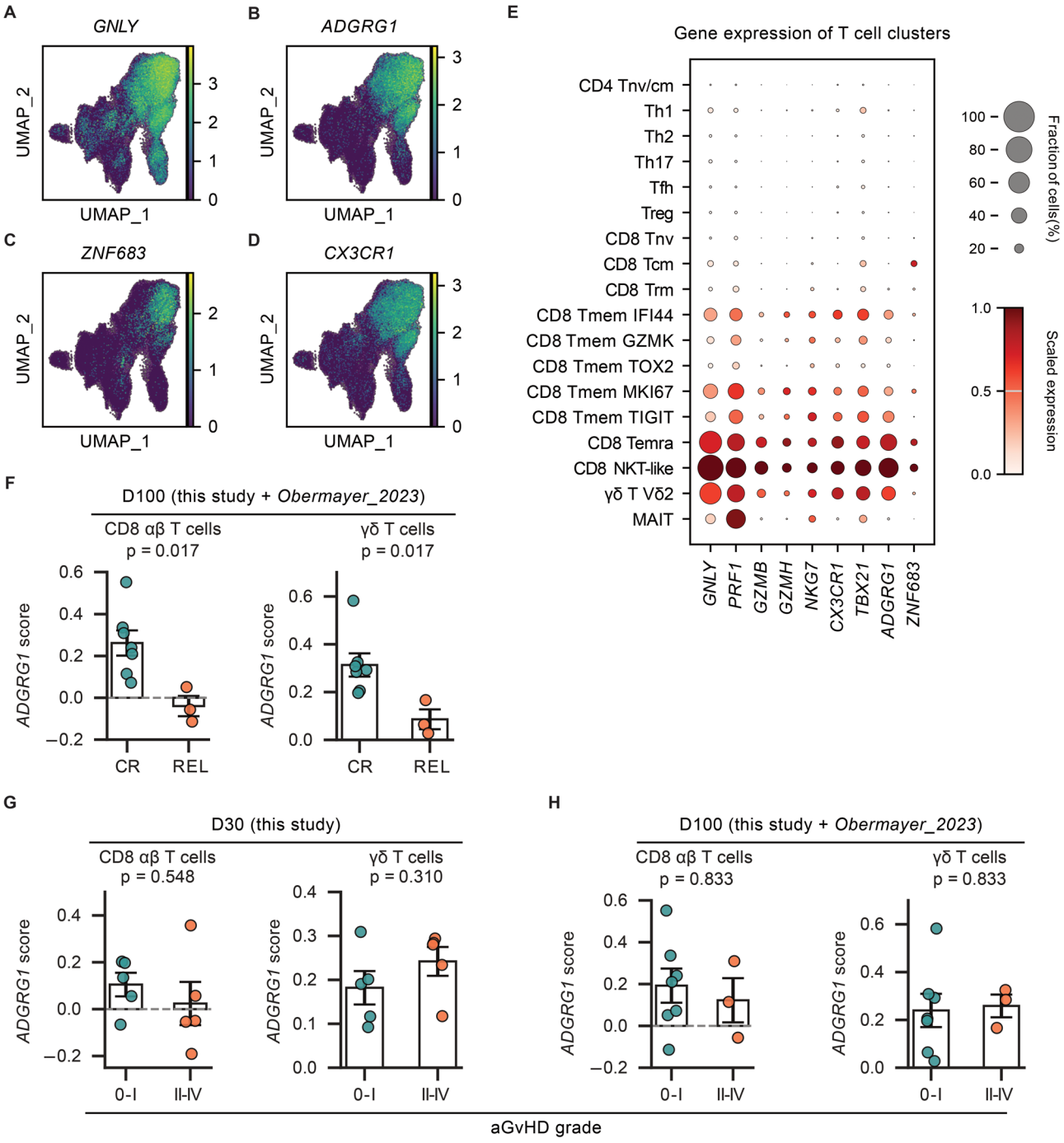


Fig. 6 Characterize *ADGRG1* expression on peripheral T cells. (**A-D**) Normalized gene expression on the T cell UMPA. (**E**) Dot plot showing the cytotoxicity-related gene expression on T cell subtypes. (**F**) Comparison of *ADGRG1* feature on $CD8^+$ T and γδ T cells at D100 between two remission status. P-values were calculated using a two-sided Mann-Whitney U test. (**G-H**) Comparison of *ADGRG1* feature on $CD8^+$ T and γδ T cells between different aGvhd outcomes at D30 (**G**) and D100 (**H**). P-values were calculated using a two-sided Mann-Whitney U test

conditioning regimen resulted in an almost complete depletion of B cells. [53] Intriguingly, we did not observe persisting lymphocytes in REL patients, possibly leading to relapse due to lack of effective GvL. [19]

Recent studies have demonstrated that cytotoxic αβ T cells and γδ T cells are beneficial for alloHSCT treatment in AML patients. [14, 15, 19, 21] However, a universal biomarker of GvL-associated cytotoxic lymphocytes remains undefined. Recent studies found that the remission status of AML patients after alloHSCT was associated with an *ADGRG1*$^+$ signature of $CD8^+$ T cells in the bone marrow. Here, we identified *ADGRG1* (also known

as GPR56) as a robust biomarker consistently expressed across peripheral cytotoxic αβ T, and γδ T cells, with cell abundance significantly correlated to AML remission status. Although our patient cohort contained only two REL patients, which clearly poses limitations on drawing general conclusions, this advocates for further exploring *ADGRG1* expression by all subsets of cytotoxic T cells in the peripheral blood as a general and easily accessible biomarker for monitoring and predicting AML remission after alloHSCT. [20]

The discovery of MDGA1 as a potential novel biomarker for inflammation, and in particular for GvHD in AML patients after alloHSCT was only possible due profiling of significantly larger numbers of cells and samples without introducing additional technical batch effects. Additionally, transcript detection sensitivity has been dramatically improved through the inclusion of random primers during reverse transcription. [48] Prior studies of aGvHD primarily focused on the known molecules associated with immune cell functions, such as the chemokine receptor CXCR3 on T cells and integrin CD11b on monocytes [22], while MDGA1 has not yet been associated with inflammatory lymphocytes and may thus represent a truly novel biomarker. Also, MDGA1 expression at the cell surface would make it tangible for detection by flow cytometry and thus qualify as an easily accessible biomarker. However, anti MDGA1 monoclonal antibodies are not commercially available, which also precludes protein-level validation in this study. Moreover, patients included in the current cohort were heterogenous, not all patients developed aGvHD on D30. While we here focused on high resolution reconstruction of the dynamics of post-transplantation immune cell reconstitution, including the discovery of the novel putative aGvHD biomarker MDGA1, the small and heterogeneous patient cohort remains a major limitation of this study. Therefore, these findings should be interpreted as hypothesis-generating and robustness of *MDGA1* as an aGvHD biomarker and its precise role in inflammatory responses still require exploration in larger patient cohorts and prospective sampling at the onset and resolution of aGvHD. Nevertheless, we also observed upregulation of MDGA1 on peripheral T cells from patients suffering from the inflammatory autoimmune disease MS, which supports the hypothesis that MDGA1 expression by lymphocytes is not specific to aGvHD in alloHSCT patients, but may serve as a broader indicator of inflammation.

Conclusions

We applied ultra-high-throughput (mega-scale) combinatorial barcoding-based scRNA-seq [48] to profile the dynamics of immune cell reconstitution from graft through two follow-up peripheral blood samples of ten AML patients who received alloHSCT treatment. We demonstrated that engrafted αβTCR$^+$ and γδTCR$^+$ effector T cells persisted in the host and exhibited enhanced activity, particularly through TCR signaling pathways. Importantly, we identified *MDGA1* and *ADGRG1* as potential complementary markers for functionally distinct T cell subsets associated with aGvHD and GvL, respectively. Our study provides a comprehensive, longitudinal characterization of immune responses related to alloHSCT in AML patients. Therefore, we suggest that these cell surface receptors serve as novel biomarkers that could facilitate the rapid diagnosis of alloHSCT outcomes and delineate the T cell subsets associated with them. This would enable timely interventions to optimize treatment efficacy and patient outcomes.

Abbreviations

scRNAseq	Single-cell RNA sequencing
aGvHD	Acute graft-versus-host disease
GvL	Graft-versus-leukemia
AML	Acute myeloid leukemia
alloHSCT	Allogeneic hematopoietic stem cell transplantation
NK cells	Natural killer cells
MHC	Major histocompatibility complex
REL	Relapse
PBMC	Peripheral Blood Mononuclear Cell
D30	Day 30
D100	Day 100
DMSO	Dimethylsulfoxid
DAPI	4′,6-diamidino-2-phenylindole
Hg38	Homo sapiens (human) genome assembly GRCh38 (hg38)
UMAP	Uniform Manifold Approximation and Projection
HVGs	Highly variable genes
PAGA	Partition-based graph abstraction
IMGT	The international immunogenetics information system
CDR3	Complementarity-determining region 3
TCR	T cell receptor
BCR	B cell receptor
IGH	Immunoglobulin heavy chain
DEA	Differential expression analysis
ORA	Over Representation Analysis
MSigDB	The Molecular Signatures Database
MS	Multiple sclerosis
log_2FC	Log_2 fold change
DCs	Dendritic cells
MRD	Measurable (minimal) residual disease

Supplementary Information

The online version contains supplementary material available at https://doi.org/10.1186/s40364-025-00868-x.

Supplementary Material 1: Supplementary Figures S1–S9

Supplementary Material 2: Supplementary Figure Legends

Supplementary Material 3: Supplementary Table 1

Acknowledgements

We thank the flow cytometry core facility (University Medical Center Hamburg-Eppendorf, Hamburg) (RRID:SCR_017156) for providing proficient support with FACS sorting for single-cell library preparation. Some elements of the schematic diagrams (Fig. 1A) and the graphical abstract were created using BioRender.com (RRID:SCR_018361).

Author contributions
Z.S. performed single-cell library preparation, conducted computational analyses, generated figures, wrote the manuscript, and contributed to the conceptual development of the study. E.K., A.B., R.M., C.W., N.Gagelmann, K.R., B.F., and F.A. organized the clinical cohort and collected patient samples. L.T., A.S., S.R., N.Gagliani, and C.K. contributed to the setup of the combinatorial barcoding-based single-cell platform. S.W. contributed to single-cell library preparation. L.T., R.J.D., E.C., C.L., and S.B. contributed to computational analyses. Y.Z. created the graphical abstract. U.P. contributed to the conceptual development of the study. N.K. and I.P. conceptualized and designed the study, supervised the project, wrote and revised the manuscript.

Funding
Open Access funding enabled and organized by Projekt DEAL. This work was supported by Deutsche Forschungsgemeinschaft (DFG) (project numbers 264599542, 395236335/FOR2799, 431861465, and 497674564 to Immo Prinz).

Data availability
Single-cell sequencing raw data have been deposited in the Gene Expression Omnibus (GEO, RRID:SCR_005012) under accession number GSE295359. Processed single-cell AnnData objects are available at Zenodo (10.5281/zenodo.15264188). Code for data processing and analysis is deposited on GitHub (https://github.com/isihh-uke/aml-sc.git) (RRID:SCR_002630). All data and code for reproducibility will be made publicly available upon manuscript acceptance.

Declarations

Ethics approval and consent to participate
The study was approved by ethics commission of the Medical Chamber of Hamburg and was performed according to the approved study protocol (version 1.1 from 01.11.2021). Written informed consent was obtained from all participants.

Consent for publication
Not applicable

Competing interests
The authors declare no competing interests.

Author details
[1]Institute of Systems Immunology, University Medical Center Hamburg-Eppendorf, Martinistr. 52, 20251 Hamburg, Germany
[2]Hamburg Center for Translational Immunology, University Medical Center Hamburg-Eppendorf, Martinistr. 52, 20251 Hamburg, Germany
[3]Department of Stem Cell Transplantation, University Medical Center Hamburg-Eppendorf, Martinistr. 52, 20251 Hamburg, Germany
[4]Department of Anaesthesia and Intensive Care and Peter Hung Pain Research Institute, The Chinese University of Hong Kong, 4/F Main Clinical Block and Trauma Centre, Prince of Wales Hospital, Shatin, New Territories, Hong Kong SAR, China
[5]Li Ka Shing Institute of Health Sciences, The Chinese University of Hong Kong; 4/F Main Clinical Block and Trauma Centre, Prince of Wales Hospital, Shatin, New Territories, Hong Kong SAR, China
[6]Institute of Immunology, Hannover Medical School; Carl-Neuberg-Str. 1, 30625 Hannover, Germany
[7]Institute of Medical Systems Bioinformatics, Center for Biomedical AI (bAIome), Center for Molecular Neurobiology (ZMNH), University Medical Center Hamburg-Eppendorf, Falkenried 94, 20251 Hamburg, Germany
[8]Department of General, Visceral and Thoracic Surgery, University Medical Center Hamburg-Eppendorf, Martinistr. 52, 20251 Hamburg, Germany
[9]I. Department of Medicine, University Medical Center Hamburg-Eppendorf, Martinistr. 52, 20251 Hamburg, Germany
[10]III. Department of Medicine, University Medical Center Hamburg-Eppendorf, Martinistr. 52, 20251 Hamburg, Germany
[11]Hamburg Center for Kidney Health (HCKH), University Medical Center Hamburg-Eppendorf, Martinistr. 52, 20251 Hamburg, Germany

Received: 10 September 2025 / Accepted: 2 November 2025
Published online: 01 December 2025

References

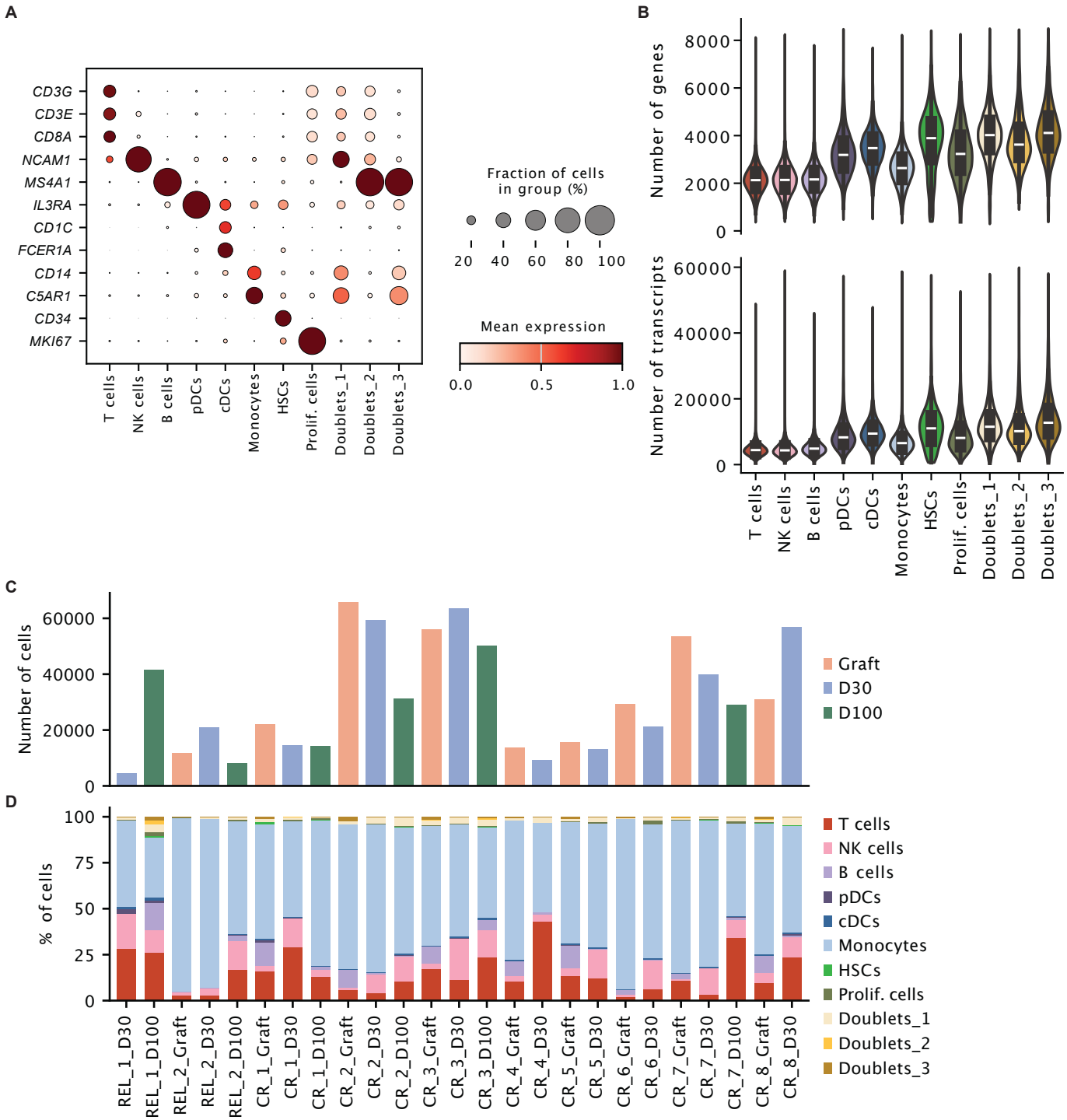
1. Kantarjian H, Kadia T, DiNardo C, Daver N, Borthakur G, Jabbour E, et al. Acute myeloid leukemia: current progress and future directions. Blood Cancer J. 2021;11(2):41. e-pub ahead of print 20210222; doi: https://doi.org/10.1038/s41408-021-00425-3.
2. Horowitz MM, Gale RP, Sondel PM, Goldman JM, Kersey J, Kolb HJ, et al. Graft-versus-leukemia reactions after bone marrow transplantation. Blood. 1990;75(3):555–62. https://doi.org/10.1182/blood.V75.3.555.555.
3. Bleakley M, Riddell SR. Molecules and mechanisms of the graft-versus-leukaemia effect. Nat Rev Cancer. 2004;4(5):371–80. https://doi.org/10.1038/nrc1365.
4. Chao NJ. Minors come of age: minor histocompatibility antigens and graft-versus-host disease. Biol Blood Marrow Transpl. 2004;10(4):215–23. https://doi.org/10.1016/j.bbmt.2003.10.003.
5. Koyama M, Hill GR. Alloantigen presentation and graft-versus-host disease: fuel for the fire. Blood. 2016;127(24):2963–70. e-pub ahead of print 20160330; doi: https://doi.org/10.1182/blood-2016-02-697250.
6. Schoemans HM, Lee SJ, Ferrara JL, Wolff D, Levine JE, Schultz KR, et al. EBMT-NIH-CIBMTR task force position statement on standardized terminology & guidance for graft-versus-host disease assessment. Bone Marrow Transpl. 2018;53(11):1401–15. e-pub ahead of print 20180605; doi: https://doi.org/10.1038/s41409-018-0204-7.
7. Ferrara JLM, Levine JE, Reddy P, Holler E. Graft-versus-host disease. Lancet. 2009;373(9674):1550–61. https://doi.org/10.1016/s0140-6736(09)60237-3.
8. Hill GR, Betts BC, Tkachev V, Kean LS, Blazar BR. Current concepts and advances in graft-versus-host disease immunology. Annu Rev Immunol. 2021;39:19–49. e-pub ahead of print 2021/01/12; doi: https://doi.org/10.1146/annurev-immunol-102119-073227.
9. Shouval R, Fein JA, Labopin M, Kroger N, Duarte RF, Bader P, et al. Outcomes of allogeneic haematopoietic stem cell transplantation from HLA-matched and alternative donors: a European society for blood and marrow transplantation registry retrospective analysis. Lancet Haematol. 2019;6(11):e573–84. e-pub ahead of print 20190830; doi: https://doi.org/10.1016/S2352-3026(19)30158-9.
10. Biernacki MA, Sheth VS, Bleakley M. T cell optimization for graft-versus-leukemia responses. Jci Insight. 2020;5(9). https://doi.org/10.1172/jci.insight.134939.
11. Yeshurun M, Weisdorf D, Rowe JM, Tallman MS, Zhang MJ, Wang HL, et al. The impact of the graft-versus-leukemia effect on survival in acute lymphoblastic leukemia. Blood Adv. 2019;3(4):670–80. https://doi.org/10.1182/bloodadvances.2018027003.
12. Weisdorf D, Zhang MJ, Arora M, Horowitz MM, Rizzo JD, Eapen M. Graft-versus-host disease induced graft-versus-leukemia effect: greater impact on relapse and disease-free survival after reduced intensity conditioning. Biol Blood Marrow Transpl. 2012;18(11):1727–33. e-pub ahead of print 20120702; doi: https://doi.org/10.1016/j.bbmt.2012.06.014.
13. Wang Z, Yin C, Zhang W, Tang W, Song X, Hu X, et al. The benefit of chronic graft-versus-host disease in patients with acute myeloid leukemia relapsed after allogeneic stem cell transplantation. Ann Hematol. 2019;98(7):1765–73. e-pub ahead of print 20190416; doi: https://doi.org/10.1007/s00277-019-03682-2.
14. Locatelli F, Merli P, Pagliara D, Li Pira G, Falco M, Pende D, et al. Outcome of children with acute leukemia given HLA-haploidentical HSCT after alphabeta T-cell and B-cell depletion. Blood. 2017;130(5):677–85. e-pub ahead of print 2017/06/08; doi: https://doi.org/10.1182/blood-2017-04-779769.
15. Airoldi I, Bertaina A, Prigione I, Zorzoli A, Pagliara D, Cocco C, et al. Gamma delta T-cell reconstitution after HLA-haploidentical hematopoietic transplantation depleted of TCR-alpha beta(+)/CD19(+) lymphocytes. Blood. 2015;125(15):2349–58. https://doi.org/10.1182/blood-2014-09-599423.
16. Mensurado S, Condeco C, Sanchez-Martinez D, Shirley S, Coelho RML, Tirado N, et al. CD155/PVR determines acute myeloid leukemia targeting by delta one T cells. Blood. 2024;143(15):1488–95. https://doi.org/10.1182/blood.2023022992.
17. Di Lorenzo B, Simoes AE, Caiado F, Tieppo P, Correia DV, Carvalho T, et al. Broad cytotoxic targeting of acute myeloid leukemia by polyclonal delta one T cells. Cancer Immunol Res. 2019;7(4):552–58. https://doi.org/10.1158/2326-6066.Cir-18-0647.
18. Savani BN, Mielke S, Adams S, Uribe M, Rezvani K, Yong AS, et al. Rapid natural killer cell recovery determines outcome after T-cell-depleted HLA-identical stem cell transplantation in patients with myeloid leukemias but not with acute lymphoblastic leukemia. Leukemia. 2007;21(10):2145–52. e-pub ahead of print 20070802; doi: https://doi.org/10.1038/sj.leu.2404892.

19. Maurer K, Park CY, Mani S, Borji M, Raths F, Kh G, 3rd et al. Coordinated immune networks in leukemia bone marrow microenvironments distinguish response to cellular therapy. Sci Immunol. 2025;10(103):eadr0782. e-pub ahead of print 20250124; doi: https://doi.org/10.1126/sciimmunol.adr0782.
20. Mei Y, Liu Y, Liu W, Chen M, Liu X, Wang S, et al. Identifying ADGRG1 as a specific marker for tumor-reactive T cells in acute myeloid leukemia. Exp Hematol Oncol. 2024;13(1):92. e-pub ahead of print 20240906; doi: https://doi.org/10.1186/s40164-024-00560-0.
21. Mathioudaki A, Wang X, Sedloev DN, Huth R, Kamal A, Hundemer M, et al. The remission status of aml patients post alloSCT is associated with a distinct single-cell bone marrow T cell signature. Blood. 2024. e-pub ahead of print 2024/01/10; doi: https://doi.org/10.1182/blood.2023021815.
22. van Halteren Ags, Suwandi JS, Tuit S, Borst J, Laban S, Tsonaka R, et al. A unique immune signature in blood separates therapy-refractory from therapy-responsive acute graft-versus-host disease. Blood. 2023;141(11):1277–92. https://doi.org/10.1182/blood.2022015734.
23. McCurdy SR, Radojcic V, Tsai H-L, Vulic A, Thompson E, Ivcevic S, et al. Signatures of GVHD and relapse after posttransplant cyclophosphamide revealed by immune profiling and machine learning. Blood. 2022;139(4):608–23. https://doi.org/10.1182/blood.2021013054.
24. Huo YY, Wu LJ, Pang AM, Li Q, Hong F, Zhu CY, et al. Single-cell dissection of human hematopoietic reconstitution after allogeneic hematopoietic stem cell transplantation. Sci Immunol. 2023;8(81). https://doi.org/10.1126/sciimmunol.abn6429.
25. Hao Y, Stuart T, Kowalski MH, Choudhary S, Hoffman P, Hartman A, et al. Dictionary learning for integrative, multimodal and scalable single-cell analysis. Nat Biotechnol. 2024;42(2):293–304. e-pub ahead of print 20230525; doi: https://doi.org/10.1038/s41587-023-01767-y.
26. Korsunsky I, Millard N, Fan J, Slowikowski K, Zhang F, Wei K, et al. Fast, sensitive and accurate integration of single-cell data with Harmony. Nat Methods. 2019;16(12):1289–96. e-pub ahead of print 20191118; doi: https://doi.org/10.1038/s41592-019-0619-0.
27. McInnes L, Healy J, Saul N, Großberger L. UMAP: uniform manifold approximation and projection. J Educ Chang Open Source Softw. 2018;3(29). https://doi.org/10.21105/joss.00861.
28. Blondel VD, Guillaume J-L, Lambiotte R, Lefebvre E. Fast unfolding of communities in large networks. J Stat Mech Theory Exp. 2008;2008(10). doi: https://doi.org/10.1088/1742-5468/2008/10/p10008.
29. Wolf FA, Angerer P, Theis FJ. SCANPY: large-scale single-cell gene expression data analysis. Genome Biol. 2018;19(1):15. e-pub ahead of print 20180206; doi: https://doi.org/10.1186/s13059-017-1382-0.
30. Virshup I, Bredikhin D, Heumos L, Palla G, Sturm G, Gayoso A, et al. The scverse project provides a computational ecosystem for single-cell omics data analysis. Nat Biotechnol. 2023;41(5):604–06. https://doi.org/10.1038/s41587-023-01733-8.
31. Wolock SL, Lopez R, Klein AM. Scrublet: computational identification of cell doublets in single-cell transcriptomic data. Cell Syst. 2019;8(4):281–91 e289. e-pub ahead of print 20190403; doi: https://doi.org/10.1016/j.cels.2018.11.005.
32. Traag VA, Waltman L, van Eck NJ. From Louvain to Leiden: guaranteeing well-connected communities. Sci Rep. 2019;9(1):5233. e-pub ahead of print 20190326; doi: https://doi.org/10.1038/s41598-019-41695-z.
33. Wolf FA, Hamey FK, Plass M, Solana J, Dahlin JS, Gottgens B, et al. PAGA: graph abstraction reconciles clustering with trajectory inference through a topology preserving map of single cells. Genome Biol. 2019;20(1):59. e-pub ahead of print 20190319; doi: https://doi.org/10.1186/s13059-019-1663-x.
34. Terekhova M, Swain A, Bohacova P, Aladyeva E, Arthur L, Laha A, et al. Single-cell atlas of healthy human blood unveils age-related loss of NKG2C(+) GZMB(-)CD8(+) memory T cells and accumulation of type 2 memory T cells. Immunity. 2023;56(12):2836–54 e2839. e-pub ahead of print 2023/11/15; doi: https://doi.org/10.1016/j.immuni.2023.10.013.
35. Song Z, Henze L, Casar C, Schwinge D, Schramm C, Fuss J, et al. Human gammadelta T cell identification from single-cell rna sequencing datasets by modular tcr expression. J Leukoc Biol. 2023;114(6):630–38. https://doi.org/10.1093/jleuko/qiad069.
36. Tan LK, Fichtner AS, Bruni E, Odak I, Sandrock I, Bubke A, et al. A fetal wave of human type 3 effector gamma delta cells with restricted TCR diversity persists into adulthood. Sci Immunol. 2021;6(58). https://doi.org/10.1126/sciimmunol.abf0125.
37. Song L, Cohen D, Ouyang Z, Cao Y, Hu X, Liu XS. TRUST4: immune repertoire reconstruction from bulk and single-cell RNA-seq data. Nat Methods. 2021;18(6):627–30. e-pub ahead of print 2021/05/15; doi: https://doi.org/10.1038/s41592-021-01142-2.
38. Love MI, Huber W, Anders S. Moderated estimation of fold change and dispersion for RNA-seq data with DESeq2. Genome Biol. 2014;15(12). https://doi.org/10.1186/s13059-014-0550-8.
39. Badia IMP, Velez Santiago J, Braunger J, Geiss C, Dimitrov D, Muller-Dott S, et al. decoupleR: ensemble of computational methods to infer biological activities from omics data. Bioinform Adv. 2022;2(1):vbac016. e-pub ahead of print 20220308; doi: https://doi.org/10.1093/bioadv/vbac016.
40. Liberzon A, Birger C, Thorvaldsdottir H, Ghandi M, Mesirov JP, Tamayo P. The molecular signatures database (MSigDB) hallmark gene set collection. Cell Syst. 2015;1(6):417–25. https://doi.org/10.1016/j.cels.2015.12.004.
41. Ostkamp P, Deffner M, Schulte-Mecklenbeck A, Wünsch C, Lu I-N, Wu GF, et al. A single-cell analysis framework allows for characterization of CSF leukocytes and their tissue of origin in multiple sclerosis. Sci Transl Med. 2022;14(673):eadc9778. https://doi.org/10.1126/scitranslmed.adc9778.
42. Bioscience P. 10 million human PBMCs in a single experiment. In. 2024. https://www.parsebiosciences.com/datasets/10-million-human-pbmcs-in-a-single-experiment/.
43. Obermayer B, Keilholz L, Conrad T, Frentsch M, Blau IW, Vuong L, et al. Single-cell clonal tracking of persistent T-cells in allogeneic hematopoietic stem cell transplantation. Front Immunol. 2023;14:1114368. e-pub ahead of print 20230210; doi: https://doi.org/10.3389/fimmu.2023.1114368.
44. Tian G, Li M, Lv G. Analysis of T-Cell receptor repertoire in transplantation: fingerprint of T cell-mediated Alloresponse. Front Immunol. 2021;12:778559. e-pub ahead of print 20220112; doi: https://doi.org/10.3389/fimmu.2021.778559.
45. van der Maas Ng, Berghuis D, van der Burg M, Lankester AC. B cell reconstitution and influencing factors after hematopoietic stem cell transplantation in children. Front Immunol. 2019;10:782. e-pub ahead of print 20190412; doi: https://doi.org/10.3389/fimmu.2019.00782.
46. Heaton H, Talman AM, Knights A, Imaz M, Gaffney DJ, Durbin R, et al. Souporcell: robust clustering of single-cell RNA-seq data by genotype without reference genotypes. Nat Methods. 2020;17(6):615–20. e-pub ahead of print 20200504; doi: https://doi.org/10.1038/s41592-020-0820-1.
47. Ghimire S, Weber D, Mavin E, Wang XN, Dickinson AM, Holler E. Pathophysiology of GvHD and other HSCT-related major complications. Front Immunol. 2017;8:79. e-pub ahead of print 20170320; doi: https://doi.org/10.3389/fimmu.2017.00079.
48. Rosenberg AB, Roco CM, Muscat RA, Kuchina A, Sample P, Yao Z, et al. Single-cell profiling of the developing mouse brain and spinal cord with split-pool barcoding. Science. 2018;360(6385):176–82. https://doi.org/10.1126/science.aam8999.
49. Tung PY, Blischak JD, Hsiao CJ, Knowles DA, Burnett JE, Pritchard JK, et al. Batch effects and the effective design of single-cell gene expression studies. Sci Rep. 2017;7:39921. e-pub ahead of print 20170103; doi: https://doi.org/10.1038/srep39921.
50. Hicks SC, Townes FW, Teng M, Irizarry RA. Missing data and technical variability in single-cell RNA-sequencing experiments. Biostatistics. 2018;19(4):562–78. https://doi.org/10.1093/biostatistics/kxx053.
51. Luecken MD, Buttner M, Chaichoompu K, Danese A, Interlandi M, Mueller MF, et al. Benchmarking atlas-level data integration in single-cell genomics. Nat Methods. 2022;19(1):41–50. e-pub ahead of print 20211223; doi: https://doi.org/10.1038/s41592-021-01336-8.
52. Tran HTN, Ang KS, Chevrier M, Zhang X, Lee NYS, Goh M, et al. A benchmark of batch-effect correction methods for single-cell rna sequencing data. Genome Biol. 2020;21(1):12. e-pub ahead of print 20200116; doi: https://doi.org/10.1186/s13059-019-1850-9.
53. Heck C, Steiner S, Kaebisch EM, Frentsch M, Wittenbecher F, Scheibenbogen C, et al. CD4+ T cell dependent B cell recovery and function after autologous hematopoietic stem cell transplantation. Front Immunol. 2021;12:736137. e-pub ahead of print 20210929; doi: https://doi.org/10.3389/fimmu.2021.736137.

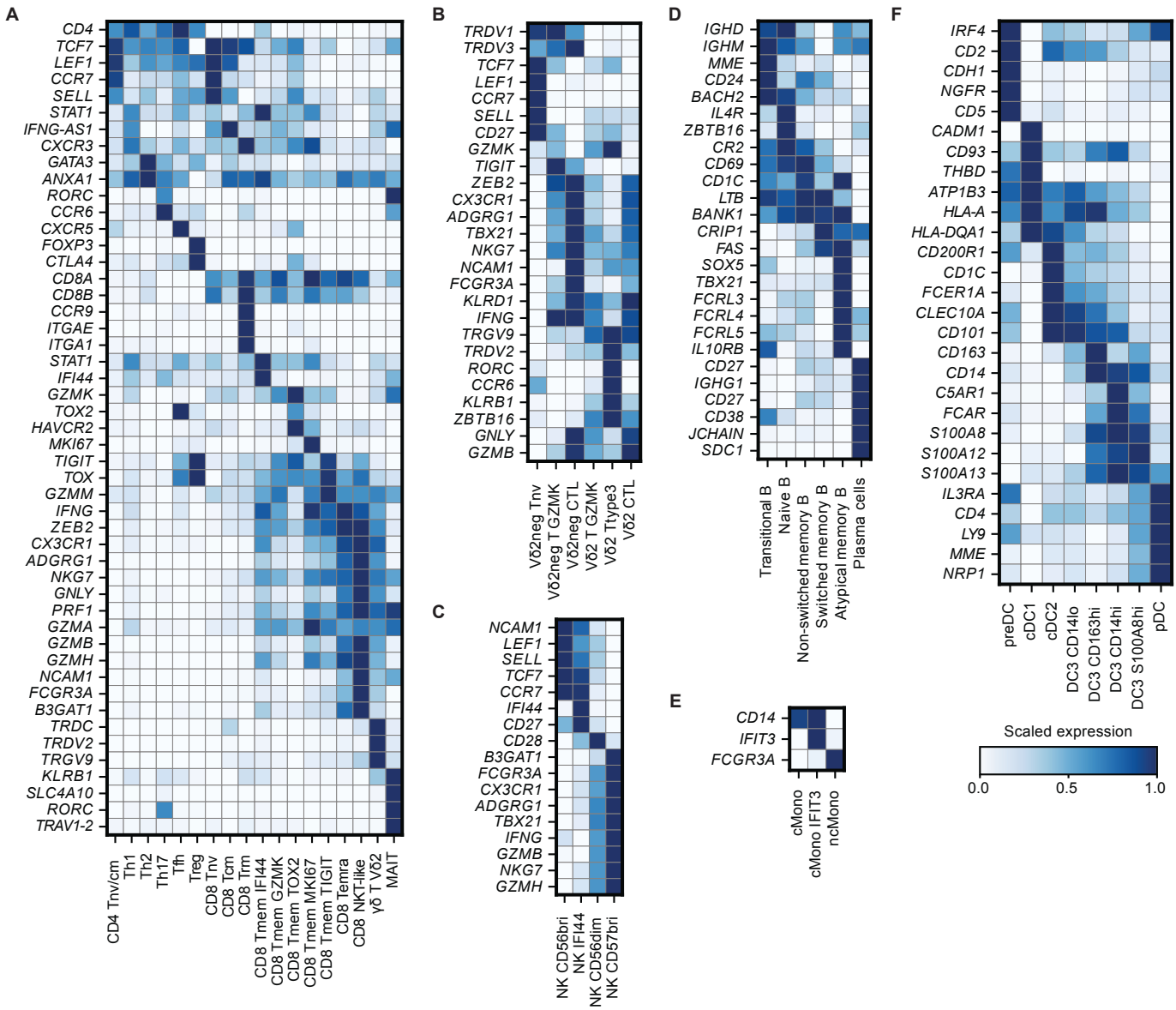
Publisher's Note

Springer Nature remains neutral with regard to jurisdictional claims in published maps and institutional affiliations.

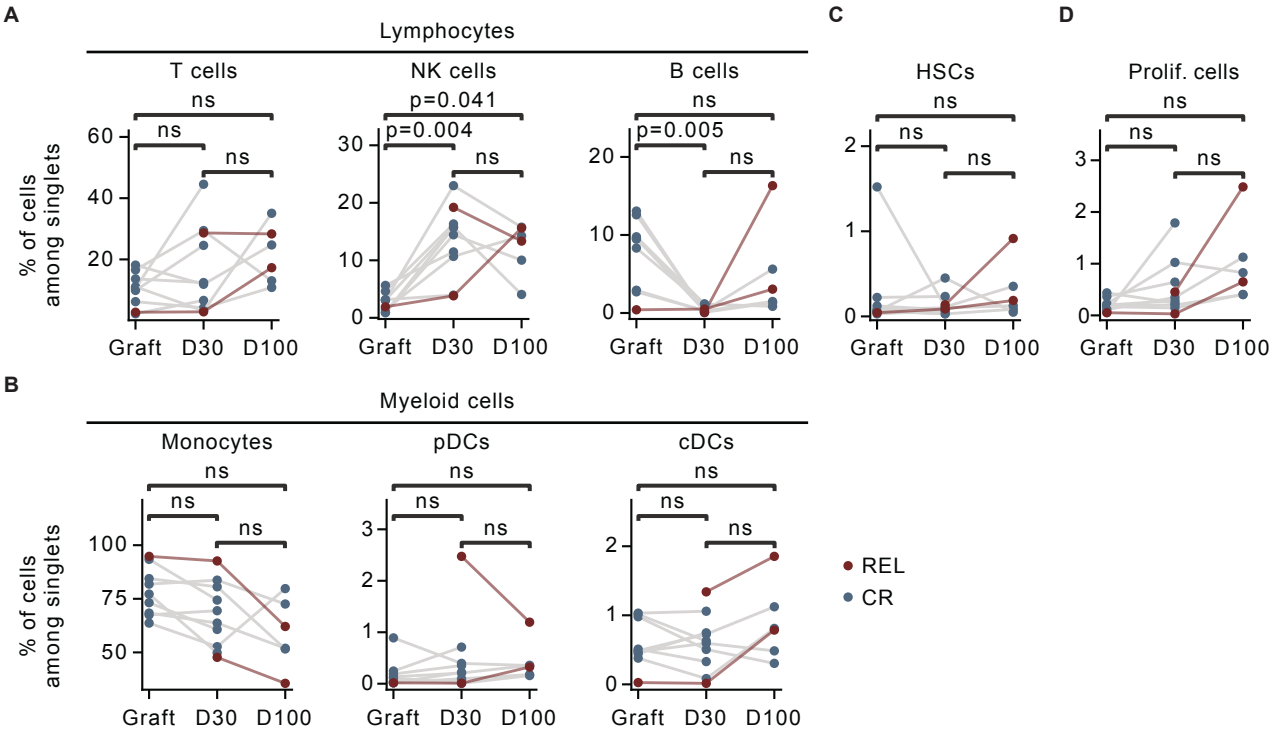
Supplementary Fig. S1



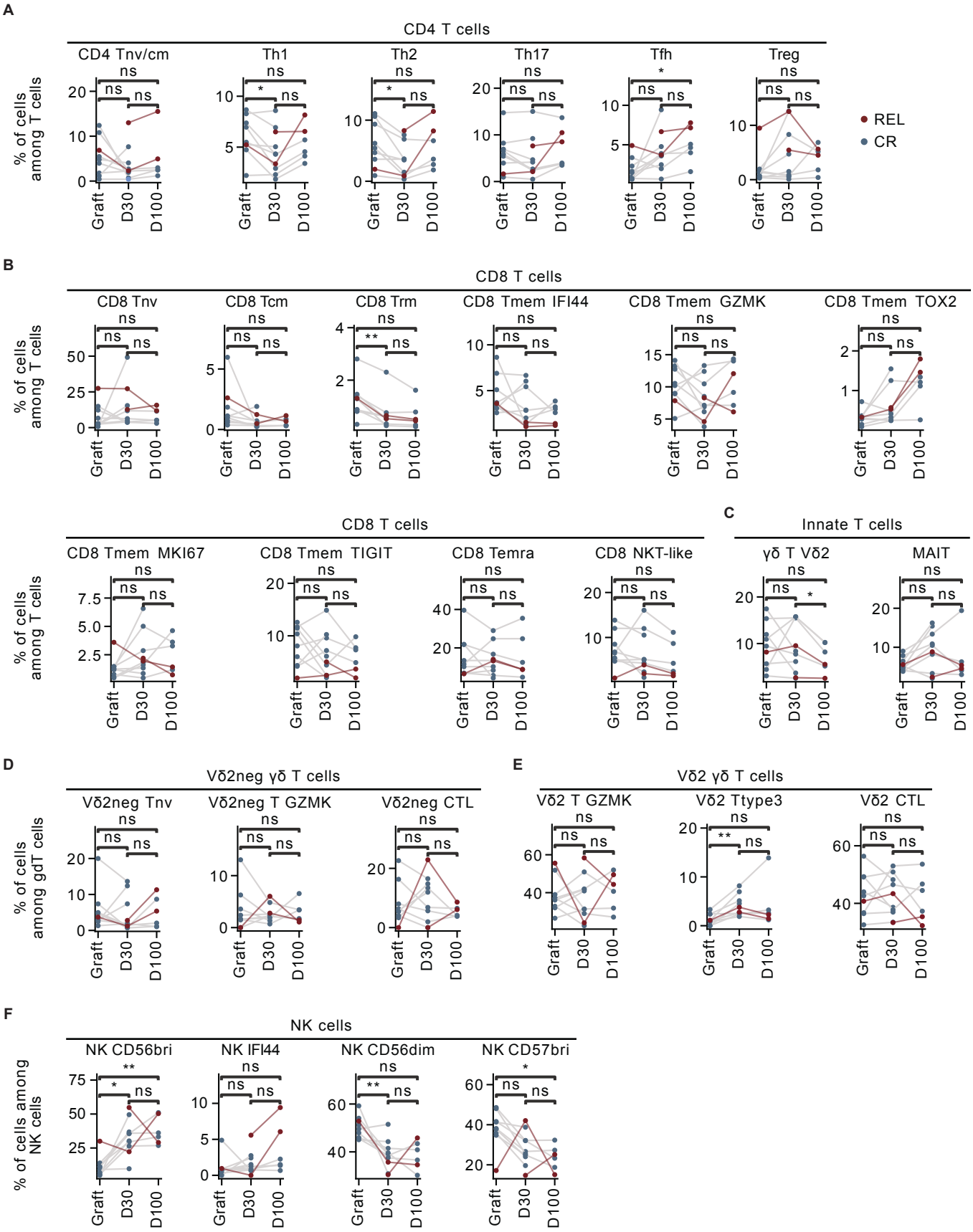
Supplementary Fig. S2



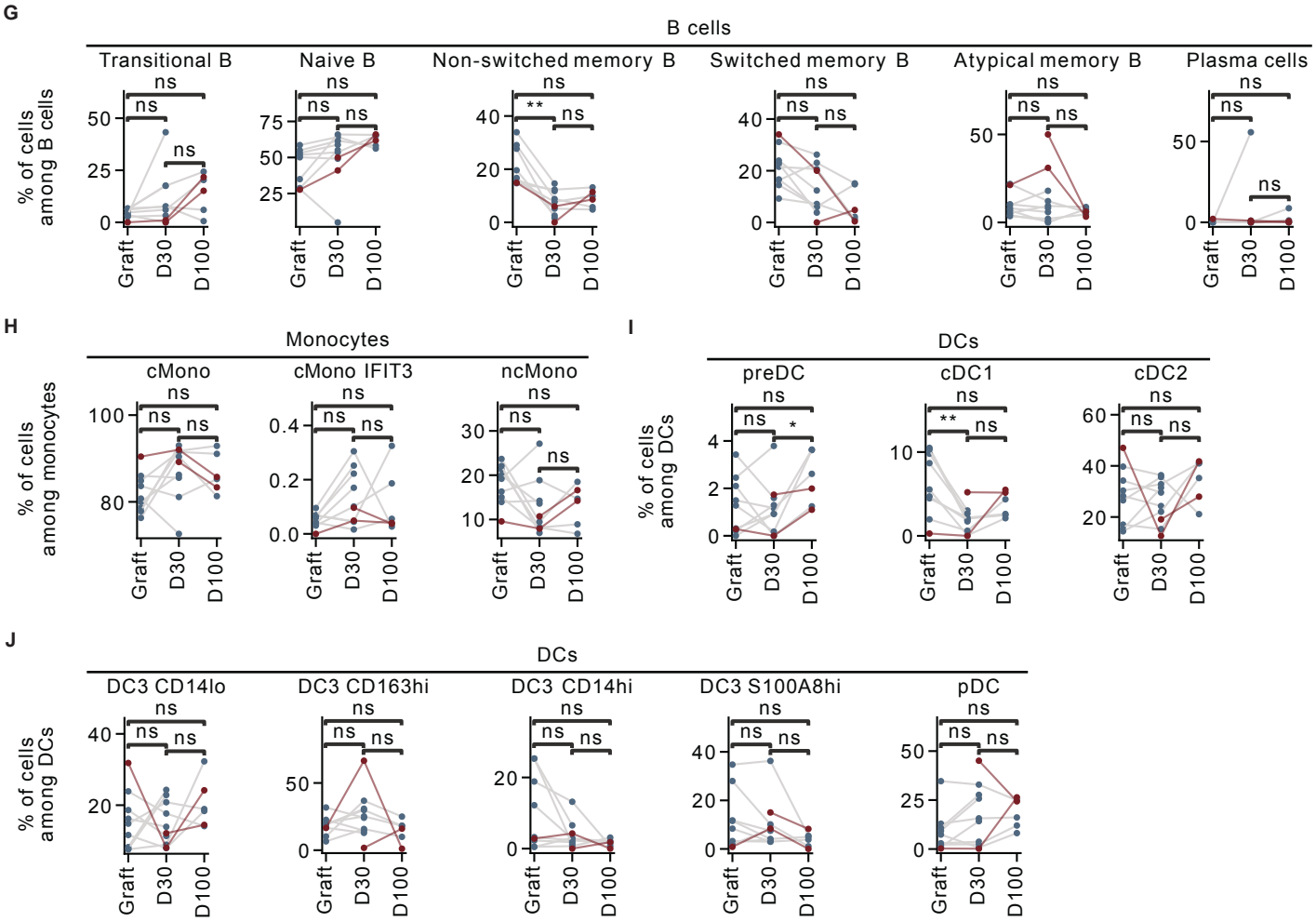
Supplementary Fig. S3



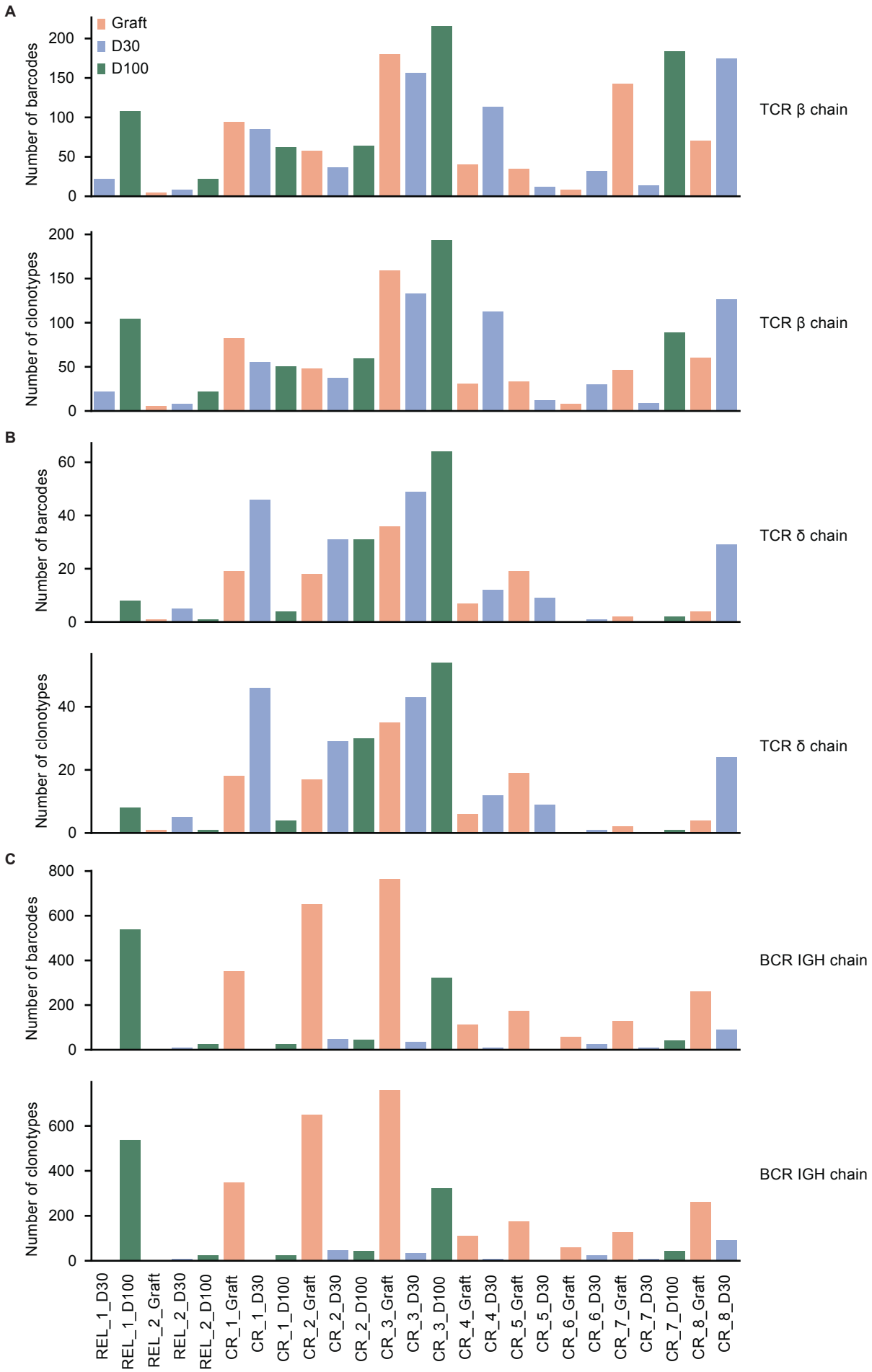
Supplementary Fig. S4



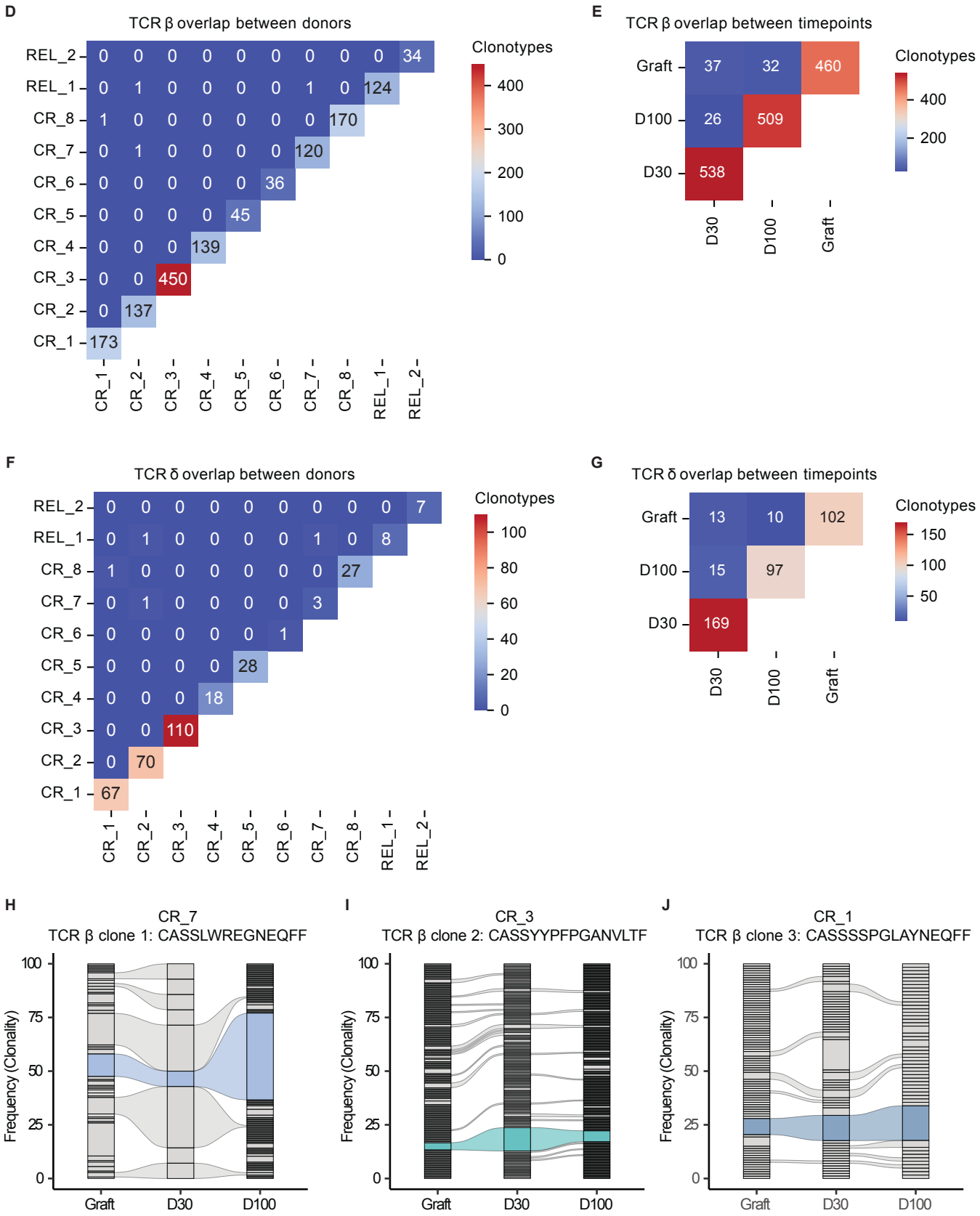
Supplementary Fig. S4



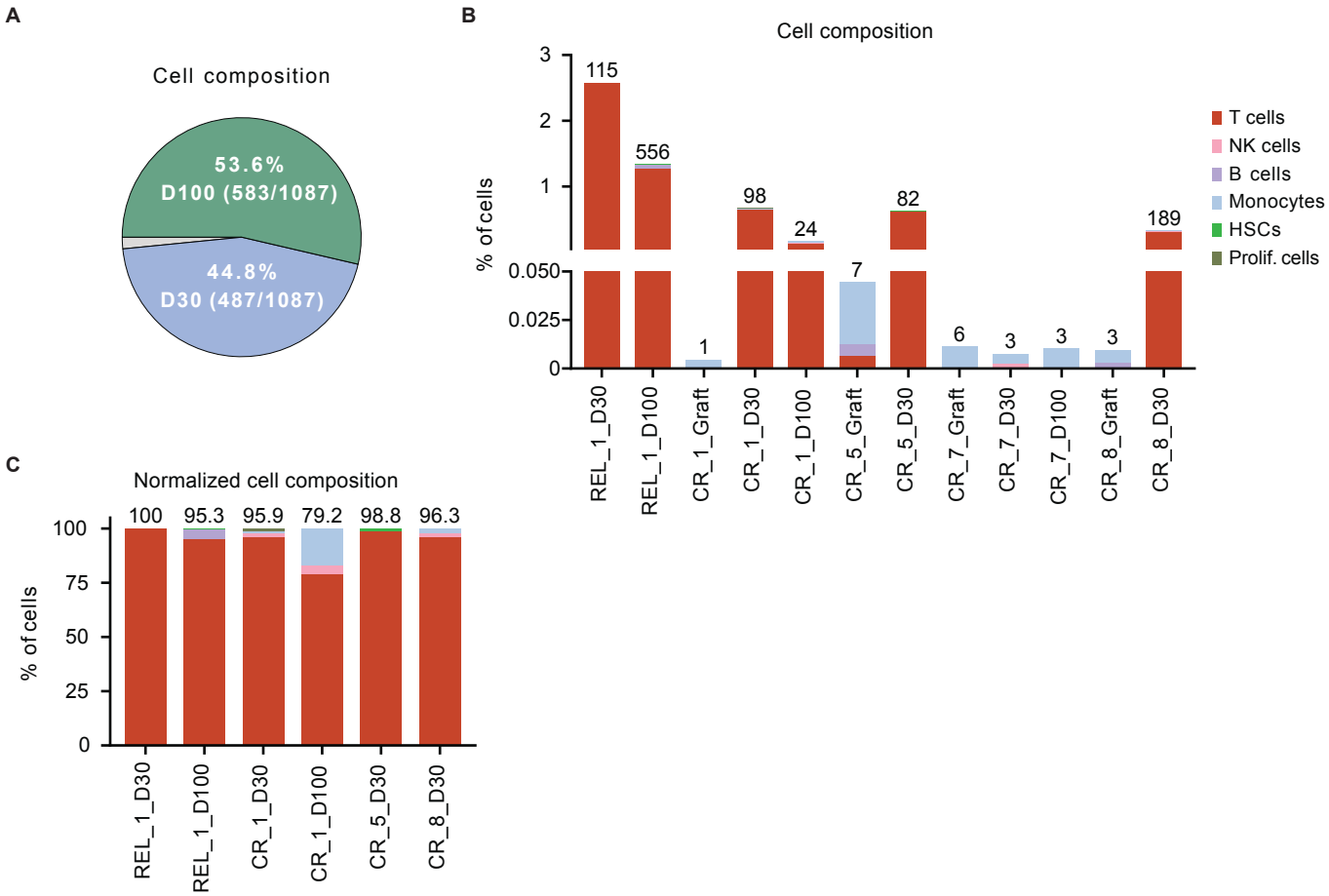
Supplementary Fig. S5



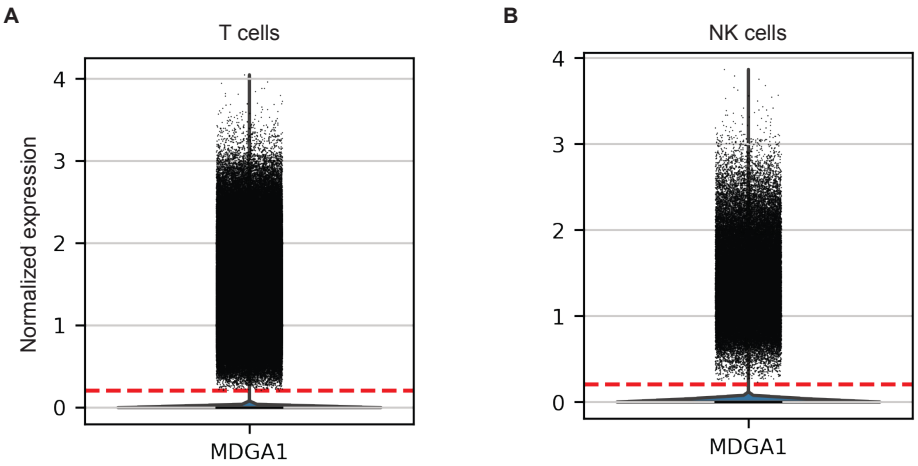
Supplementary Fig. S5



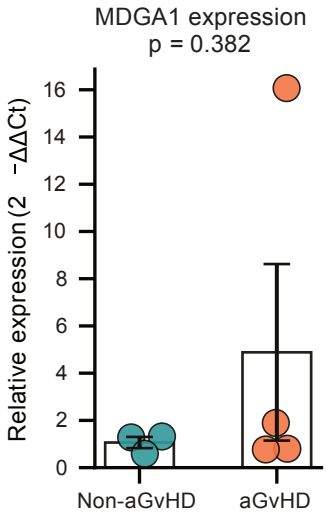
Supplementary Fig. S6



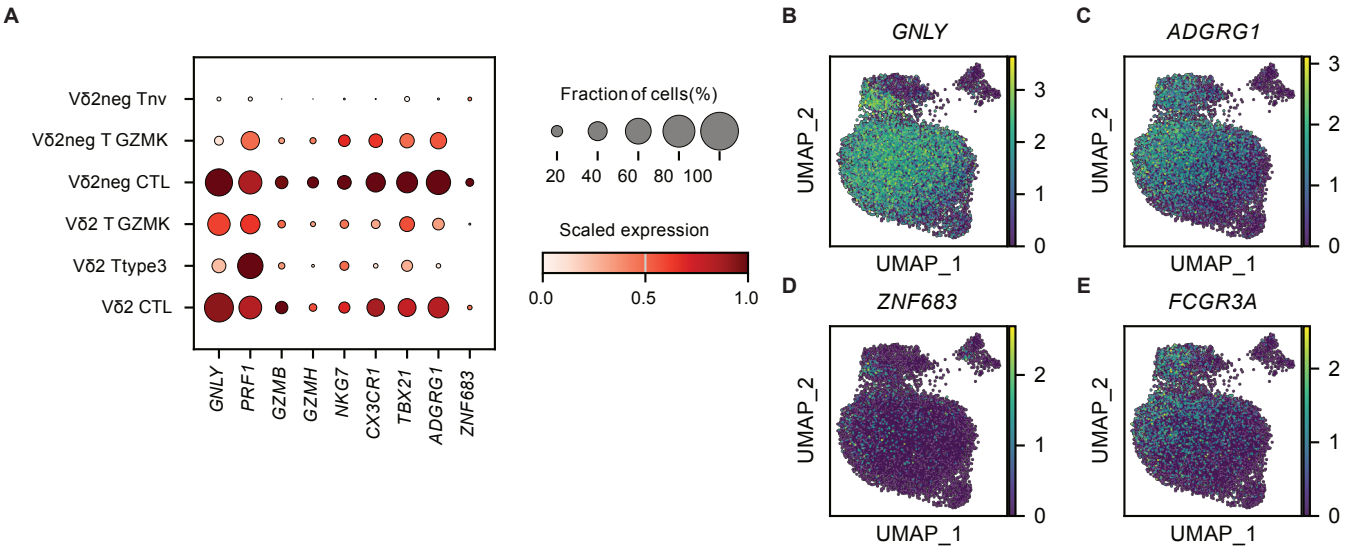
Supplementary Fig. S7



Supplementary Fig. S8



Supplementary Fig. S9



Supplementary figure legends

Supplementary Fig. S1 Overview of the scRNA-seq dataset

(A) Dotplot showing the marker gene expression of major cell populations. (B) Gene number (upper) and transcripts number (lower) of major cell populations. (C-D) Cell number (upper) and cell composition (lower) of each sample.

Supplementary Fig. S2 Marker gene expression of subpopulations

(A-F) Matrixplot showing marker gene expression of total T cells (A), γδ T cells (B), Natural Killer cells (NK) (C), B cells (D), monocytes (E), dendritic cells (DCs) (F). Gene expression are scaled between 0 and 1.

Supplementary Fig. S3 Comparison of cell frequency between different timepoints

(A-D) Comparison the frequency of lymphocytes (A), myeloid cells (B), HSCs (C), and Prolif. cells (D). Each dot represents one sample and is colored by the remission status of the patient. P-values were calculated using a two-sided paired Student's t-test and adjusted by Bonferroni correction.

Supplementary Fig. S4 Comparison of subtype frequency between different timepoints

(A-J) Comparison the frequency of $CD4^+$ T cells (A), $CD8^+$ T cells (B), innate T cells (C), Vδ2neg γδ T cells (D), Vδ2 γδ T cells (E), NK cells (F), B cells (G), monocytes (H), and DCs (I-J). Each dot represents one sample and is colored by the remission status of the patient. P-values were calculated using a two-sided paired Student's t-test and adjusted by Bonferroni correction. *: $p < 0.05$, **: $p < 0.01$.

Supplementary Fig. S5 Overview of immune repertoire

(A-C) The number of barcodes and clonotypes of TCR β chain (A), TCR δ chain (B), and BCR IGH chain (C) of each sample. (D-E) The overlap of TCR β clonotypes between different donors (D) or between different timepoints (E). (F-G) The overlap of TCR δ clonotypes between different donors (F) or between different timepoints (G). (H-J) The overlap and clonality of indicated clones between different timepoints.

Supplementary Fig. S6 Overview of residual host-derived cells

(A) Pie plot showing the cell composition of timepoints. Cell number and percentage are indicated. (B-C) The frequencies (B) and normalized frequencies (C) of residual host-derived cells from indicated samples same as that in Fig. 3B. The numbers on the top of the bar are the absolute cell number of the residual host-derived cells (B) or proportion of T cells (C). Bars are colored by cell type.

Supplementary Fig. S7 Definition of *MDGA1*$^{+}$ T and NK cells

(A-B) Violin plot showing the expression of *MDGA1* on T cells (A) and NK cells (B). Cell with expression above the red dashed line (y = 0.2) was defined as MDGA1^{+}.

Supplementary Fig. S8 Validation of *MDGA1* expression in T cells from patients with acute GvHD after allogeneic hematopoietic stem cell transplantation by qPCR

Comparison of normalized *MDGA1* expression of T cells between patients with and without aGvHD. Each dot represents one patient. P-values were calculated using a two-sided Student's t-test.

Supplementary Fig. S9 Characterization of ADGRG1 expression on γδ T cells

(A) Dot plot showing the cytotoxicity-related gene expression on γδ T cell subtypes.

(B-E) Normalized gene expression on the T cell UMAP.

Supplementary Table S1

Patient	Age	Disease	Dose of $CD34^+$ cells	aGvHD	Relapse
A	53	MCL	6 Mio/kg BW	II	no
B	56	BPDCN	5.4 Mio/kg BW	I	no
C	65	AML	5.3 Mio/kg BW	I	no
D	54	MDS	6.2 Mio/kg BW	0	yes
E	43	AML	4.6 Mio/kg BW	I	no

Supplementary Table 1: Clinical details for the pairs A-E from public dataset *Obermayer_2023*, according to reference 43. MCL: Mantle cell lymphoma; BPDCN: Blastic plasmacytoid dendritic cell neoplasm; AML: Acute myeloid leukemia; MDS: Myelodysplastic syndrome; BW: Body weight

Chapter 4: Unpublished Manuscript

Decade-long persistence of adaptive γδ T effectors in recurrent malaria

Specific contributions:

The following manuscript is being prepared for submission to a journal. I am the first author of the manuscript. I performed the single-cell library preparation, conducted the computational analyses, generated the figures, drafted the manuscript, and contributed to the conceptual development of the study.

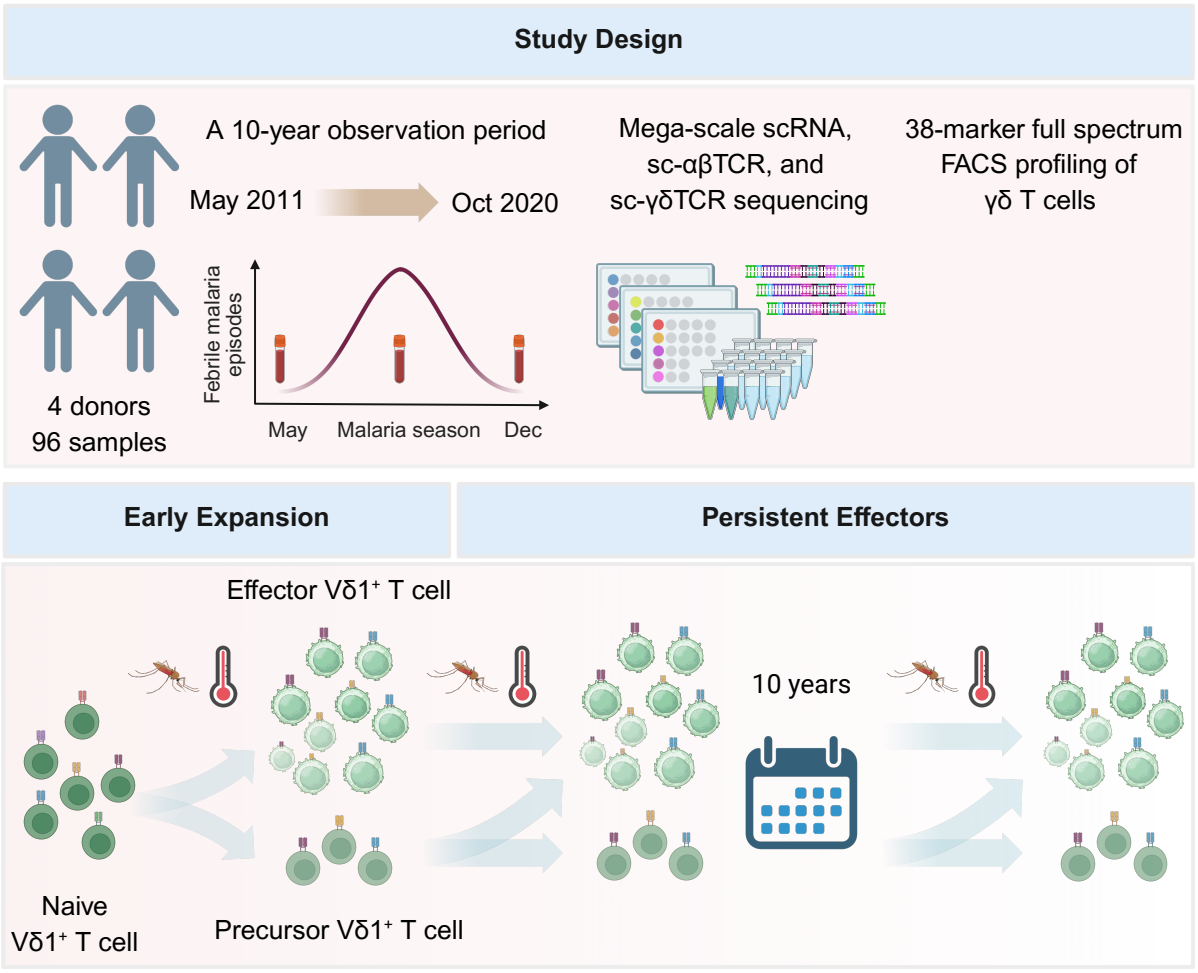
I, Immo Prinz, agree with the above statements as the direct supervisor.

Signature _____

Universitätsklinikum Hamburg-Eppendorf
Hamburg Center for Translational Immunology (HCTI)
Prof. Dr. Immo Prinz
Institute of Systems Immunology
Martinistraße 52 • 20246 Hamburg • Germany
Tel.: +49 40 7410 56028 • Email: i.prinz@uke.de

Date & Place 30.03.2026, Hamburg

Graphic Abstract



Working title:

Decade-long persistence of adaptive γδ T effectors in recurrent malaria

Running title:

Effector Vδ1^{+} T cells persist over 10 years

Potential List of Authors:

Zheng Song[1,2], Rosie Sanders[3], Helen George[4,5], Carolin Maack[1,2], Freya Sibbertsen[1,2], *xxx-tba*, Aissata Ongoiba[6], Safiatou Doumbo[6], Didier Doumtabe[6], Shanping Li[7], Kassoum Kayentao[6], Peter D. Crompton[7], Maria Mackroth[4,8], Christine S. Hopp[4], Martin Davey[3], Immo Prinz[1,2#]

Affiliations:

[1]Institute of Systems Immunology, University Medical Center Hamburg-Eppendorf, Hamburg, Germany.

[2]Hamburg Center for Translational Immunology, University Medical Center Hamburg-Eppendorf, Hamburg, Germany.

[3]Division of Biomedical Sciences, Warwick Medical School, University of Warwick, Coventry, UK.

[4]B cell Immunology in Malaria, Bernhard Nocht Institute for Tropical Medicine, Hamburg, Germany.

[5]Protozoa Immunology, Bernhard Nocht Institute for Tropical Medicine, Hamburg, Germany.

[6]Malaria Research and Training Centre, Department of Epidemiology of Parasitic Diseases, International Center of Excellence in Research, University of Sciences, Technique and Technology of Bamako, Mali.

[7]Malaria Infection Biology and Immunity Section, Laboratory of Immunogenetics, Division of Intramural Research, NIAID, NIH, Rockville, MD.

[8]Institute for Translational Medicine, Medical School Hamburg, Germany.

[#] I.P. and *tba* are joint senior authors.

Corresponding author: Immo Prinz, email: i.prinz@uke.de.

Abstract (200 words)

Human adaptive γδ T cells, expressing a Vδ1 T cell receptor (TCR), participate in immune responses to infections and cancer, showing durable clonal expansion and sustained functional competence. However, the lack of longitudinal studies with integrated clonal-phenotypic resolution limits our understanding of their functional plasticity, and longevity mechanisms. We used single-cell RNA and γδ TCR sequencing (scRNA-seq and sc-γδTCR-seq) to profile peripheral γδ T cell phenotypes and clonotypes in a 10–year longitudinal cohort of four Malian children (aged 4–5 years at enrollment) exposed to yearly seasonal malaria transmission. Repeated infection drove clonal expansion of two distinct Vδ1$^+$ effector populations with either regulatory (*CX3CR1*, *PDCD1*, and *IL10*) or cytotoxic (*CX3CR1*, *GNLY*, *INFG*, and *PRF1*) phenotypes, alongside the establishment of a previously unrecognized precursor-like Vδ1$^+$ subset co-expressing self-renewal (*TCF7*) and exhaustion-associated markers (*TOX*, *PDCD1*, *TIGIT*, and *HAVCR2*). Clonal tracking revealed that the dominant Vδ1$^+$ clonotypes in each individual persisted over the decade with stable effector phenotypes, maintained by self-renewal and involving a precursor-like memory pool. Together, these findings define mechanisms of durable adaptive γδ T cell immunity during recurrent malaria, instructing the development of γδ T cell–based immunotherapies for infectious diseases and cancer.

Introduction

Adaptive human γδ T cells, dominated by Vδ1 and Vδ3 T cell receptor (TCR) δ-chain usage, undergo marked clonal expansion in response to chronic infections including cytomegalovirus (CMV)[1-8], *Mycobacterium tuberculosis* (*Mtb*)[9-11], *Plasmodium falciparum* (*P. falciparum*)[12-14], and they are involved in anti-cancer immunity[15-31]. γδ TCR tracking revealed that expanded Vδ1$^+$ γδ T clones persist more than six months in immunocompromised patients after allogeneic stem cell transplantation with CMV reactivation and for over 18 months in healthy adults, supporting the idea that ongoing antigen exposure may sustain durable Vδ1$^+$ T cell responses[3,5-7,32]. This contrasts with CD8$^+$ αβ T cells, in which continuous TCR stimulation drives exhaustion along the establishment of a TCF1$^+$ memory precursor-exhausted pool[33-43]. This divergence is further supported by clonally expanded tumor-infiltrating Vδ1$^+$ T cells, which retain functional plasticity despite elevated inhibitory receptor expression (PD1, TIM3, TIGIT), as reported across leukemia[16,27,29], melanoma[17], colorectal cancer[21,22,28,30], breast cancer[18], renal cell carcinoma[23], non–small-cell lung cancer[20], and Merkel cell carcinoma[26]. These observations raise the question how Vδ1$^+$ T cells maintain sustained responses across prolonged or repeated antigen exposure without contraction or functional exhaustion. Therefore, the long-term stability and phenotypic plasticity of Vδ1$^+$ T cells should be addressed through longitudinal γδ TCR clonal tracking across repeated infections in humans.

Malaria provides an opportune natural setting to interrogate the durability of Vδ1$^+$ T cell responses. Repeated *P. falciparum* exposure drives the expansion of circulating effector Vδ1$^+$ T cells in controlled human malaria infection (CHMI) and in individuals living in malaria-endemic regions with annual seasonal transmission[14]. Notably, these *P. falciparum*-challenged γδ T cells are able to mount recall responses that were largely maintained ~14 months after a single *P. falciparum* episode[44]. Moreover, in clinically immune individuals, expanded circulating Vδ1$^+$ T cells produce IL-10 alongside IFN-γ in response to *P. falciparum* antigens, mirroring the type 1 regulatory (Tr1)–like cytokine profile[45-56]. Together, these observations suggest long-lived, exposure-associated Vδ1$^+$ T cell responsiveness in malaria, but it remains unclear whether this represents bona fide "γδ T cell memory" with persistent clonotypes and reproducible recall across repeated *P. falciparum* infections. This gap arises because circulating Vδ1$^+$ T cells are rare, and traditional approaches, such as bulk TCR sequencing and flow cytometry, lack the phenotypic–clonotypic resolution needed for longitudinal tracking of Vδ1$^+$ T cell responses in malaria.

To overcome these limitations, we employed single-cell profiling to longitudinally track peripheral γδ T cells at clonal-phenotypic resolution over 10 years in four Malian children exposed to seasonal malaria each year. We uncovered decade-long persistence of malaria-induced Vδ1$^+$ T cell expansions with a stable effector program, sustained by ongoing self-renewal and a previously unrecognized memory-precursor population.

Results

Longitudinal single-cell profiling of circulating T cell dynamics over a decade of recurrent malaria

To study human T cell responses to repeated episodes of malaria in an unbiased way, we employed ultra-high-throughput combinatorial barcoding-based single–cell RNA and TCR sequencing of circulating $CD3^+$ T cells in a 10-year longitudinal cohort including four Malian children (aged 4 to 5 years at the time of enrollment) exposed to intense seasonal malaria transmission (**Figure 1a**). From a total of 96 PBMC samples, collected at two annual cross–sectional blood–draws and individually shortly after febrile malaria episodes, we recovered 381,638 high quality $CD3^+$ T cells (**Figure 1b**). Based on canonical lineage markers and T cell functional gene programs, we identified 28 distinct T cell populations across $CD4^+$ αβ T, $CD8^+$ αβ T, Vγ9Vδ2 γδ T, and non–Vγ9Vδ2 γδ T compartments (**Figure 1c-e**).

Repeated malaria episodes were associated with a marked expansion of $CD4^+$ αβ T cells (from ~40% in year 1 to ~80% in year 10) (**Figure 1f**), consistent with prior reports. In contrast to these dynamic αβ T cell shifts, non–Vγ9Vδ2 γδ T cells remained consistently expanded over the decade, reaching atypically high frequencies comparable to the Vγ9Vδ2 γδ T cell compartment (**Figure 1f**). This dataset provides a comprehensive 10–year single–cell atlas of circulating αβ and γδ T cell dynamics in recurrent malaria and identifies the consistent expansion of non–Vγ9Vδ2 γδ T cells in malaria–exposed children.

Figure 1 Decade-long single-cell profiling of T cell dynamics in Malian children

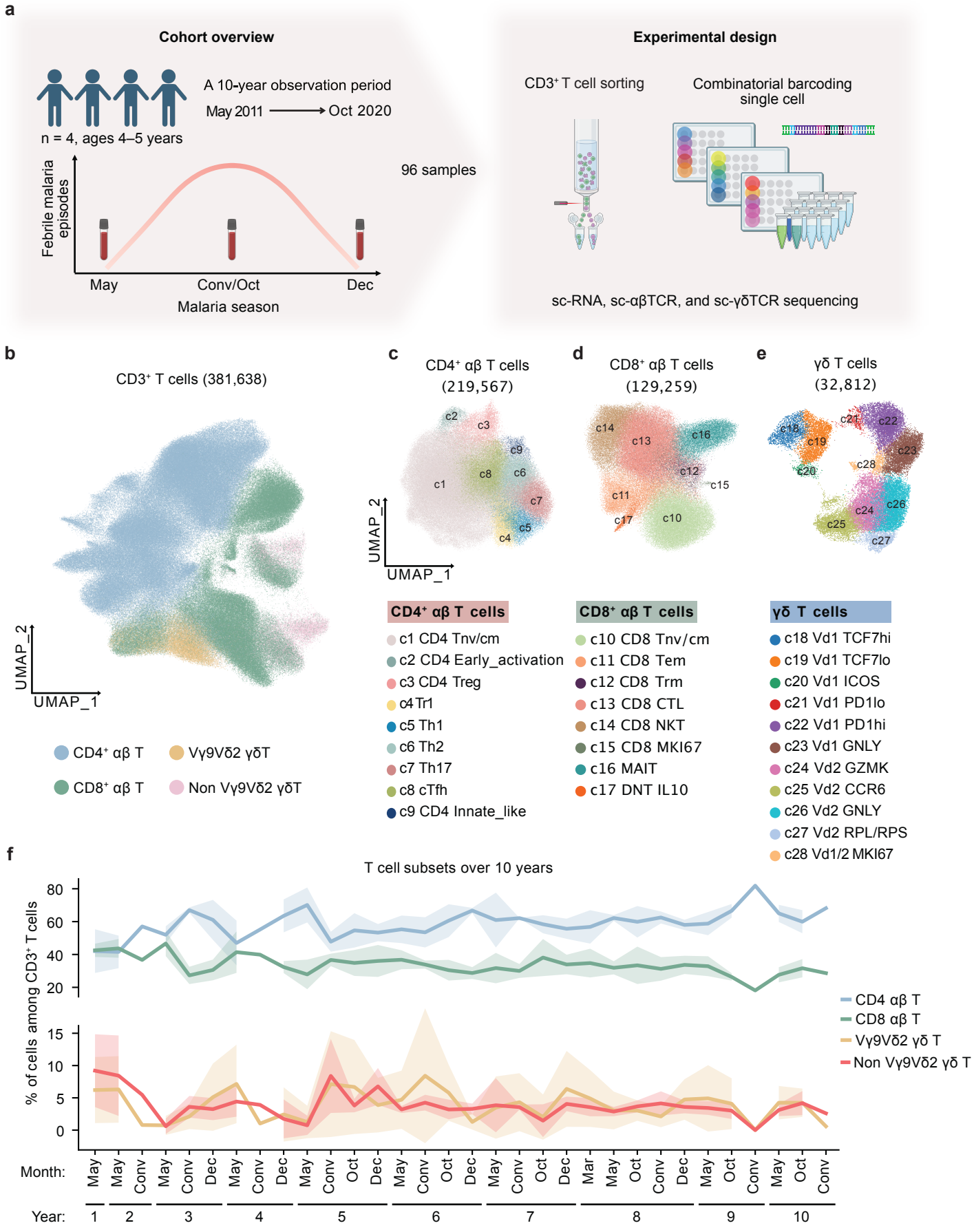


Figure 1. Decade-long single-cell profiling of T cell dynamics in Malian children

a, Schematic of the experimental design.

b, UMAP of the 381,638 high-quality $CD3^+$ T cells. Cells are colored by T cell subset.

c-e, UMAP of 219,567 $CD4^+$ αβ T (**c**), 129,259 $CD8^+$ αβ T (**d**), and 32,812 γδ T cells (**e**). Cells are colored by annotation.

f, Frequencies of $CD4^+$ αβ T, $CD8^+$ αβ T, and Vγ9Vδ2 γδ T (Vδ2) and non-Vγ9Vδ2 γδ T (Vδ1) cells across the 10-year observation period. Lines and shaded areas are colored by cell subset and denote mean ± s.d. Conv represents convalescent period after acute infection.

Repeated malaria exposure drives expansion of distinct circulating Vδ1⁺ T cell subsets

To generalize our observations, we reanalyzed a cross-sectional single–cell dataset of circulating T cells from children in malaria-endemic Burkina Faso and found enriched Vδ1⁺ T cells, contrasting to the predominated circulating Vδ2⁺ cells in age–matched non–endemic Western children (**Figure 2a, b**). Consistently, in our longitudinal cohort, circulating Vδ1⁺ T cells expanded robustly within individuals during acute malaria and remained elevated after infection compared with pre–season baseline samples (**Figure 2c**). This expansion was attributable to several phenotypically distinct Vδ1⁺ subsets including an effector population (c22 Vd1 PD1hi), a proliferative population (c28 Vd1/2 MKI67), and a naïve–like population (c19 Vd1 TCF7lo) (**Figure 2d**). Prior study showed that repeated *P. falciparum* infections drove the clonal selection and expansion of circulating effector Vδ1⁺ T cells in controlled human malaria infection (CHMI). To investigate whether those phenotypic states represented a shared T cell differentiation continuum or independent lineages, we leveraged γδ TCR sequences to track clonotypes across clusters. Strikingly, γδ TCR clonotypes were highly shared among the effector populations (c22 Vd1 PD1hi and c23 Vd1 GNLY), the proliferative population (c28 Vd1/2 MKI67), and a small memory-precursor population (c21 Vd1 PD1lo), but displayed only minimal clonotype sharing with the naïve–like populations (**Figure 2e**). This suggests that prior infections established a pool of memory Vδ1⁺ T cells that preferentially contributed to effector responses upon reinfection. Effector Vδ1⁺ T cells with overlapping TCR clonotypes comprised two transcriptionally distinct cytotoxic populations, namely the c22 Vd1 PD1hi cluster expressing *EOMES*, *TOX*, *PDCD1*, and *IL10*, consistent with a Tr1–like program, whereas the c23 Vd1 GNLY cluster expressed *GNLY*, *PRF1*, and *IFNG*, consistent with a Th1–like cytotoxic program (**Figure 2f**). Notably, the relative abundance of these two effector populations remained proportionally stable across children aged 5 to 12 years residing in a malaria-endemic region (**Figure 2g**). Together, these data suggest that malaria exposure drives the expansion of two phenotypically distinct yet clonally related cytotoxic effector states and maintains these via a previously unappreciated memory–precursor Vδ1⁺ population.

Figure 2 Distinct effector Vδ1⁺ T cells are expanded in repeated malaria

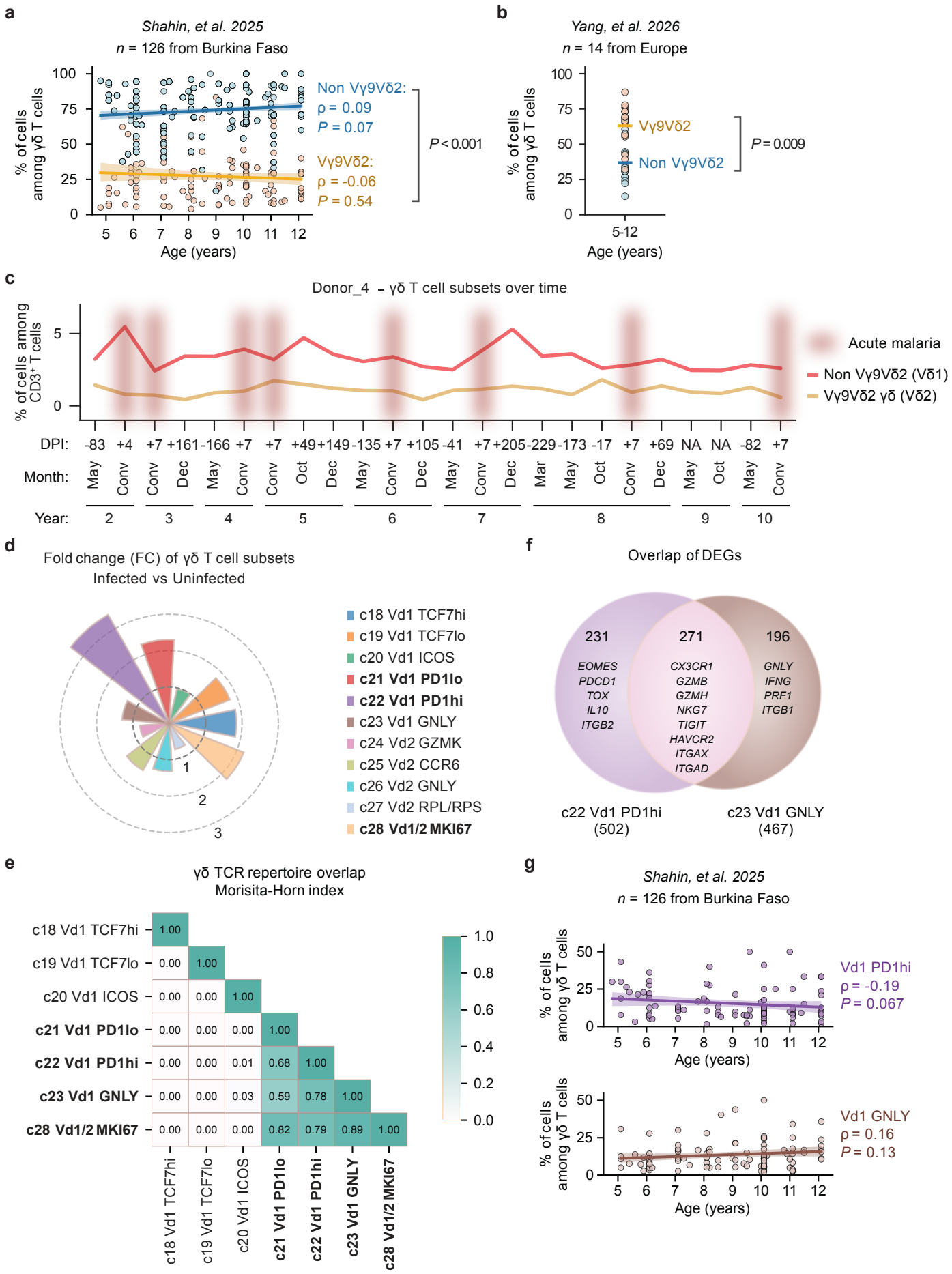


Figure 2. Distinct effector Vδ1$^+$ T cells are expanded in repeated malaria

a, Correlations between age and non-Vγ9Vδ2 γδ T (Vδ1) or Vγ9Vδ2 γδ T (Vδ2) frequency among γδ T cells in children residing in Burkina Faso were assessed using two-sided Spearman's rank correlation (ρ); ρ and *P* values are shown. Solid lines indicate the fitted trend and dashed lines denote the 95% confidence interval. Paired comparisons between Vδ1 and Vδ2 frequencies within donors were assessed using a two-sided paired t-test (*n* = 126 pairs, *P* < 0.001).

b, Frequencies of non-Vγ9Vδ2 γδ T (Vδ1) and Vγ9Vδ2 γδ T (Vδ2) among γδ T cells in children residing in Europe. Paired comparisons between Vδ1 and Vδ2 frequencies within donors were assessed using a two-sided paired t-test (*n* = 14 pairs, *P* = 0.009).

c, Frequencies of Vγ9Vδ2 γδ T (Vδ2) and non-Vγ9Vδ2 γδ T (Vδ1) cells in Donor_4 across the observation period. Acute malaria episodes are indicated.

d, Fold change (FC) of γδ T cell subsets in paired infected versus uninfected samples within each donor: Donor_1 (2018_conv vs 2018_may), Donor_2 (2015_conv vs 2015_oct), Donor_3 (2018_dec vs 2018_may), Donor_4 (2012_conv vs 2012_may). c18 Vd1 TCF7hi, *P* = 0.125; c22 Vd1 PD-1hi, *P* = 0.125; c28 Vd1/2 MKI67, *P* = 0.125. *P* values were calculated using a two-sided Wilcoxon matched-pairs signed-rank test with paired samples within each donor (n = 4 donor pairs).

e, γδ TCR repertoire similarity between clusters quantified by the Morisita–Horn index using TCR δ CDR3 amino acid sequences. Values range from 0 (minimum) to 1 (maximum) and are shown as a white-to-green gradient (0 = white, 1 = green).

f, Comparison of differentially expressed genes (DEGs) between c22 Vd1 PD1hi and c23 Vd1 GNLY clusters. c22-specific DEGs, n = 231; shared DEGs, n = 271; c23-specific DEGs, n = 196. Total DEGs: c22, n = 502; c23, n = 467. Immune-related gene examples are indicated.

g, Correlations between age and c22 Vd1 PD1hi and c23 Vd1 GNLY frequency among γδ T cells in children residing in Burkina Faso (*n* = 126) were assessed using two-sided Spearman's rank correlation (ρ); ρ and P values are shown. Solid lines indicate the fitted trend and dashed lines denote the 95% confidence interval.

Decade-long persistence of dominant Vδ1$^+$ clonotypes despite infection-associated repertoire remodeling

The stability and TCR repertoire overlap of Vδ1$^+$ effector states in exposed individuals suggested that malaria may maintain sustained clonal selection and self-renewal of the Vδ1$^+$ T cell repertoire. We therefore compared clonality across Vδ1$^+$ subsets and found that Vδ1$^+$ effector clusters (c22 Vδ1 PD1hi and c23 Vδ1 GNLY) showed higher clonality than naïve and memory Vδ1$^+$ populations (**Figure 3a, b**). To establish a baseline for longitudinal tracking, we then quantified clonality at the earliest observation timepoint and found that the γδ TCR repertoire at an age of 4-5 years was already dominated by a small number of Vδ1 clonotypes (**Figure 3c-e**), contrasting with the Vδ2 predominance reported in children from non-endemic regions. Strikingly, most expanded Vδ1$^+$ clonotypes persisted throughout the 10-year observation period, accompanied by few newly expanded Vδ1 and Vδ3 clonotypes that emerged after multiple infections and remained detectable in subsequent years (**Figure 3f**). In line with this, similarity analyses indicated that the Vδ1$^+$ TCR repertoire remained relatively stable over the decade, driven by the long-term persistence of dominant clonotypes (**Figure 3g, h**). Although repeated infections were associated with fluctuations in the broader Vδ1$^+$ repertoire, the established dominant clonotypes remained largely unchanged (Figure 3H). Thus, longitudinal clonal tracking supports that malaria-associated Vδ1$^+$ effector clones are long-lived and persist for at least a decade, rather than being reshaped de novo with each malaria episode.

Figure 3 Established Vδ1⁺ TCR repertoires persist over 10 years

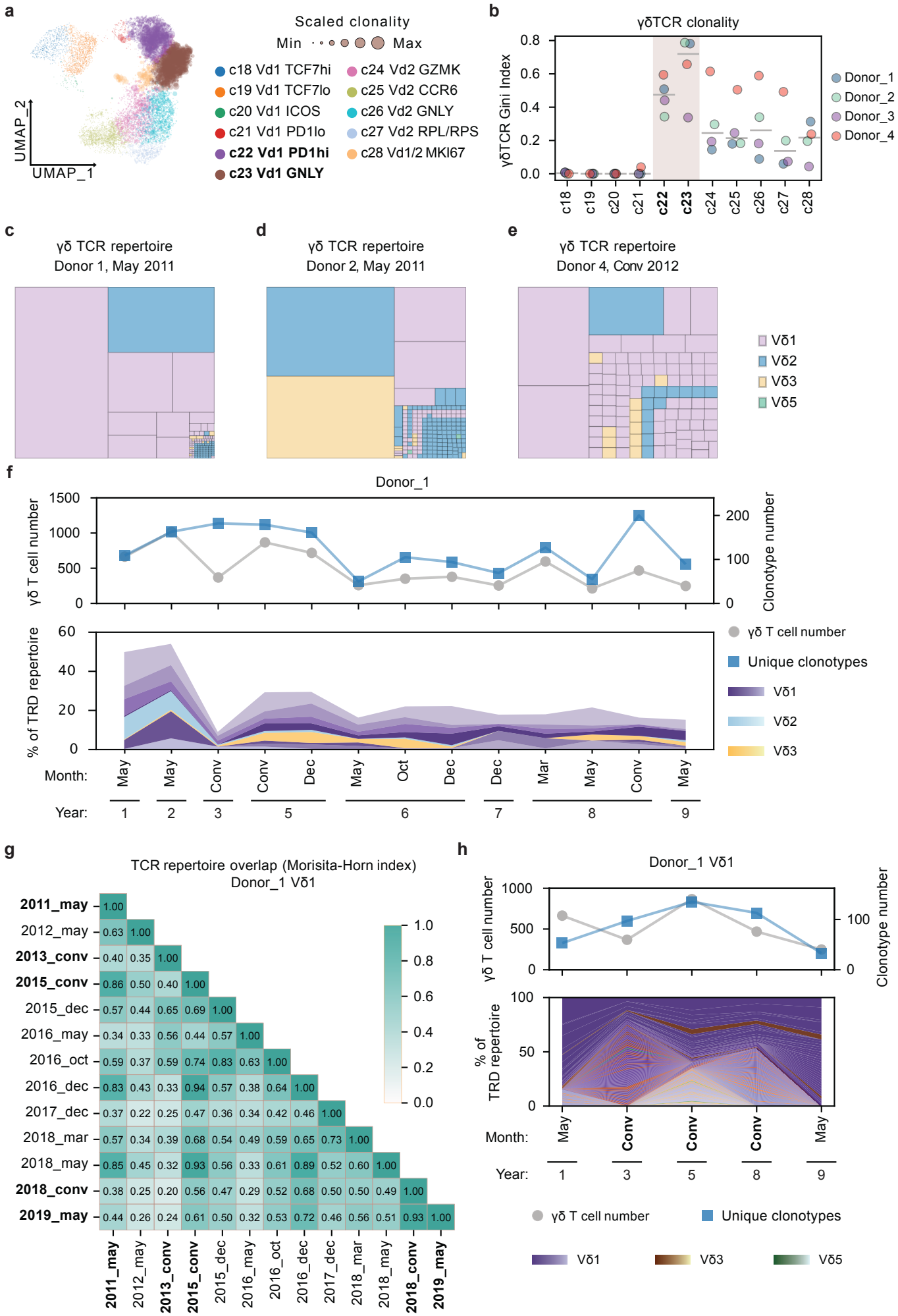


Figure 3. Established Vδ1$^+$ TCR repertoires persist over 10 years

a, Clonality of γδ TCR (TCR δ chain) on UMAP. Dot size indicates scaled clonality and colors denote clusters.

b, Gini index of γδ TCR (TCRδ chain) repertoires. Dots are colored by donor, and the gray line indicates the mean Gini index for each cluster.

c-e, Treemaps showing TCRδ CDR3 clonotype usage for the indicated samples. Clonotypes are colored by TCRδ chain usage.

f, Abundance of the top 10 γδ TCR (TCR δ chain) clones across the observation period in Donor_1. The line plot shows γδ T cell number (gray) and the number of unique TCRδ CDR3 clonotypes (blue) per sample. Clonotypes are colored by TCR δ chain usage. Conv indicates the convalescent period after acute infection.

g, γδ TCR repertoire similarity between timepoints quantified by the Morisita–Horn index using TCR δ CDR3 amino acid sequences. Values range from 0 (minimum) to 1 (maximum) and are shown as a white-to-green gradient (0 = white, 1 = green).

h, Abundance of Vδ1 TCR repertoire over the indicated timepoint (Donor_1). Conv represents convalescent period after acute infection. Line plot shows γδ T cell number (gray) and unique γδ TCR (TCR δ chain) clonotypes (blue) for each sample. Clonotypes are colored by TCR δ chain usage.

Vδ1$^+$ effector pool is maintained by self-proliferation and memory precursors across repeated malaria

The observed durable Vδ1$^+$ effector responses across repeated malaria provided a unique opportunity to investigate the mechanisms of their long-term persistence. Because the newly identified Vδ1$^+$ precursor-like cells shared a highly overlapping TCR repertoire with effector and proliferative populations (**Figures 2e, 4a**), we asked whether they contribute to sustaining Vδ1$^+$ effector responses. Using *PhyloVelo* to reconstruct γδ T cell clonal lineages, we identified two distinct differentiation trajectories (branch A: c21 Vd1 PD1lo to c22 Vd1 PD1hi; branch B: c28 Vd1/2 MKI67 to c23 Vd1 GNLY) (**Figure 4b**). Given the highly overlapping TCR repertoires of c22 Vδ1 PD1hi and c23 Vδ1 GNLY, we tested whether dominant Vδ1$^+$ clones switch between these effector programs over disease courses. Longitudinal tracking of the top expanded Vδ1$^+$ clonotypes revealed largely stable effector phenotypes across most timepoints, supporting the functional stability Vδ1$^+$ T cells during recurrent malaria (**Figure 4c, d**). Notably, clonal lineage tracing suggested that these expanded clones adopted a precursor-like memory program and transiently entered a proliferative state following acute malaria (**Figure 4b-d**). Collectively, these results suggest that Vδ1$^+$ effector persistence is maintained through self-proliferation and replenishment from a precursor-like reservoir.

Figure 4 Vδ1⁺ effector pool is maintained by self-proliferation and memory precursors

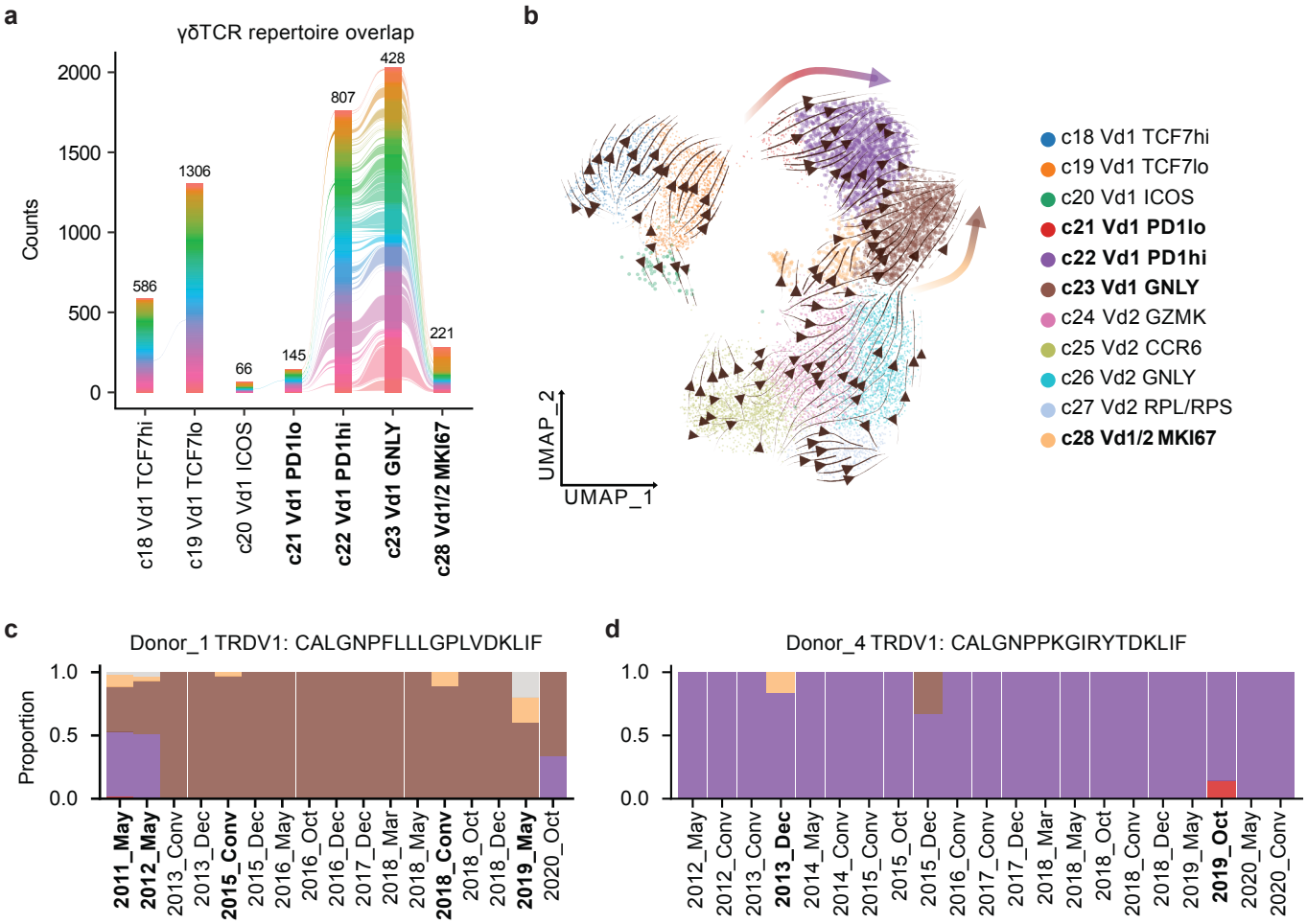


Figure 4. Effector Vδ1^{+} T cells are expanded in repeated malaria

a, Alluvial plots showing γδ TCR (TCR δ chain) clonal expansion and repertoire overlap. Bar height indicates clonotype count among all sequenced cells of each cluster, whereas color corresponds to phenotype. Bands connect clonotypes observed across multiple samples. The number of unique clonotypes for each cluster is indicated.

b, γδ TCR (TCR δ CDR3) clonotypes were used to trace clonal lineages, and phylogeny-informed transcriptomic velocity (*PhyloVelo*) was overlaid on the UMAP to visualize clonal trajectories. Black arrows indicate the forward *PhyloVelo* velocity field, pointing toward inferred future transcriptional states. The purple arrow highlights lineage 1 (c21 Vd1 PD1lo to c22 Vd1 PD1hi), and the yellow arrow highlights lineage 2 (c28 Vd1/2 MKI67 to c23 Vd1 GNLY).

c-d, Cell states of the indicated clonotype (TCR δ CDR3) across the indicated timepoints. Cells are colored by clusters as indicated in in (**b**).

Discussion

In contrast to Vγ9Vδ2 γδ T cells, which are phenotypically preprogrammed in utero[4,57], expand after birth[58,59], and persist into adulthood[3,60-62], Vδ1$^+$ γδ T cells are shaped by postnatal antigen exposure, showing individualized clonal expansions later in life[5,6,63]. Accumulating studies have revealed the persistence and functional durability of these clonally expanded Vδ1$^+$ T cells[16-18,20-23,26-30,44]. To define the mechanisms of this durability in humans, we systematically profiled long-lived Vδ1$^+$ T cells at single-cell, clonal–phenotypic resolution in a 10-year longitudinal cohort of children that were repeatedly exposed to seasonal malaria. We found that malaria-driven effector Vδ1$^+$ expansions are maintained through ongoing self-renewal and replenishment from a previously unappreciated memory-precursor population. Our study provides the first direct evidence that Vδ1$^+$ T cells can couple decade-long clonal stability with functional plasticity during repeated malaria.

Clonally expanded Vδ1$^+$ effectors remain remarkably stable over time, even after *P. falciparum* clearance[64]. Similarly focused adaptive γδ repertoires, dominated by a few high-frequency Vδ1 clonotypes, have also been reported in CMV[1-3,5-7,62,65], *Mtb*-infected individuals[9-11], and adults at steady state[62,66]. The driving force of these dominant expansions remains unclear, because the ligands are largely unknown. A plausible hypothesis, informed by γδ TCR ligands identified to date, is that infection-induced host-derived ligands persist beyond acute infection and provide sustained stimulation that preserves these adapted pools[67,68]. Even in the absence of defined ligands, several non-mutually exclusive mechanisms could contribute to the long-term maintenance of these individually effector Vδ1 pools, including (i) self-renewal of effector cells[5,69], reminiscent of long-lived tissue-resident invariant γδ T cell populations in mice[70-73]; (ii) enhanced survival programs, including expression of anti-apoptotic factors (e.g., *Bcl2a1*)[74], potentially linked to immune checkpoint receptor expression[18,20,21,23,26,75]; and (iii) a pool of 'stem-like' memory precursors, which in our data is by a precursor-like population characterized with the expression of *TCF7*, *TOX*, and *EOMES*[39,55].

The supernumerary proliferative potential of T cells has been demonstrated in an experimental mouse model with iterative immunization, where antigen-specific αβ T cells sustained recall proliferation and effector function for >10 years, despite acquiring canonical exhaustion-associated features[76]. As a major obstacle to long-term functional T cell longevity, T cell exhaustion characterized by constrained effector capacity, is closely linked to clinical outcomes in chronic infection and cancer, including responses to T cell–based immunotherapy[37,40,77,78]. In long-term responders to CD19 CAR T therapy, an early wave of Vδ1$^+$ CAR T cells expanded and persisted for more than 3 years during the initial response phase, before the CAR T compartment shifted into a decade-long remission phase dominated by proliferative, cytolytic CD4$^+$ CAR T cells with a Tr1-like phenotype[79]. Beyond their cytotoxic potential, Tr1 cells have paradoxically emerged as key immunoregulatory effectors that restrain excessive inflammation and limit immunopathology across autoimmunity, infection, transplantation, and immunotherapy[52]. In this study, we identified malaria-driven effector Vδ1$^+$ T cells (c22 Vd1 PD1hi) with Tr1-like signatures.

Consistent with phenotypic fidelity of Tr1, these expanded Vδ1 clonotypes maintained the regulatory transcriptional state across timepoints, indicating long-term stability of their effector programs[53,55,56]. Moreover, leveraging TCR-based lineage tracing, we uncovered a previously unappreciated precursor-like Vδ1$^+$ T (c21 Vd1 PD1lo) population that sustains the long-term effector pool. Together, these findings position Vδ1$^+$ T cells as long-lived effectors that mediate immune surveillance[80,81], warrant immune homeostasis[82], and with implications for γδ T cell–based immunotherapy[25].

γδ T cells contribute to both anti-parasite immunity and anti-disease tolerance during malaria[12-14,44,45,83-94]. Vδ2$^+$ γδ T cells can directly kill *P. falciparum*–infected erythrocytes through both TCR-dependent cytotoxicity and antibody-dependent cellular cytotoxicity (ADCC)[84,91,92]. However, this Vδ2-mediated anti-parasites responses may be accompanied by excessive inflammation, as repeated exposure with progressive loss and dysfunction of Vδ2$^+$ cells correlate with the development of asymptomatic infection in endemic settings[86]. In CHMI, repeated *P. falciparum* infection consistently drives clonal expansion of an adaptive γδ repertoire, highlighting the potential roles of Vδ1$^+$ T cells in acquiring long-term immunity to malaria[14]. Here we found that one donor (Donor_4), who experienced more frequent symptomatic malaria, was dominated by persistent Vδ2 clonotypes alongside a long-lived regulatory Vδ1$^+$ population (c22 Vd1 PD1hi), which could contribute to limiting excessive inflammation. In contrast, donors with less frequent symptomatic malaria showed preferential persistence of a cytotoxic Vδ1$^+$ population (c23 Vδ1 GNLY). Together, these observations strongly support a link between durable Vδ1$^+$ γδ T cell responses and clinical immunity to malaria[88], although validation in larger cohorts will be required.

The protective memory potential of γδ T cells has been demonstrated in mice[70-73] and macaques[95], but it remains poorly defined in humans because γδ T cell responses to most infections are not well characterized and longitudinal cohorts capturing naturally repeated exposure are limited. Malaria provides an ideal framework to address this question: it triggers strong acute immune activation and, with repeated exposure in endemic settings, robustly drives clonal expansion of Vδ1$^+$ T cells[12,14,83,93]. Importantly, malaria is predominantly a blood-borne infection, making serial sampling highly feasible[90]—whereas in many other settings, such as solid tumors, adaptive γδ T cells are largely tissue-resident and thus difficult to sample repeatedly over time. By revealing the cellular programs underpinning the long-term Vδ1$^+$ T cell persistence, our work shows that human adaptive γδ T cells can adapt a memory-like program akin to αβ T cells and points to a strategy for leveraging these durable responses in malaria vaccine development.

Methods

scRNA-seq library preparation and sequencing

All CD3+ T cells were sorted from frozen PBMC samples. The sorted cells were fixed and permeabilized using Evercode™ Cell Fixation v2 (Parse Biosciences, Cat. ECF2001) following the manufacturer's protocol. Fixed cells were stored at −80°C. All samples were then processed together to prepare single-cell libraries using one Evercode TCR Mega, Human TCR + WT Kit (Parse Biosciences, Cat. ECIT3500), according to the manufacturer's instructions. Fifteen sub-libraries were sequenced on the Illumina NovaSeqX 25B flow cell platform using PE150 chemistry with a sequencing depth of 25,000 reads per cell.

scRNA-seq analysis

Raw fastq data were aligned to human genome assembly GRCh38 (hg38) and quantified using split-pipe software suite (Parse Biosciences, v1.4.0). The filtered feature-barcode matrices containing only cellular barcodes were used for further analysis. Single cell gene expression matrices were analyzed using Scanpy (v1.9.6). Detailed parameters for data clean and dimensional reduction are shown in **Supplementary Methods**.

Statistical analysis

Statistical analyses were performed using Python (v3.8.10) with the scipy package (v1.10.1).

Code and data sharing statement

Single-cell sequencing raw data have been deposited in the Gene Expression Omnibus (GEO) under accession number GSExxx. To review GEO accession GSExxx: Go to xxx and enter token (xxx) into the box. Processed single-cell AnnData objects are available at Zenodo (xxx). Code for data processing and analysis is deposited on GitHub (xxx). All data and code for reproducibility will be made publicly available upon manuscript acceptance.

Acknowledgments

We thank the flow cytometry core facility (University Medical Center Hamburg-Eppendorf, Hamburg) for providing proficient support with FACS sorting. Some elements of the schematic diagrams (Fig. 1A) and the graphical abstract were created using BioRender.com.

This work was supported by Deutsche Forschungsgemeinschaft (DFG, project numbers 264599542, 395236335 /FOR2799, 431861465, and 497674564 to I.P.).

Authorship contributions

Z.S. performed single-cell library preparation, conducted computational analyses, generated figures, wrote the manuscript, and conceptualized the study.

tba

I.P. conceptualized and designed the study, supervised the project, and revised the manuscript.

Conflict of interest disclosures

The authors declare no conflict of interest.

References

1 Déchanet, J. *et al.* Major expansion of γδ T lymphocytes following cytomegalovirus infection in kidney allograft recipients. *J Infect Dis* **179**, 1-8 (1999). https://doi.org:10.1086/314568

2 Déchanet, J. *et al.* Implication of gammadelta T cells in the human immune response to cytomegalovirus. *J Clin Invest* **103**, 1437-1449 (1999). https://doi.org:10.1172/jci5409

3 Pitard, V. *et al.* Long-term expansion of effector/memory Vδ2$^-$ γδ T cells is a specific blood signature of CMV infection. *Blood* **112**, 1317-1324 (2008). https://doi.org:10.1182/blood-2008-01-136713

4 Vermijlen, D. *et al.* Human cytomegalovirus elicits fetal gamma delta T cell responses in utero. *Journal of Experimental Medicine* **207**, 807-821 (2010). https://doi.org:10.1084/jem.20090348

5 Davey, M. S. *et al.* Clonal selection in the human Vδ1 T cell repertoire indicates γδ TCR-dependent adaptive immune surveillance. *Nature communications* **8** (2017). https://doi.org:10.1038/ncomms14760

6 Ravens, S. *et al.* Human gammadelta T cells are quickly reconstituted after stem-cell transplantation and show adaptive clonal expansion in response to viral infection. *Nat Immunol* **18**, 393-401 (2017). https://doi.org:10.1038/ni.3686

7 Deseke, M. *et al.* A CMV-induced adaptive human Vδ1$^+$ γδ T cell clone recognizes HLA-DR. *The Journal of experimental medicine* **219** (2022). https://doi.org:10.1084/jem.20212525

8 Davey, M. S. *et al.* The human Vdelta2(+) T-cell compartment comprises distinct innate-like Vgamma9(+) and adaptive Vgamma9(-) subsets. *Nat Commun* **9**, 1760 (2018). https://doi.org:10.1038/s41467-018-04076-0

9 Roy Chowdhury, R. *et al.* NK-like CD8$^+$ γδ T cells are expanded in persistent Mycobacterium tuberculosis infection. *Science Immunology* **8**, eade3525 (2023). https://doi.org:10.1126/sciimmunol.ade3525

10 Kearns, K. *et al.* Enrichment of a CD4$^-$CD8$^-$ NK-like cytotoxic Vδ1/3 T cell subset in tuberculosis disease. *bioRxiv* (2025). https://doi.org:10.1101/2025.11.12.688134

11 Maerz, M. D. *et al.* BCG vaccination induces antibacterial effector functions among Vδ1/3 T cells that are associated with protection against tuberculosis. *Cell Rep Med*, 102536 (2026). https://doi.org:10.1016/j.xcrm.2025.102536

12 Hviid, L., Smith-Togobo, C. & Willcox, B. E. Human Vδ1^{+} T Cells in the Immune Response to *Plasmodium falciparum* Infection. *Frontiers in immunology* **10** (2019). https://doi.org:10.3389/fimmu.2019.00259

13 Rutishauser, T. *et al.* Activation of TCR Vδ1^{+} and Vδ1^{-}Vδ2^{-} γδ T Cells upon Controlled Infection with *Plasmodium falciparum* in Tanzanian Volunteers. *Journal of Immunology* **204**, 180-191 (2020). https://doi.org:10.4049/jimmunol.1900669

14 von Borstel, A. *et al.* Repeated Plasmodium falciparum infection in humans drives the clonal expansion of an adaptive γδ T cell repertoire. *Science Translational Medicine* **13**, eabe7430 (2021). https://doi.org:doi:10.1126/scitranslmed.abe7430

15 Halary, F. *et al.* Shared reactivity of Vδ2neg γδ T cells against cytomegalovirus-infected cells and tumor intestinal epithelial cells. *The Journal of experimental medicine* **201**, 1567-1578 (2005). https://doi.org:10.1084/jem.20041851

16 Airoldi, I. *et al.* γδ T-cell reconstitution after HLA-haploidentical hematopoietic transplantation depleted of TCR-αβ+/CD19+ lymphocytes. *Blood* **125**, 2349-2358 (2015). https://doi.org:10.1182/blood-2014-09-599423

17 Benveniste, P. M. *et al.* Generation and molecular recognition of melanoma-associated antigen-specific human γδ T cells. *Science Immunology* **3**, eaav4036 (2018). https://doi.org:doi:10.1126/sciimmunol.aav4036

18 Wu, Y. *et al.* An innate-like Vδ1^{+} γδ T cell compartment in the human breast is associated with remission in triple-negative breast cancer. *Science Translational Medicine* **11**, eaax9364 (2019). https://doi.org:doi:10.1126/scitranslmed.aax9364

19 Makkouk, A. *et al.* Off-the-shelf Vδ1 γδ T cells engineered with glypican-3 (GPC-3)-specific chimeric antigen receptor (CAR) and soluble IL-15 display robust antitumor efficacy against hepatocellular carcinoma. *J Immunother Cancer* **9** (2021). https://doi.org:10.1136/jitc-2021-003441

20 Wu, Y. *et al.* A local human Vδ1 T cell population is associated with survival in nonsmall-cell lung cancer. *Nature Cancer* (2022). https://doi.org:10.1038/s43018-022-00376-z

21 de Vries, N. L. *et al.* γδ T cells are effectors of immunotherapy in cancers with HLA class I defects. *Nature* **613**, 743-750 (2023). https://doi.org:10.1038/s41586-022-05593-1

22 Harmon, C. *et al.* γδ T cell dichotomy with opposing cytotoxic and wound healing functions in human solid tumors. *Nat Cancer* **4**, 1122-1137 (2023). https://doi.org:10.1038/s43018-023-00589-w

23 Rancan, C. *et al.* Exhausted intratumoral Vδ2^{-} γδ T cells in human kidney cancer retain effector function. *Nat Immunology* (2023). https://doi.org:10.1038/s41590-023-01448-7

24 Davies, D. *et al.* PD-1 defines a distinct, functional, tissue-adapted state in Vδ1+ T cells with implications for cancer immunotherapy. *Nature Cancer* **5**, 1-1 (2024). https://doi.org:10.1038/s43018-023-00690-0

25 Hayday, A., Dechanet-Merville, J., Rossjohn, J. & Silva-Santos, B. Cancer immunotherapy by γδ T cells. *Science* **386**, eabq7248 (2024). https://doi.org:doi:10.1126/science.abq7248

26 Lien, S. C. *et al.* Tumor reactive γδ T cells contribute to a complete response to PD-1 blockade in a Merkel cell carcinoma patient. *Nature communications* **15** (2024). https://doi.org:10.1038/s41467-024-45449-y

27 Mensurado, S. *et al.* CD155/PVR determines acute myeloid leukemia targeting by Delta One T cells. *Blood* **143**, 1488-1495 (2024). https://doi.org:10.1182/blood.2023022992

28 Blanco-Domínguez, R. *et al.* Dual modulation of cytotoxic and checkpoint receptors tunes the efficacy of adoptive Delta One T cell therapy against colorectal cancer. *Nature Cancer* **6** (2025). https://doi.org:10.1038/s43018-025-00948-9

29 Scheper, W. *et al.* γδT cells elicited by CMV reactivation after allo-SCT cross-recognize CMV and leukemia. *Leukemia* **27**, 1328-1338 (2013). https://doi.org:10.1038/leu.2012.374

30 Mikulak, J. *et al.* NKp46-expressing human gut-resident intraepithelial Vδ1 T cell subpopulation exhibits high antitumor activity against colorectal cancer. *JCI Insight* **4** (2019). https://doi.org:10.1172/jci.insight.125884

31 Hao, Q. *et al.* A pan-cancer single cell landscape reveals heterogeneity and functional diversity of double-negative T cells. *Mol Cancer* (2026). https://doi.org:10.1186/s12943-025-02548-8

32 Davey, M. S. *et al.* Clonal selection in the human Vdelta1 T cell repertoire indicates gammadelta TCR-dependent adaptive immune surveillance. *Nat Commun* **8**, 14760 (2017). https://doi.org:10.1038/ncomms14760

33 Moskophidis, D., Lechner, F., Pircher, H. & Zinkernagel, R. M. Virus persistence in acutely infected immunocompetent mice by exhaustion of antiviral cytotoxic effector T cells. *Nature* **362**, 758-761 (1993). https://doi.org:10.1038/362758a0

34 Lee, P. P. *et al.* Characterization of circulating T cells specific for tumor-associated antigens in melanoma patients. *Nature Medicine* **5**, 677-685 (1999). https://doi.org:10.1038/9525

35 Utzschneider, D. T. *et al.* T Cell Factor 1-Expressing Memory-like CD8⁺ T Cells Sustain the Immune Response to Chronic Viral Infections. *Immunity* **45**, 415-427 (2016). https://doi.org:10.1016/j.immuni.2016.07.021

36 Hashimoto, M. *et al.* CD8 T Cell Exhaustion in Chronic Infection and Cancer: Opportunities for Interventions. *Annu Rev Med* **69**, 301-318 (2018). https://doi.org:10.1146/annurev-med-012017-043208

37 Blank, C. U. *et al.* Defining 'T cell exhaustion'. *Nature reviews. Immunology* **19**, 665-674 (2019). https://doi.org:10.1038/s41577-019-0221-9

38 McLane, L. M., Abdel-Hakeem, M. S. & Wherry, E. J. CD8 T Cell Exhaustion During Chronic Viral Infection and Cancer. *Annual review of immunology* **37**, 457-495 (2019). https://doi.org:10.1146/annurev-immunol-041015-055318

39 Zehn, D., Thimme, R., Lugli, E., de Almeida, G. P. & Oxenius, A. 'Stem-like' precursors are the fount to sustain persistent $CD8^+$ T cell responses. *Nat Immunology* **23**, 836-847 (2022). https://doi.org:10.1038/s41590-022-01219-w

40 Sun, Q. & Dong, C. Regulators of CD8(+) T cell exhaustion. *Nature reviews. Immunology* (2025). https://doi.org:10.1038/s41577-025-01221-x

41 Utzschneider, D. T. *et al.* Early precursor T cells establish and propagate T cell exhaustion in chronic infection. *Nature immunology* **21**, 1256-1266 (2020). https://doi.org:10.1038/s41590-020-0760-z

42 Chu, T. *et al.* Precursors of exhausted T cells are pre-emptively formed in acute infection. *Nature* **640**, 782-792 (2025). https://doi.org:10.1038/s41586-024-08451-4

43 McManus, D. T. *et al.* An early precursor $CD8^+$ T cell that adapts to acute or chronic viral infection. *Nature* **640**, 772-781 (2025). https://doi.org:10.1038/s41586-024-08562-y

44 Teirlinck, A. C. *et al.* Longevity and Composition of Cellular Immune Responses Following Experimental Plasmodium falciparum Malaria Infection in Humans. *PLoS pathogens* **7** (2011). https://doi.org:10.1371/journal.ppat.1002389

45 Taniguchi, T. *et al.* A Unique Subset of γδ T Cells Expands and Produces IL-10 in Patients with Naturally Acquired Immunity against Falciparum Malaria. *Frontiers in Microbiology* **8** (2017). https://doi.org:10.3389/fmicb.2017.01288

46 Groux, H. *et al.* A $CD4^+$T-cell subset inhibits antigen-specific T-cell responses and prevents colitis. *Nature* **389**, 737-742 (1997). https://doi.org:10.1038/39614

47 Couper, K. N. *et al.* IL-10 from $CD4^+CD25^-Foxp3^-CD127^-$ adaptive regulatory T cells modulates parasite clearance and pathology during malaria infection. *Plos Pathogens* (2008). https://doi.org:10.1371/journal.ppat.1000004

48 Jagannathan, P. *et al.* IFNγ/IL-10 Co-producing Cells Dominate the CD4 Response to Malaria in Highly Exposed Children. *Plos Pathogens* (2014). https://doi.org:10.1371/journal.ppat.1003864

49 Boyle, M. J. *et al.* The Development of Plasmodium falciparum-specific IL10 CD4 T Cells and Protection from Malaria in Children in an Area of High Malaria Transmission. *Frontiers in Immunology* (2017). https://doi.org:10.3389/fimmu.2017.01329

50 Levings, M. K. *et al.* IFN-α and IL-10 induce the differentiation of human type 1 T regulatory cells. *Journal of Immunology* (2001).

51 Zhang, P. *et al.* Eomesodermin promotes the development of type 1 regulatory T (T_R1) cells. *Science Immunology* **2**, eaah7152 (2017). https://doi.org:doi:10.1126/sciimmunol.aah7152

52 Freeborn, R. A., Strubbe, S. & Roncarolo, M. G. Type 1 regulatory T cell-mediated tolerance in health and disease. *Frontiers in Immunology* (2022). https://doi.org:10.3389/fimmu.2022.1032575

53 Edwards, C. L. *et al.* IL^-10^-producing Th1 cells possess a distinct molecular signature in malaria. *Journal of Clinical Investigation* (2023). https://doi.org:10.1172/jci169299

54 Munoz Sandoval, D. *et al.* Plasmodium falciparum infection induces T cell tolerance that is associated with decreased disease severity upon re-infection. *The Journal of experimental medicine* **222** (2025). https://doi.org:10.1084/jem.20241667

55 Zhang, P. *et al.* $Eomesodermin^+$ $CD4^+$ T cells are critical for curative immunotherapy outcomes. *Immunity* **58**, 3024-3039 e3027 (2025). https://doi.org:10.1016/j.immuni.2025.09.004

56 Nideffer, J. *et al.* Clone tracking through repeated malaria identifies high-fidelity memory CD4 T cell responses. *Science Immunology* **10**, eads2957 (2025). https://doi.org:doi:10.1126/sciimmunol.ads2957

57 Dimova, T. *et al.* Effector Vγ9Vδ2 T cells dominate the human fetal γδ T-cell repertoire. *Proceedings of the National Academy of Sciences of the United States of America* **112**, E556-E565 (2015). https://doi.org:10.1073/pnas.1412058112

58 Papadopoulou, M. *et al.* Fetal public Vγ9Vδ2 T cells expand and gain potent cytotoxic functions early after birth. *Proceedings of the National Academy of Sciences of the United States of America* **117**, 18638-18648 (2020). https://doi.org:10.1073/pnas.1922595117

59 Ravens, S. *et al.* Microbial exposure drives polyclonal expansion of innate gamma delta T cells immediately after birth. *Proceedings of the National Academy of Sciences of the United States of America* **117**, 18649-18660 (2020). https://doi.org:10.1073/pnas.1922588117

60 Tan, L. K. *et al.* A fetal wave of human type 3 effector gamma delta cells with restricted TCR diversity persists into adulthood. *Science Immunology* **6** (2021). https://doi.org:10.1126/sciimmunol.abf0125

61 Ryan, P. L. *et al.* Heterogeneous yet stable $V\delta2^{(+)}$ T-cell profiles define distinct cytotoxic effector potentials in healthy human individuals. *Proceedings of the National Academy of Sciences of the United States of America* **113**, 14378-14383 (2016). https://doi.org:10.1073/pnas.1611098113

62 Davey, M. S. *et al.* The human $V\delta2^{+}$ T-cell compartment comprises distinct innate-like $V\gamma9^{+}$ and adaptive $V\gamma9^{-}$ subsets. *Nature communications* **9** (2018). https://doi.org:10.1038/s41467-018-04076-0

63 Ravens, S. *et al.* Human γδ T Cell Receptor Repertoires in Peripheral Blood Remain Stable Despite Clearance of Persistent Hepatitis C Virus Infection by Direct-Acting Antiviral Drug Therapy. *Frontiers in immunology* **9** (2018). https://doi.org:10.3389/fimmu.2018.00510

64 . (!!! INVALID CITATION !!! 11-13,42,43,46,52,62-68).

65 Willcox, C. R. *et al.* Cytomegalovirus and tumor stress surveillance by binding of a human γδ T cell antigen receptor to endothelial protein C receptor. *Nature Immunology* **13**, 872-879 (2012). https://doi.org:10.1038/ni.2394

66 Hviid, L. *et al.* High frequency of circulating γδ T cells with dominance of the Vδ1 subset in a healthy population. *International immunology* **12**, 797-805 (2000). https://doi.org:10.1093/intimm/12.6.797

67 Willcox, B. E. & Willcox, C. R. γδ TCR ligands: the quest to solve a 500-million-year-old mystery. *Nature Immunology* **20**, 121-128 (2019). https://doi.org:10.1038/s41590-018-0304-y

68 Deseke, M. & Prinz, I. Ligand recognition by the γδ TCR and discrimination between homeostasis and stress conditions. *Cellular & Molecular Immunology* **17**, 914-924 (2020). https://doi.org:10.1038/s41423-020-0503-y

69 Pizzolato, G. *et al.* Single-cell RNA sequencing unveils the shared and the distinct cytotoxic hallmarks of human TCRVdelta1 and TCRVdelta2 gammadelta T lymphocytes. *Proceedings of the National Academy of Sciences of the United States of America* **116**, 11906-11915 (2019). https://doi.org:10.1073/pnas.1818488116

70 Sheridan, Brian S. *et al.* γδ T Cells Exhibit Multifunctional and Protective Memory in Intestinal Tissues. *Immunity* **39**, 184-195 (2013). https://doi.org:https://doi.org/10.1016/j.immuni.2013.06.015

71 Murphy, A. G. *et al.* Staphylococcus aureus Infection of Mice Expands a Population of Memory γδ T Cells That Are Protective against Subsequent Infection. *The Journal of Immunology* **192**, 3697-3708 (2014). https://doi.org:10.4049/jimmunol.1303420

72 Hartwig, T., Pantelyushin, S., Croxford, A. L., Kulig, P. & Becher, B. Dermal IL-17-producing gamma delta T cells establish long-lived memory in the skin. *European Journal of Immunology* **45**, 3022-3033 (2015). https://doi.org:10.1002/eji.201545883

73 Ramirez-Valle, F., Gray, E. E. & Cyster, J. G. Inflammation induces dermal Vγ4^{+} γδ T17 memory-like cells that travel to distant skin and accelerate secondary IL-17-driven responses. *Proceedings of the National Academy of Sciences of the United States of America* **112**, 8046-8051 (2015). https://doi.org:10.1073/pnas.1508990112

74 Tan, L. K. *et al.* Single-Cell Transcriptomics Identifies the Adaptation of Scart1^{+}Vγ6^{+} T Cells to Skin Residency as Activated Effector Cells. *Cell reports* **27**, 3657-+ (2019). https://doi.org:10.1016/j.celrep.2019.05.064

75 Catafal-Tardos, E. *et al.* Dynamics of checkpoint receptors in γδ T cell subsets are associated with clinical response during anti-PD-1 immunotherapies. *EMBO Mol Med* **18**, 91-119 (2026). https://doi.org:10.1038/s44321-025-00338-9

76 Soerens, A. G. *et al.* Functional T cells are capable of supernumerary cell division and longevity. *Nature* **614**, 762-766 (2023). https://doi.org:10.1038/s41586-022-05626-9

77 June, C. H., O'Connor, R. S., Kawalekar, O. U., Ghassemi, S. & Milone, M. C. CAR T cell immunotherapy for human cancer. *Science* **359**, 1361-1365 (2018). https://doi.org:doi:10.1126/science.aar6711

78 Bai, Z. *et al.* Single-cell CAR T atlas reveals type 2 function in 8-year leukaemia remission. *Nature* **634**, 702-711 (2024). https://doi.org:10.1038/s41586-024-07762-w

79 Melenhorst, J. J. *et al.* Decade-long leukaemia remissions with persistence of CD4(+) CAR T cells. *Nature* **602**, 503-509 (2022). https://doi.org:10.1038/s41586-021-04390-6

80 Vantourout, P. & Hayday, A. Six-of-the-best: unique contributions of γδ T cells to immunology. *Nature Reviews Immunology* **13**, 88-100 (2013). https://doi.org:10.1038/nri3384

81 Hayday, A. C. γδ T Cell Update: Adaptate Orchestrators of Immune Surveillance. *Journal of Immunology* **203**, 311-320 (2019). https://doi.org:10.4049/jimmunol.1800934

82 Nielsen, M. M., Witherden, D. A. & Havran, W. L. gamma delta T cells in homeostasis and host defence of epithelial barrier tissues. *Nature Reviews Immunology* **17**, 733-745 (2017). https://doi.org:10.1038/nri.2017.101

83 Marsh, K. & Kinyanjui, S. Immune effector mechanisms in malaria. *Parasite Immunology* **28**, 51-60 (2006). https://doi.org:10.1111/j.1365-3024.2006.00808.x

84 Costa, G. *et al.* Control of Plasmodium falciparum erythrocytic cycle: γδ T cells target the red blood cell–invasive merozoites. *Blood* **118**, 6952-6962 (2011). https://doi.org:10.1182/blood-2011-08-376111

85 Seder, R. A. *et al.* Protection Against Malaria by Intravenous Immunization with a Nonreplicating Sporozoite Vaccine. *Science* **341**, 1359-1365 (2013). https://doi.org:doi:10.1126/science.1241800

86 Jagannathan, P. *et al.* Loss and dysfunction of $V\delta2^+$ γδ T cells are associated with clinical tolerance to malaria. *Science Translational Medicine* **6**, 251ra117-251ra117 (2014). https://doi.org:doi:10.1126/scitranslmed.3009793

87 Ishizuka, A. S. *et al.* Protection against malaria at 1 year and immune correlates following PfSPZ vaccination. *Nature Medicine* **22**, 614-+ (2016). https://doi.org:10.1038/nm.4110

88 Zaidi, I. *et al.* γδ T Cells Are Required for the Induction of Sterile Immunity during Irradiated Sporozoite Vaccinations. *Journal of immunology (Baltimore, Md. : 1950)* **199**, 3781-3788 (2017). https://doi.org:10.4049/jimmunol.1700314

89 Mamedov, M. R. *et al.* A Macrophage Colony-Stimulating-Factor-Producing gamma delta T Cell Subset Prevents Malarial Parasitemic Recurrence. *Immunity* **48**, 350-+ (2018). https://doi.org:10.1016/j.immuni.2018.01.009

90 Kurup, S. P., Butler, N. S. & Harty, J. T. T cell-mediated immunity to malaria. *Nature Reviews Immunology* (2019). https://doi.org:10.1038/s41577-019-0158-z

91 Farrington, L. A. *et al.* Opsonized antigen activates Vδ2+T cells via CD16/FCγRIIIa in individuals with chronic malaria exposure. *Plos Pathogens* **16** (2020). https://doi.org:10.1371/journal.ppat.1008997

92 Junqueira, C. *et al.* γδ T cells suppress *Plasmodium falciparum* blood-stage infection by direct killing and phagocytosis. *Nature immunology* **22**, 347-+ (2021). https://doi.org:10.1038/s41590-020-00847-4

93 León-Lara, X. *et al.* Evidence for an Adult-Like Type 1-Immunity Phenotype of Vδ1, Vδ2 and Vδ3 T Cells in Ghanaian Children With Repeated Exposure to Malaria. *Frontiers in immunology* **13** (2022). https://doi.org:10.3389/fimmu.2022.807765

94 Sissoko, M. S. *et al.* Safety and efficacy of a three-dose regimen of Plasmodium falciparum sporozoite vaccine in adults during an intense malaria transmission season in Mali: a randomised, controlled phase 1 trial. *The Lancet Infectious Diseases* **22**, 377-389 (2022). https://doi.org:https://doi.org/10.1016/S1473-3099(21)00332-7

95 Shen, Y. *et al.* Adaptive Immune Response of Vγ2Vδ2^{+} T Cells During Mycobacterial Infections. *Science* **295**, 2255-2258 (2002). https://doi.org:doi:10.1126/science.1068819

Chapter 5: Discussion

5.1 Clonal Tracking Unlocks Novel Insights into Immunity

Single-cell TCR clonal tracking has been employed to longitudinally track individual T cell clones in infections[118,205], vaccinations[206-208], and cancer[119,209]. The integration of transcriptome and clonotypes enables characterization of T cell differentiation, persistence, functional states, and lineage relationships at single-cell resolution[116].

In this dissertation, we employed TCR tracking to investigate the long-term maintenance of graft-derived T cells and showed that both $CD8^+$ αβ and γδ T cells remain detectable after transplantation while displaying alloreactivity characterized with increased proliferation and metabolic activities. In parallel, we used TCR tracking to investigate γδ T cell dynamics in children living in a malaria-endemic region and uncovered the decade-long persistence of adaptive effector γδ T cells, sustained by self-proliferation and a previously unrecognized precursor-memory population, thereby deepening our understanding of the mechanisms underlying γδ T cell longevity. Similarly, TCR clonal tracking has been used to demonstrate the high clonal fidelity of $CD4^+$ αβ T cells during repeated malaria, showing that most clonotypes maintain stable subset identities over time and that Tr1 cells dominate the parasite-specific memory $CD4^+$ T cell response[118].

In $CD8^+$ T cells, clonal tracking has further revealed that clonally related progenitor populations in the tumor draining lymph nodes sustain the long-term persistence of tumor-specific T cells during immune checkpoint blockade, highlighting lineage coupling between lymphoid and intratumoral T cell states[119]. Similarly, recent cross-tissue TCR repertoire comparisons revealed that Trm and tumor-associated Tex cells are clonally distinct, thereby helping define the lineage architecture and functional T cell subsets that contribute to anti-tumor immunity[120,210]. Such concept extends to tumor-reactive γδ T cells, as the TCR repertoires of melanoma-infiltrating γδ T cells and peripheral blood γδ T cells are highly overlapped indicating clonal relatedness across circulating and intratumoral compartments[121].

Clonal tracking has also been extended to NK cells by using somatic mitochondrial DNA mutations as endogenous molecular barcodes, revealing substantial clonal expansion of adaptive NK cells in HCMV-seropositive individuals[211-213]. Similarly, longitudinal CAR T cell clonal tracking through lentiviral vector integration site (LVIS) analysis have revealed that the expansion, persistence, and eventual clonal focusing of distinct CAR T cell subsets, including

highly activated cytotoxic $CD4^+$ T cell populations which are linked to the therapeutic efficacy and long-term remission[214].

In summary, single-cell clonal tracking has emerged as a powerful approach for investigating T cell responses in cancer and infection, providing a more precise, robust, and broadly feasible framework than conventional FACS- or function-based assays, particularly for γδ T cells, whose cognate ligands remain largely unknown.

5.2 T Cell Composition and TCR Repertoire Predict AlloHSCT Outcomes

In **Chapter 3**, we showed that the phenotypes of both αβ and γδ T cells were strongly associated with alloHSCT outcomes. Particularly increased frequencies of *ADGRG1* cytotoxic αβ and γδ T cells in peripheral blood at an early post-alloHSCT stage were linked to improved relapse-free survival in patients with AML[215,216]. A similar population was also detected in the bone marrow, where it showed comparable associations with clinical outcome[217]. These cells are clonally expanded and terminally differentiated and partially from graft as revealed by TCR clonal tracking[218]. This raises the debate that whether these cells are mediating anti-leukemia activity or just function as a biomarker although the direct kill leukemia blast capacity has been revealed by in vitro functional assay[109,112,137]. One potential explanation is the cross-reactivity of TCR as has been observed for CMV-reactive γδ TCR[219].

However, whether this pronounced cytotoxicity is linked to GvHD remains to be fully determined, particularly given the reported positive association between graft-versus-leukemia (GvL) and graft-versus-host disease (GvHD)[126,127,220,221]. To address this challenge, multiple graft-engineering strategies has been explored. Notably, one clinical trial using αβ T cell- and B cell-depleted grafts in pediatric leukemia demonstrated improved GVHD-free, relapse-free survival (GRFS), consistent with observations that enhanced early γδ T cell reconstitution is associated with superior outcomes[110,112,137]. These findings highlight the need to dissect graft T cell composition in greater detail. In this context, our study provides a framework for profiling graft-derived T cell phenotypes and clonotypes at single-cell resolution, thereby enabling a more precise definition of the cellular populations linked to beneficial versus adverse alloHSCT outcomes[136].

Beyond clonal tracking, immune receptor sequencing has recently been applied to disease classification. The next step would be to exploit T cell phenotypes and repertoire features for disease outcome prediction[222-228]. This approach is particularly attractive because integration of T cell phenotype with immune repertoire could precisely dissect functional T cell states involved in GvL or GvHD, thereby connecting immune identity with disease prognosis and treatment response. Specifically, given our finding that γδ T cells adapt to a stable phenotype and repertoire to perform long-term immunosurveillance and their reported beneficial roles in anti-leukemia, employing the γδ TCR repertories combined with their phenotypes to predict the outcomes of alloHSCT would be a promising direction.

In the long term, this concept could be translated into a clinically relevant tool for assessing graft quality, based on the premise that the cellular composition and functional properties of graft-derived T cells shape post-transplant immune responses. Accordingly, future studies in large cohorts should focus on establishing a robust scoring system that integrates T cell composition, repertoire features, and clinical parameters to evaluate graft quality, inform graft engineering, and support early clinical interventions aimed at improving alloHSCT outcomes.

5.3 The Need for a Cross-Tissue, Pan-Disease Human γδ T Cell Atlas

In **Chapter 4**, we identified two new peripheral γδ T cell subsets, termed 'stem-like' memory Vδ1 and IL10$^+$ Vδ1 T cells, in single-cell datasets from the malaria cohort. The 'stem-like' memory Vδ1 subset was defined by a distinct transcriptional phenotype characterized by *TCF7*, *TOX*, *EOMES*, *IL10*, and *PDCD1* expression, and showed clonotypic overlap with effector Vδ1 T cells. The identification of this population was enabled by unsupervised clustering of single-cell data, highlighting how recent advances in single-cell technologies have revolutionized our understanding of γδ cell heterogeneity in an unbiased manner. Consistently, recent single-cell analyses in human ulcerative colitis also uncovered previously unappreciated γδ T cell subsets, including 'stem-like' TCF1$^+$ PD-1$^+$ cells and cytotoxic effector-like populations, highlighting the power of these approaches to resolve functionally distinct γδ T cell states in human disease[229].

Building on this, the generation of a cross-tissue human γδ T cell atlas would substantially advance our understanding of γδ T cell biology. Given their pronounced tissue-specific distribution, and phenotype heterogeneity, such an atlas would first provide a reference framework for the physiological compartmentation of γδ T cells across human organs[6,15,81]. This is necessary because γδ T cells, especially adaptive Vδ1$^+$ subsets, are preferentially distributed in epithelial tissues, where they are implicated in maintaining barrier integrity and tissue homeostasis[7,57,81]. Moreover, γδ T cells are uniquely adapted for tissue immunosurveillance by detecting stress-induced and transformation-associated signals[13,15].

This cross-tissue atlas of healthy states could then be extended across diseases to define how γδ T cell states are remodeled in pathological contexts, thereby distinguishing shared tissue programs from disease-specific adaptations in cancer, infection, autoimmunity, and transplantation. Recent studies have revealed the human γδ T cells are not uniformly anti-tumor but instead undergo tumor- and tissue-specific functional polarization. For example, whereas colorectal tumors promote an AREG-producing Vδ1 state with features linked to tissue repair, endometrial tumors preferentially harbor cytotoxic γδ T cells[104]. A similar immunoregulatory, tumor-promoting role for γδ T cells has been described in pancreatic ductal adenocarcinoma, where they suppress protective αβ T-cell responses through checkpoint-ligand-mediated crosstalk[230]. This is also supported by the distinct clonally expand regulatory and cytotoxic Vδ1 T cells in malaria infected individuals[158,161,164,231-233].

However, generating a de novo cross-tissue, pan-disease γδ T cell atlas would require a substantial number of samples and considerable financial resources. To address this challenge, our here-introduced new method to link combinatorial barcoding-based single cell sequencing and single cell γδ TCR sequencing should help to overcome the bottleneck of generating sufficient high-quality datasets. Furthermore, we present a robust strategy for retrieving γδ T cells from public single-cell datasets. Beyond γδ T cell atlas generation, this approach can also help evaluate and refine T-cell annotation, as Vδ1 T cells often phenotypically overlap with cytotoxic CD8 αβ T cells[204]. Such an atlas would provide a valuable resource for understanding how diseases reshape γδ T cell, and in turn help identify therapeutic targets and guide the optimization of γδ T cell-based immunotherapies for cancer and infectious disease[8].

Reference

1 Sun, L., Su, Y., Jiao, A., Wang, X. & Zhang, B. T cells in health and disease. *Signal Transduct Target Ther* **8**, 235 (2023). https://doi.org/10.1038/s41392-023-01471-y

2 Kumar, B. V., Connors, T. J. & Farber, D. L. Human T Cell Development, Localization, and Function throughout Life. *Immunity* **48**, 202–213 (2018). https://doi.org/10.1016/j.immuni.2018.01.007

3 Davis, M. M. & Bjorkman, P. J. T-cell antigen receptor genes and T-cell recognition. *Nature* **334**, 395–402 (1988). https://doi.org/10.1038/334395a0

4 Rossjohn, J. *et al.* in *Annual Review of Immunology Vol 33* Vol. 33 *Annual Review of Immunology* (eds D. R. Littman & W. M. Yokoyama) 169–200 (2015).

5 Morath, A. & Schamel, W. W. alphabeta and gammadelta T cell receptors: Similar but different. *J Leukoc Biol* **107**, 1045–1055 (2020). https://doi.org/10.1002/JLB.2MR1219-233R

6 Hu, Y. *et al.* γδ T cells: origin and fate, subsets, diseases and immunotherapy. *Signal Transduction and Targeted Therapy* **8** (2023). https://doi.org/10.1038/s41392-023-01653-8

7 Hayday, A. C. γδ Cells: A Right Time and a Right Place for a Conserved Third Way of Protection. *Annual review of immunology* **18**, 975–1026 (2000). https://doi.org/https://doi.org/10.1146/annurev.immunol.18.1.975

8 Hayday, A., Dechanet-Merville, J., Rossjohn, J. & Silva-Santos, B. Cancer immunotherapy by γδ T cells. *Science* **386**, eabq7248 (2024). https://doi.org/doi:10.1126/science.abq7248

9 Waldman, A. D., Fritz, J. M. & Lenardo, M. J. A guide to cancer immunotherapy: from T cell basic science to clinical practice. *Nature reviews. Immunology* **20**, 651–668 (2020). https://doi.org/10.1038/s41577-020-0306-5

10 Sakaguchi, S. *et al.* in *Annual Review of Immunology, Vol 38* Vol. 38 *Annual Review of Immunology* (ed W. M. Yokoyama) 541–566 (2020).

11 Brunkow, M. E. *et al.* Disruption of a new forkhead/winged-helix protein, scurfin, results in the fatal lymphoproliferative disorder of the scurfy mouse. *Nature genetics* **27**, 68–73 (2001). https://doi.org/10.1038/83784

12 Chien, Y.-h., Jores, R. & Crowley, M. P. RECOGNITION BY γ/δ T CELLS. *Annual review of immunology* **14**, 511–532 (1996). https://doi.org/https://doi.org/10.1146/annurev.immunol.14.1.511

13 Willcox, B. E. & Willcox, C. R. γδ TCR ligands: the quest to solve a 500-million-year-old mystery. *Nature immunology* **20**, 121–128 (2019). https://doi.org/10.1038/s41590-018-0304-y

14 Deseke, M. & Prinz, I. Ligand recognition by the γδ TCR and discrimination between homeostasis and stress conditions. *Cellular & Molecular Immunology* **17**, 914–924 (2020). https://doi.org/10.1038/s41423-020-0503-y

15 Fichtner, A. S., Ravens, S. & Prinz, I. Human gamma delta TCR Repertoires in Health and Disease. *Cells* **9** (2020). https://doi.org/10.3390/cells9040800

16 von Boehmer, H. Thymic selection: a matter of life and death. *Immunology Today* **13**, 454–458 (1992). https://doi.org/https://doi.org/10.1016/0167-5699(92)90075-I

17 Zhu, J., Yamane, H. & Paul, W. E. Differentiation of effector CD4 T cell populations. *Annual review of immunology* **28**, 445–489 (2010). https://doi.org/10.1146/annurev-immunol-030409-101212

18 Kunzli, M. & Masopust, D. CD4(+) T cell memory. *Nature immunology* **24**, 903–914 (2023). https://doi.org/10.1038/s41590-023-01510-4

19 Szabo, S. J. *et al.* A Novel Transcription Factor, T-bet, Directs Th1 Lineage Commitment. *Cell* **100**, 655–669 (2000). https://doi.org/https://doi.org/10.1016/S0092-8674(00)80702-3

20 Mosmann, T. R. & Coffman, R. L. TH1 and TH2 Cells: Different Patterns of Lymphokine Secretion Lead to Different Functional Properties. *Annual review of immunology* **7**, 145–173 (1989). https://doi.org/https://doi.org/10.1146/annurev.iy.07.040189.001045

21 Zheng, W.-p. & Flavell, R. A. The Transcription Factor GATA-3 Is Necessary and Sufficient for Th2 Cytokine Gene Expression in CD4 T Cells. *Cell* **89**, 587–596 (1997). https://doi.org/https://doi.org/10.1016/S0092-8674(00)80240-8

22 Paul, W. E. & Zhu, J. How are T(H)2-type immune responses initiated and amplified? *Nature reviews. Immunology* **10**, 225–235 (2010). https://doi.org/10.1038/nri2735

23 Korn, T., Bettelli, E., Oukka, M. & Kuchroo, V. K. IL-17 and Th17 Cells. *Annual review of immunology* **27**, 485–517 (2009). https://doi.org/https://doi.org/10.1146/annurev.immunol.021908.132710

24 Mucida, D. *et al.* Reciprocal TH17 and Regulatory T Cell Differentiation Mediated by Retinoic Acid. *Science* **317**, 256–260 (2007). https://doi.org/doi:10.1126/science.1145697

25 Nurieva, R. I. *et al.* Bcl6 Mediates the Development of T Follicular Helper Cells. *Science* **325**, 1001–1005 (2009). https://doi.org/doi:10.1126/science.1176676

26 Crotty, S. T Follicular Helper Cell Biology: A Decade of Discovery and Diseases. *Immunity* **50**, 1132–1148 (2019). https://doi.org/10.1016/j.immuni.2019.04.011

27 Curotto de Lafaille, M. A. & Lafaille, J. J. Natural and adaptive foxp3+ regulatory T cells: more of the same or a division of labor? *Immunity* **30**, 626–635 (2009). https://doi.org/10.1016/j.immuni.2009.05.002

28 Sun, Q. *et al.* Facile induction of immune tolerance by an interleukin-2-TGFbeta surrogate agonist. *Nature* (2026). https://doi.org/10.1038/s41586-026-10208-0

29 Brockmann, L. *et al.* IL-10 Receptor Signaling Is Essential for TR1 Cell Function In Vivo. *Journal of immunology (Baltimore, Md. : 1950)* **198**, 1130–1141 (2017). https://doi.org/10.4049/jimmunol.1601045

30 Wang, H. *et al.* IL-27 induces the differentiation of Tr1-like cells from human naive CD4+ T cells via the phosphorylation of STAT1 and STAT3. *Immunology letters* **136**, 21–28 (2011). https://doi.org/https://doi.org/10.1016/j.imlet.2010.11.007

31 Gagliani, N. *et al.* Coexpression of CD49b and LAG-3 identifies human and mouse T regulatory type 1 cells. *Nature Medicine* **19**, 739–746 (2013). https://doi.org/10.1038/nm.3179

32 Roncarolo, M. G., Gregori, S., Bacchetta, R., Battaglia, M. & Gagliani, N. The Biology of T Regulatory Type 1 Cells and Their Therapeutic Application in Immune-Mediated Diseases. *Immunity* **49**, 1004–1019 (2018). https://doi.org/https://doi.org/10.1016/j.immuni.2018.12.001

33 Giles, J. R., Globig, A. M., Kaech, S. M. & Wherry, E. J. CD8(+) T cells in the cancer-immunity cycle. *Immunity* **56**, 2231–2253 (2023). https://doi.org/10.1016/j.immuni.2023.09.005

34 Zhang, N. & Bevan, M. J. CD8(+) T cells: foot soldiers of the immune system. *Immunity* **35**, 161–168 (2011). https://doi.org/10.1016/j.immuni.2011.07.010

35 Galluzzi, L., Smith, K. N., Liston, A. & Garg, A. D. The diversity of CD8(+) T cell dysfunction in cancer and viral infection. *Nature reviews. Immunology* **25**, 662–679 (2025). https://doi.org/10.1038/s41577-025-01161-6

36 Jameson, S. C. & Masopust, D. Understanding Subset Diversity in T Cell Memory. *Immunity* **48**, 214–226 (2018). https://doi.org/10.1016/j.immuni.2018.02.010

37 Masopust, D. *et al.* Guidelines for T cell nomenclature. *Nature reviews. Immunology* (2025). https://doi.org/10.1038/s41577-025-01238-2

38 Chang, J. T., Wherry, E. J. & Goldrath, A. W. Molecular regulation of effector and memory T cell differentiation. *Nature immunology* **15**, 1104–1115 (2014). https://doi.org/10.1038/ni.3031

39 Rausch, L. & Kallies, A. Molecular Mechanisms Governing CD8 T Cell Differentiation and Checkpoint Inhibitor Response in Cancer. *Annual review of immunology* **43**, 515–543 (2025). https://doi.org/10.1146/annurev-immunol-082223-044122

40 Wherry, E. J. T cell exhaustion. *Nature immunology* **12**, 492–499 (2011). https://doi.org/10.1038/ni.2035

41 Moskophidis, D., Lechner, F., Pircher, H. & Zinkernagel, R. M. Virus persistence in acutely infected immunocompetent mice by exhaustion of antiviral cytotoxic effector T cells. *Nature* **362**, 758–761 (1993). https://doi.org/10.1038/362758a0

42 Zajac, A. J. *et al.* Viral immune evasion due to persistence of activated T cells without effector function. *The Journal of experimental medicine* **188**, 2205–2213 (1998). https://doi.org/10.1084/jem.188.12.2205

43 Alfei, F. *et al.* TOX reinforces the phenotype and longevity of exhausted T cells in chronic viral infection. *Nature* **571**, 265–+ (2019). https://doi.org/10.1038/s41586-019-1326-9

44 Khan, O. *et al.* TOX transcriptionally and epigenetically programs CD8(+) T cell exhaustion. *Nature* **571**, 211–+ (2019). https://doi.org/10.1038/s41586-019-1325-x

45 Yao, C. *et al.* Single-cell RNA-seq reveals TOX as a key regulator of CD8(+) T cell persistence in chronic infection. *Nature immunology* **20**, 890–901 (2019). https://doi.org/10.1038/s41590-019-0403-4

46 Wherry, E. J. & Kurachi, M. Molecular and cellular insights into T cell exhaustion. *Nature Reviews Immunology* **15**, 486–499 (2015). https://doi.org/10.1038/nri3862

47 Zehn, D., Thimme, R., Lugli, E., de Almeida, G. P. & Oxenius, A. 'Stem-like' precursors are the fount to sustain persistent $CD8^+$ T cell responses. *Nat Immunology* **23**, 836–847 (2022). https://doi.org/10.1038/s41590-022-01219-w

48 Chu, T. *et al.* Precursors of exhausted T cells are pre-emptively formed in acute infection. *Nature* **640**, 782–792 (2025). https://doi.org/10.1038/s41586-024-08451-4

49 McManus, D. T. *et al.* An early precursor $CD8^+$ T cell that adapts to acute or chronic viral infection. *Nature* **640**, 772–781 (2025). https://doi.org/10.1038/s41586-024-08562-y

50 He, R. *et al.* Follicular CXCR5-expressing CD8+ T cells curtail chronic viral infection. *Nature* **537**, 412–416 (2016). https://doi.org/10.1038/nature19317

51 Utzschneider, D. T. *et al.* T Cell Factor 1-Expressing Memory-like CD8+ T Cells Sustain the Immune Response to Chronic Viral Infections. *Immunity* **45**, 415–427 (2016). https://doi.org/https://doi.org/10.1016/j.immuni.2016.07.021

52 Iwai, Y., Hamanishi, J., Chamoto, K. & Honjo, T. Cancer immunotherapies targeting the PD-1 signaling pathway. *J Biomed Sci* **24**, 26 (2017). https://doi.org/10.1186/s12929-017-0329-9

53 Miller, B. C. *et al.* Subsets of exhausted CD8+ T cells differentially mediate tumor control and respond to checkpoint blockade. *Nature immunology* **20**, 326–336 (2019). https://doi.org/10.1038/s41590-019-0312-6

54 Siddiqui, I. *et al.* Intratumoral Tcf1+PD-1+CD8+ T Cells with Stem-like Properties Promote Tumor Control in Response to Vaccination and Checkpoint Blockade Immunotherapy. *Immunity* **50**, 195–211.e110 (2019). https://doi.org/https://doi.org/10.1016/j.immuni.2018.12.021

55 Curran, M. A., Montalvo, W., Yagita, H. & Allison, J. P. PD-1 and CTLA-4 combination blockade expands infiltrating T cells and reduces regulatory T and myeloid cells within B16 melanoma tumors. *Proceedings of the National Academy of Sciences of the United States of America* **107**, 4275–4280 (2010). https://doi.org/10.1073/pnas.0915174107

56 Topalian, S. L. *et al.* Safety, Activity, and Immune Correlates of Anti–PD-1 Antibody in Cancer. *New England Journal of Medicine* **366**, 2443–2454 (2012). https://doi.org/doi:10.1056/NEJMoa1200690

57 Vantourout, P. & Hayday, A. Six-of-the-best: unique contributions of γδ T cells to immunology. *Nature Reviews Immunology* **13**, 88–100 (2013). https://doi.org/10.1038/nri3384

58 Dimova, T. *et al.* Effector Vγ9Vδ2 T cells dominate the human fetal γδ T-cell repertoire. *Proceedings of the National Academy of Sciences of the United States of America* **112**, E556–E565 (2015). https://doi.org/10.1073/pnas.1412058112

59 Papadopoulou, M. *et al.* Fetal public Vγ9Vδ2 T cells expand and gain potent cytotoxic functions early after birth. *Proceedings of the National Academy of Sciences of the United States of America* **117**, 18638–18648 (2020). https://doi.org/10.1073/pnas.1922595117

60 Ravens, S. *et al.* Microbial exposure drives polyclonal expansion of innate gamma delta T cells immediately after birth. *Proceedings of the National Academy of Sciences of the*

United States of America **117**, 18649–18660 (2020). https://doi.org/10.1073/pnas.1922588117

61 Ryan, P. L. *et al.* Heterogeneous yet stable Vδ2$^{(+)}$ T-cell profiles define distinct cytotoxic effector potentials in healthy human individuals. *Proceedings of the National Academy of Sciences of the United States of America* **113**, 14378–14383 (2016). https://doi.org/10.1073/pnas.1611098113

62 Jomaa, H. *et al.* Vγ9/Vδ2 T cell activation induced by bacterial low molecular mass compounds depends on the 1-deoxy-D-xylulose 5-phosphate pathway of isoprenoid biosynthesis. *FEMS Immunology & Medical Microbiology* **25**, 371–378 (1999). https://doi.org/10.1111/j.1574-695X.1999.tb01362.x

63 Puan, K.-J. *et al.* Preferential recognition of a microbial metabolite by human Vγ2Vδ2 T cells. *International immunology* **19**, 657–673 (2007). https://doi.org/10.1093/intimm/dxm031

64 Yuan, L. *et al.* Phosphoantigens glue butyrophilin 3A1 and 2A1 to activate Vgamma9Vdelta2 T cells. *Nature* **621**, 840–848 (2023). https://doi.org/10.1038/s41586-023-06525-3

65 Karunakaran, M. M. *et al.* Butyrophilin-2A1 Directly Binds Germline-Encoded Regions of the V gamma 9V delta 2 TCR and Is Essential for Phosphoantigen Sensing. *Immunity* **52**, 487–+ (2020). https://doi.org/10.1016/j.immuni.2020.02.014

66 Sandoz, P. A. *et al.* Modulation of lytic molecules restrain serial killing in γδ T lymphocytes. *Nature communications* **14** (2023). https://doi.org/10.1038/s41467-023-41634-7

67 Sandstrom, A. *et al.* The Intracellular B30.2 Domain of Butyrophilin 3A1 Binds Phosphoantigens to Mediate Activation of Human V gamma 9V delta 2 T Cells. *Immunity* **40**, 490–500 (2014). https://doi.org/10.1016/j.immuni.2014.03.003

68 Rigau, M. *et al.* Butyrophilin 2A1 is essential for phosphoantigen reactivity by gamma delta T cells. *Science* **367**, 642–+ (2020). https://doi.org/10.1126/science.aay5516

69 Dieli, F. *et al.* Vgamma9/Vdelta2 T lymphocytes reduce the viability of intracellular Mycobacterium tuberculosis. *Eur J Immunol* **30**, 1512–1519 (2000). https://doi.org/10.1002/(sici)1521-4141(200005)30:5<1512::Aid-immu1512>3.0.Co;2-3

70 Li, H. *et al.* Human Vγ9Vδ2-T cells efficiently kill influenza virus-infected lung alveolar epithelial cells. *Cellular & Molecular Immunology* **10**, 159–164 (2013). https://doi.org/10.1038/cmi.2012.70

71 Junqueira, C. *et al.* γδ T cells suppress Plasmodium falciparum blood-stage infection by direct killing and phagocytosis. *Nature immunology* **22**, 347–357 (2021). https://doi.org/10.1038/s41590-020-00847-4

72 Chitadze, G. *et al.* NKG2D- and T-cell receptor-dependent lysis of malignant glioma cell lines by human γδ T cells: Modulation by temozolomide and A disintegrin and metalloproteases 10 and 17 inhibitors. *Oncoimmunology* **5**, e1093276 (2016). https://doi.org/10.1080/2162402x.2015.1093276

73 King, L. A. *et al.* A Bispecific gammadelta T-cell Engager Targeting EGFR Activates a Potent Vgamma9Vdelta2 T cell-Mediated Immune Response against EGFR-Expressing Tumors. *Cancer Immunol Res* **11**, 1237–1252 (2023). https://doi.org/10.1158/2326-6066.CIR-23-0189

74 Xu, Y. *et al.* Allogeneic V gamma 9V delta 2 T-cell immunotherapy exhibits promising clinical safety and prolongs the survival of patients with late-stage lung or liver cancer. *Cellular & Molecular Immunology* **18**, 427–439 (2021). https://doi.org/10.1038/s41423-020-0515-7

75 Wilhelm, M. *et al.* Gammadelta T cells for immune therapy of patients with lymphoid malignancies. *Blood* **102**, 200–206 (2003). https://doi.org/10.1182/blood-2002-12-3665

76 Meraviglia, S. *et al.* In vivo manipulation of Vgamma9Vdelta2 T cells with zoledronate and low-dose interleukin-2 for immunotherapy of advanced breast cancer patients. *Clin Exp Immunol* **161**, 290–297 (2010). https://doi.org/10.1111/j.1365-2249.2010.04167.x

77 De Gassart, A. *et al.* Development of ICT01, a first-in-class, anti-BTN3A antibody for activating Vγ9Vδ2 T cell–mediated antitumor immune response. *Science Translational Medicine* **13**, eabj0835 (2021). https://doi.org/doi:10.1126/scitranslmed.abj0835

78 Chowers, Y., Holtmeier, W., Harwood, J., Morzycka-Wroblewska, E. & Kagnoff, M. F. The V delta 1 T cell receptor repertoire in human small intestine and colon. *The Journal of experimental medicine* **180**, 183–190 (1994). https://doi.org/10.1084/jem.180.1.183

79 Söderström, K. *et al.* High expression of V gamma 8 is a shared feature of human gamma delta T cells in the epithelium of the gut and in the inflamed synovial tissue. *Journal of immunology (Baltimore, Md. : 1950)* **152**, 6017–6027 (1994).

80 Hunter, S. *et al.* Human liver infiltrating gamma delta T cells are composed of clonally expanded circulating and tissue-resident populations. *Journal of Hepatology* **69**, 654–665 (2018). https://doi.org/10.1016/j.jhep.2018.05.007

81 Gray, J. I. *et al.* Human γδ T cells in diverse tissues exhibit site-specific maturation dynamics across the life span. *Science Immunology* **9** (2024). https://doi.org/10.1126/sciimmunol.adn3954

82 Davey, M. S. *et al.* The human Vδ2^{+} T-cell compartment comprises distinct innate-like Vγ9^{+} and adaptive Vγ9^{-} subsets. *Nature communications* **9** (2018). https://doi.org/10.1038/s41467-018-04076-0

83 Davey, M. S. *et al.* Clonal selection in the human Vδ1 T cell repertoire indicates γδ TCR-dependent adaptive immune surveillance. *Nature communications* **8** (2017). https://doi.org/10.1038/ncomms14760

84 Ravens, S. *et al.* Human γδ T cells are quickly reconstituted after stem-cell transplantation and show adaptive clonal expansion in response to viral infection. *Nature immunology* **18**, 393–401 (2017). https://doi.org/10.1038/ni.3686

85 Ravens, S. *et al.* Human γδ T Cell Receptor Repertoires in Peripheral Blood Remain Stable Despite Clearance of Persistent Hepatitis C Virus Infection by Direct-Acting Antiviral Drug Therapy. *Frontiers in immunology* **9** (2018). https://doi.org/10.3389/fimmu.2018.00510

86 Déchanet, J. *et al.* Major expansion of γδ T lymphocytes following cytomegalovirus infection in kidney allograft recipients. *J Infect Dis* **179**, 1–8 (1999). https://doi.org/10.1086/314568

87 Déchanet, J. *et al.* Implication of gammadelta T cells in the human immune response to cytomegalovirus. *J Clin Invest* **103**, 1437–1449 (1999). https://doi.org/10.1172/jci5409

88 Pitard, V. *et al.* Long-term expansion of effector/memory Vδ2^{-} γδ T cells is a specific blood signature of CMV infection. *Blood* **112**, 1317–1324 (2008). https://doi.org/10.1182/blood-2008-01-136713

89 Vermijlen, D. *et al.* Human cytomegalovirus elicits fetal gamma delta T cell responses in utero. *Journal of Experimental Medicine* **207**, 807–821 (2010). https://doi.org/10.1084/jem.20090348

90 Willcox, C. R. *et al.* Cytomegalovirus and tumor stress surveillance by binding of a human γδ T cell antigen receptor to endothelial protein C receptor. *Nature immunology* **13**, 872–879 (2012). https://doi.org/10.1038/ni.2394

91 Scheper, W. *et al.* γδT cells elicited by CMV reactivation after allo-SCT cross-recognize CMV and leukemia. *Leukemia* **27**, 1328–1338 (2013). https://doi.org/10.1038/leu.2012.374

92 Deseke, M. *et al.* A CMV-induced adaptive human Vδ1^{+} γδ T cell clone recognizes HLA-DR. *The Journal of experimental medicine* **219** (2022). https://doi.org/10.1084/jem.20212525

93 Goodier, M. *et al.* γδ T cells in the peripheral blood of individuals from an area of holoendemic *Plasmodium falciparum* transmission. *Transactions of the Royal Society of Tropical Medicine and Hygiene* **87**, 692–696 (1993). https://doi.org/https://doi.org/10.1016/0035-9203(93)90299-6

94 Jagannathan, P. *et al.* IFNγ/IL-10 Co-producing Cells Dominate the CD4 Response to Malaria in Highly Exposed Children. *PLoS pathogens* (2014). https://doi.org/10.1371/journal.ppat.1003864

95 Benveniste, P. M. *et al.* Generation and molecular recognition of melanoma-associated antigen-specific human γδ T cells. *Science Immunology* **3**, eaav4036 (2018). https://doi.org/doi:10.1126/sciimmunol.aav4036

96 Le Nours, J. *et al.* A class of γδ T cell receptors recognize the underside of the antigen-presenting molecule MR1. *Science* **366**, 1522–1527 (2019). https://doi.org/doi:10.1126/science.aav3900

97 Luoma, Adrienne M. *et al.* Crystal Structure of Vδ1 T Cell Receptor in Complex with CD1d-Sulfatide Shows MHC-like Recognition of a Self-Lipid by Human γδ T Cells. *Immunity* **39**, 1032–1042 (2013). https://doi.org/https://doi.org/10.1016/j.immuni.2013.11.001

98 Uldrich, A. P. *et al.* CD1d-lipid antigen recognition by the γδ TCR. *Nature immunology* **14**, 1137–1145 (2013). https://doi.org/10.1038/ni.2713

99 Bai, L. *et al.* The majority of CD1d-sulfatide-specific T cells in human blood use a semiinvariant Vdelta1 TCR. *Eur J Immunol* **42**, 2505–2510 (2012). https://doi.org/10.1002/eji.201242531

100 Marlin, R. *et al.* Sensing of cell stress by human γδ TCR-dependent recognition of annexin A2. *Proceedings of the National Academy of Sciences* **114**, 3163–3168 (2017). https://doi.org/doi:10.1073/pnas.1621052114

101 Wu, Y. *et al.* A local human Vδ1 T cell population is associated with survival in nonsmall-cell lung cancer. *Nature Cancer* (2022). https://doi.org/10.1038/s43018-022-00376-z

102 Mikulak, J. *et al.* NKp46-expressing human gut-resident intraepithelial Vδ1 T cell subpopulation exhibits high antitumor activity against colorectal cancer. *JCI Insight* **4** (2019). https://doi.org/10.1172/jci.insight.125884

103 de Vries, N. L. *et al.* γδ T cells are effectors of immunotherapy in cancers with HLA class I defects. *Nature* **613**, 743–750 (2023). https://doi.org/10.1038/s41586-022-05593-1

104 Harmon, C. *et al.* γδ T cell dichotomy with opposing cytotoxic and wound healing functions in human solid tumors. *Nat Cancer* **4**, 1122–1137 (2023). https://doi.org/10.1038/s43018-023-00589-w

105 Blanco-Domínguez, R. *et al.* Dual modulation of cytotoxic and checkpoint receptors tunes the efficacy of adoptive Delta One T cell therapy against colorectal cancer. *Nature Cancer* **6** (2025). https://doi.org/10.1038/s43018-025-00948-9

106 Rancan, C. *et al.* Exhausted intratumoral Vδ2$^-$ γδ T cells in human kidney cancer retain effector function. *Nat Immunology* (2023). https://doi.org/10.1038/s41590-023-01448-7

107 Airoldi, I. *et al.* γδ T-cell reconstitution after HLA-haploidentical hematopoietic transplantation depleted of TCR-αβ+/CD19+ lymphocytes. *Blood* **125**, 2349–2358 (2015). https://doi.org/10.1182/blood-2014-09-599423

108 Di Lorenzo, B. *et al.* Broad Cytotoxic Targeting of Acute Myeloid Leukemia by Polyclonal Delta One T Cells. *Cancer Immunol. Res.* **7**, 552–558 (2019). https://doi.org/10.1158/2326-6066.Cir-18-0647

109 Airoldi, I. *et al.* gamma delta T-cell reconstitution after HLA-haploidentical hematopoietic transplantation depleted of TCR-alpha beta(+)/CD19(+) lymphocytes. *Blood* **125**, 2349–2358 (2015). https://doi.org/10.1182/blood-2014-09-599423

110 Klyuchnikov, E. *et al.* Enhanced Immune Reconstitution of gammadelta T Cells after Allogeneic Stem Cell Transplantation Overcomes the Negative Impact of Pretransplantation Minimal Residual Disease-Positive Status in Patients with Acute Myelogenous Leukemia. *Transplant Cell Ther* **27**, 841–850 (2021). https://doi.org/10.1016/j.jtct.2021.06.003

111 Holtan, S. G. *et al.* Composite end point of graft-versus-host disease-free, relapse-free survival after allogeneic hematopoietic cell transplantation. *Blood* **125**, 1333–1338 (2015). https://doi.org/10.1182/blood-2014-10-609032

112 Mensurado, S. *et al.* CD155/PVR determines acute myeloid leukemia targeting by Delta One T cells. *Blood* **143**, 1488–1495 (2024). https://doi.org/10.1182/blood.2023022992

113 Silva-Santos, B., Serre, K. & Norell, H. gamma delta T cells in cancer. *Nature Reviews Immunology* **15**, 683–691 (2015). https://doi.org/10.1038/nri3904

114 Mensurado, S., Blanco-Dominguez, R. & Silva-Santos, B. The emerging roles of gammadelta T cells in cancer immunotherapy. *Nat Rev Clin Oncol* **20**, 178–191 (2023). https://doi.org/10.1038/s41571-022-00722-1

115 Nikolich-Zugich, J., Slifka, M. K. & Messaoudi, I. The many important facets of T-cell repertoire diversity. *Nature reviews. Immunology* **4**, 123–132 (2004). https://doi.org/10.1038/nri1292

116 Pai, J. A. & Satpathy, A. T. High-throughput and single-cell T cell receptor sequencing technologies. *Nature Methods* **18**, 881–892 (2021). https://doi.org/10.1038/s41592-021-01201-8

117 Chien, Y.-h. & Konigshofer, Y. Antigen recognition by γδ T cells. *Immunological reviews* **215**, 46–58 (2007). https://doi.org/https://doi.org/10.1111/j.1600-065X.2006.00470.x

118 Nideffer, J. *et al.* Clone tracking through repeated malaria identifies high-fidelity memory CD4 T cell responses. *Science Immunology* **10**, eads2957 (2025). https://doi.org/doi:10.1126/sciimmunol.ads2957

119 Pai, J. A. *et al.* Lineage tracing reveals clonal progenitors and long-term persistence of tumor-specific T cells during immune checkpoint blockade. *Cancer Cell* (2023). https://doi.org/10.1016/j.ccell.2023.03.009

120 Burn, T. N. *et al.* Antigen reactivity defines tissue-resident memory and exhausted T cells in tumors. *Nature immunology* **27**, 98–109 (2026). https://doi.org/10.1038/s41590-025-02347-9

121 Herold, N. *et al.* Vδ1 T-cell subset appears to be responsive to PD-1 blockade therapy and is associated with survival in melanoma. *Journal for ImmunoTherapy of Cancer* **14**, e011224 (2026). https://doi.org/10.1136/jitc-2024-011224

122 Shimony, S., Stahl, M. & Stone, R. M. Acute Myeloid Leukemia: 2025 Update on Diagnosis, Risk-Stratification, and Management. *American Journal of Hematology* **100**, 860–891 (2025). https://doi.org/https://doi.org/10.1002/ajh.27625

123 Kantarjian, H. *et al.* Acute myeloid leukemia: current progress and future directions. *Blood Cancer J* **11**, 41 (2021). https://doi.org/10.1038/s41408-021-00425-3

124 Sauerer, T., Velazquez, G. F. & Schmid, C. Relapse of acute myeloid leukemia after allogeneic stem cell transplantation: immune escape mechanisms and current implications for therapy. *Mol Cancer* **22**, 180 (2023). https://doi.org/10.1186/s12943-023-01889-6

125 Shouval, R. *et al.* Outcomes of allogeneic haematopoietic stem cell transplantation from HLA-matched and alternative donors: a European Society for Blood and Marrow Transplantation registry retrospective analysis. *Lancet Haematol* **6**, e573–e584 (2019). https://doi.org/10.1016/S2352-3026(19)30158-9

126 Horowitz, M. M. *et al.* Graft-versus-leukemia reactions after bone marrow transplantation. *Blood* **75**, 555–562 (1990). https://doi.org/10.1182/blood.V75.3.555.555

127 Bleakley, M. & Riddell, S. R. Molecules and mechanisms of the graft-versus-leukaemia effect. *Nat Rev Cancer* **4**, 371–380 (2004). https://doi.org/10.1038/nrc1365

128 Weisdorf, D. *et al.* Graft-versus-host disease induced graft-versus-leukemia effect: greater impact on relapse and disease-free survival after reduced intensity conditioning. *Biol Blood Marrow Transplant* **18**, 1727–1733 (2012). https://doi.org/10.1016/j.bbmt.2012.06.014

129 Wang, Z. *et al.* The benefit of chronic graft-versus-host disease in patients with acute myeloid leukemia relapsed after allogeneic stem cell transplantation. *Ann Hematol* **98**, 1765–1773 (2019). https://doi.org/10.1007/s00277-019-03682-2

130 Yeshurun, M. *et al.* The impact of the graft-versus-leukemia effect on survival in acute lymphoblastic leukemia. *Blood Adv* **3**, 670–680 (2019). https://doi.org/10.1182/bloodadvances.2018027003

131 Christopher, M. J. *et al.* Immune Escape of Relapsed AML Cells after Allogeneic Transplantation. *N Engl J Med* **379**, 2330–2341 (2018). https://doi.org/10.1056/NEJMoa1808777

132 Zeiser, R. & Blazar, B. R. Acute Graft-versus-Host Disease - Biologic Process, Prevention, and Therapy. *New England Journal of Medicine* **377**, 2167–2179 (2017). https://doi.org/10.1056/NEJMra1609337

133 Ferrara, J. L. M., Levine, J. E., Reddy, P. & Holler, E. Graft-versus-host disease. *Lancet (London, England)* **373**, 1550–1561 (2009). https://doi.org/10.1016/s0140-6736(09)60237-3

134 Koyama, M. & Hill, G. R. Alloantigen presentation and graft-versus-host disease: fuel for the fire. *Blood* **127**, 2963–2970 (2016). https://doi.org/10.1182/blood-2016-02-697250

135 Hill, G. R., Betts, B. C., Tkachev, V., Kean, L. S. & Blazar, B. R. Current Concepts and Advances in Graft-Versus-Host Disease Immunology. *Annual review of*

immunology **39**, 19–49 (2021). https://doi.org/10.1146/annurev-immunol-102119-073227

136 Biernacki, M. A., Sheth, V. S. & Bleakley, M. T cell optimization for graft-versus-leukemia responses. *Jci Insight* **5** (2020). https://doi.org/10.1172/jci.insight.134939

137 Locatelli, F. *et al.* Outcome of children with acute leukemia given HLA-haploidentical HSCT after alphabeta T-cell and B-cell depletion. *Blood* **130**, 677–685 (2017). https://doi.org/10.1182/blood-2017-04-779769

138 Kurup, S. P., Butler, N. S. & Harty, J. T. T cell-mediated immunity to malaria. *Nature Reviews Immunology* (2019). https://doi.org/10.1038/s41577-019-0158-z

139 Florens, L. *et al.* A proteomic view of the Plasmodium falciparum life cycle. *Nature* **419**, 520–526 (2002). https://doi.org/10.1038/nature01107

140 Overstreet, M. G., Cockburn, I. A., Chen, Y. C. & Zavala, F. Protective CD8 T cells against Plasmodium liver stages: immunobiology of an 'unnatural' immune response. *Immunological reviews* **225**, 272–283 (2008). https://doi.org/10.1111/j.1600-065X.2008.00671.x

141 Fernandez-Ruiz, D. *et al.* Liver-Resident Memory CD8(+) T Cells Form a Front-Line Defense against Malaria Liver-Stage Infection. *Immunity* **45**, 889–902 (2016). https://doi.org/10.1016/j.immuni.2016.08.011

142 Kurup, S. P. *et al.* Monocyte-Derived CD11c+ Cells Acquire Plasmodium from Hepatocytes to Prime CD8 T Cell Immunity to Liver-Stage Malaria. *Cell Host & Microbe* **25**, 565–577.e566 (2019). https://doi.org/https://doi.org/10.1016/j.chom.2019.02.014

143 Weiss, W. R., Sedegah, M., Beaudoin, R. L., Miller, L. H. & Good, M. F. CD8+ T cells (cytotoxic/suppressors) are required for protection in mice immunized with malaria sporozoites. *Proceedings of the National Academy of Sciences of the United States of America* **85**, 573–576 (1988). https://doi.org/10.1073/pnas.85.2.573

144 Chakravarty, S. *et al.* CD8+ T lymphocytes protective against malaria liver stages are primed in skin-draining lymph nodes. *Nature Medicine* **13**, 1035–1041 (2007). https://doi.org/10.1038/nm1628

145 Kurup, S. P. *et al.* Monocyte-Derived CD11c⁺ Cells Acquire Plasmodium from Hepatocytes to Prime CD8 T Cell Immunity to Liver-Stage Malaria. *Cell Host & Microbe* **25**, 565–577.e566 (2019). https://doi.org/10.1016/j.chom.2019.02.014

146 Butler, Noah S. *et al.* Superior Antimalarial Immunity after Vaccination with Late Liver Stage-Arresting Genetically Attenuated Parasites. *Cell Host & Microbe* **9**, 451–462 (2011). https://doi.org/10.1016/j.chom.2011.05.008

147 van Dijk, H. *et al.* Epitope and HLA specificity of human TCRs against Plasmodium falciparum circumsporozoite protein. *The Journal of experimental medicine* **222** (2025). https://doi.org/10.1084/jem.20250044

148 Obeng-Adjei, N. *et al.* Circulating Th1-Cell-type Tfh Cells that Exhibit Impaired B Cell Help Are Preferentially Activated during Acute Malaria in Children. *Cell reports* **13**, 425–439 (2015). https://doi.org/10.1016/j.celrep.2015.09.004

149 Kurup, S. P. *et al.* Regulatory T cells impede acute and long-term immunity to blood-stage malaria through CTLA-4. *Nature Medicine* **23**, 1220–1225 (2017). https://doi.org/10.1038/nm.4395

150 Zander, R. A. *et al.* Th1-like Plasmodium-Specific Memory CD4⁺ T Cells Support Humoral Immunity. *Cell reports* **21**, 1839–1852 (2017). https://doi.org/10.1016/j.celrep.2017.10.077

151 Jagannathan, P. *et al.* IFNγ/IL-10 Co-producing Cells Dominate the CD4 Response to Malaria in Highly Exposed Children. *PLoS pathogens* **10**, e1003864 (2014). https://doi.org/10.1371/journal.ppat.1003864

152 Zander, R. A. *et al.* Type I Interferons Induce T Regulatory 1 Responses and Restrict Humoral Immunity during Experimental Malaria. *PLoS pathogens* **12**, e1005945 (2016). https://doi.org/10.1371/journal.ppat.1005945

153 Montes de Oca, M. *et al.* Type I Interferons Regulate Immune Responses in Humans with Blood-Stage Plasmodium falciparum Infection. *Cell reports* **17**, 399–412 (2016). https://doi.org/10.1016/j.celrep.2016.09.015

154 Barbosa, A. *et al.* Plasmodium falciparum-Specific Cellular Immune Responses after Immunization with the RTS,S/AS02D Candidate Malaria Vaccine in Infants Living in an Area of High Endemicity in Mozambique. *Infection and Immunity* **77**, 4502–4509 (2009). https://doi.org/10.1128/iai.00442-09

155 Edwards, C. L. *et al.* IL^{-}10^{-}producing Th1 cells possess a distinct molecular signature in malaria. *Journal of Clinical Investigation* (2023). https://doi.org/10.1172/jci169299

156 Kumar, R., Ng, S. & Engwerda, C. The Role of IL-10 in Malaria: A Double Edged Sword. *Frontiers in immunology* **Volume 10 - 2019** (2019). https://doi.org/10.3389/fimmu.2019.00229

157 Marsh, K. & Kinyanjui, S. Immune effector mechanisms in malaria. *Parasite Immunology* **28**, 51–60 (2006). https://doi.org/10.1111/j.1365-3024.2006.00808.x

158 Junqueira, C. *et al.* γδ T cells suppress *Plasmodium falciparum* blood-stage infection by direct killing and phagocytosis. *Nature immunology* **22**, 347–+ (2021). https://doi.org/10.1038/s41590-020-00847-4

159 Farrington, L. A. *et al.* Opsonized antigen activates Vδ2+T cells via CD16/FCγRIIIa in individuals with chronic malaria exposure. *PLoS pathogens* **16** (2020). https://doi.org/10.1371/journal.ppat.1008997

160 Costa, G. *et al.* Control of Plasmodium falciparum erythrocytic cycle: γδ T cells target the red blood cell–invasive merozoites. *Blood* **118**, 6952–6962 (2011). https://doi.org/10.1182/blood-2011-08-376111

161 Jagannathan, P. *et al.* Loss and dysfunction of $V\delta2^+$ γδ T cells are associated with clinical tolerance to malaria. *Science Translational Medicine* **6**, 251ra117–251ra117 (2014). https://doi.org/doi:10.1126/scitranslmed.3009793

162 von Borstel, A. *et al.* Repeated Plasmodium falciparum infection in humans drives the clonal expansion of an adaptive γδ T cell repertoire. *Science Translational Medicine* **13**, eabe7430 (2021). https://doi.org/doi:10.1126/scitranslmed.abe7430

163 Teirlinck, A. C. *et al.* Longevity and Composition of Cellular Immune Responses Following Experimental Plasmodium falciparum Malaria Infection in Humans. *PLoS pathogens* **7** (2011). https://doi.org/10.1371/journal.ppat.1002389

164 Taniguchi, T. *et al.* A Unique Subset of γδ T Cells Expands and Produces IL-10 in Patients with Naturally Acquired Immunity against Falciparum Malaria. *Frontiers in Microbiology* **8** (2017). https://doi.org/10.3389/fmicb.2017.01288

165 Howie, B. *et al.* High-throughput pairing of T cell receptor α and β sequences. *Science Translational Medicine* **7**, 301ra131–301ra131 (2015). https://doi.org/doi:10.1126/scitranslmed.aac5624

166 Redmond, D., Poran, A. & Elemento, O. Single-cell TCRseq: paired recovery of entire T-cell alpha and beta chain transcripts in T-cell receptors from single-cell RNAseq. *Genome Med* **8**, 80 (2016). https://doi.org/10.1186/s13073-016-0335-7

167 Stoeckius, M. *et al.* Simultaneous epitope and transcriptome measurement in single cells. *Nature Methods* **14**, 865–868 (2017). https://doi.org/10.1038/nmeth.4380

168 Buenrostro, J. D. *et al.* Single-cell chromatin accessibility reveals principles of regulatory variation. *Nature* **523**, 486–490 (2015). https://doi.org/10.1038/nature14590

169 Smallwood, S. A. *et al.* Single-cell genome-wide bisulfite sequencing for assessing epigenetic heterogeneity. *Nat Methods* **11**, 817–820 (2014). https://doi.org/10.1038/nmeth.3035

170 Tang, F. *et al.* mRNA-Seq whole-transcriptome analysis of a single cell. *Nat Methods* **6**, 377–382 (2009). https://doi.org/10.1038/nmeth.1315

171 Klein, Allon M. *et al.* Droplet Barcoding for Single-Cell Transcriptomics Applied to Embryonic Stem Cells. *Cell* **161**, 1187–1201 (2015). https://doi.org/https://doi.org/10.1016/j.cell.2015.04.044

172 Picelli, S. *et al.* Full-length RNA-seq from single cells using Smart-seq2. *Nature Protocols* **9**, 171–181 (2014). https://doi.org/10.1038/nprot.2014.006

173 Hwang, B., Lee, J. H. & Bang, D. Single-cell RNA sequencing technologies and bioinformaticspipelines. *Experimental & Molecular Medicine* **50**, 1–14 (2018). https://doi.org/10.1038/s12276-018-0071-8

174 Kolodziejczyk, Aleksandra A., Kim, J. K., Svensson, V., Marioni, John C. & Teichmann, Sarah A. The Technology and Biology of Single-Cell RNA Sequencing. *Molecular Cell* **58**, 610–620 (2015). https://doi.org/https://doi.org/10.1016/j.molcel.2015.04.005

175 Heumos, L. *et al.* Best practices for single-cell analysis across modalities. *Nature Reviews Genetics* **24**, 550–572 (2023). https://doi.org/10.1038/s41576-023-00586-w

176 Rosenberg, A. B. *et al.* Single-cell profiling of the developing mouse brain and spinal cord with split-pool barcoding. *Science* **360**, 176–182 (2018). https://doi.org/doi:10.1126/science.aam8999

177 Cao, J. *et al.* The single-cell transcriptional landscape of mammalian organogenesis. *Nature* **566**, 496–502 (2019). https://doi.org/10.1038/s41586-019-0969-x

178 Cao, J. *et al.* Comprehensive single-cell transcriptional profiling of a multicellular organism. *Science* **357**, 661–667 (2017). https://doi.org/doi:10.1126/science.aam8940

179 Cao, J. *et al.* Joint profiling of chromatin accessibility and gene expression in thousands of single cells. *Science* **361**, 1380–1385 (2018). https://doi.org/doi:10.1126/science.aau0730

180 Cao, J. *et al.* A human cell atlas of fetal gene expression. *Science* **370**, eaba7721 (2020). https://doi.org/doi:10.1126/science.aba7721

181 Domcke, S. *et al.* A human cell atlas of fetal chromatin accessibility. *Science* **370**, eaba7612 (2020). https://doi.org/10.1126/science.aba7612

182 Qiu, C. *et al.* Systematic reconstruction of cellular trajectories across mouse embryogenesis. *Nature genetics* **54**, 328–341 (2022). https://doi.org/10.1038/s41588-022-01018-x

183 Qiu, C. *et al.* A single-cell time-lapse of mouse prenatal development from gastrula to birth. *Nature* **626**, 1084–1093 (2024). https://doi.org/10.1038/s41586-024-07069-w

184 Cao, J., Zhou, W., Steemers, F., Trapnell, C. & Shendure, J. Sci-fate characterizes the dynamics of gene expression in single cells. *Nature biotechnology* **38**, 980–988 (2020). https://doi.org/10.1038/s41587-020-0480-9

185 Sziraki, A. *et al.* A global view of aging and Alzheimer's pathogenesis-associated cell population dynamics and molecular signatures in human and mouse brains. *Nature genetics* **55**, 2104–2116 (2023). https://doi.org/10.1038/s41588-023-01572-y

186 Zhang, Z. *et al.* A panoramic view of cell population dynamics in mammalian aging. *Science* **387**, eadn3949 https://doi.org/10.1126/science.adn3949

187 Wolf, F. A., Angerer, P. & Theis, F. J. SCANPY: large-scale single-cell gene expression data analysis. *Genome Biol* **19**, 15 (2018). https://doi.org/10.1186/s13059-017-1382-0

188 Hao, Y. *et al.* Dictionary learning for integrative, multimodal and scalable single-cell analysis. *Nature biotechnology* **42**, 293–304 (2024). https://doi.org/10.1038/s41587-023-01767-y

189 Luecken, M. D. & Theis, F. J. Current best practices in single-cell RNA-seq analysis: a tutorial. *Mol Syst Biol* **15**, e8746 (2019). https://doi.org/10.15252/msb.20188746

190 Young, M. D. & Behjati, S. SoupX removes ambient RNA contamination from droplet-based single-cell RNA sequencing data. *GigaScience* **9**, giaa151 (2020). https://doi.org/10.1093/gigascience/giaa151

191 Fleming, S. J. *et al.* Unsupervised removal of systematic background noise from droplet-based single-cell experiments using CellBender. *Nature Methods* **20**, 1323–1335 (2023). https://doi.org/10.1038/s41592-023-01943-7

192 Yang, S. *et al.* Decontamination of ambient RNA in single-cell RNA-seq with DecontX. *Genome Biology* **21**, 57 (2020). https://doi.org/10.1186/s13059-020-1950-6

193 McGinnis, C. S., Murrow, L. M. & Gartner, Z. J. DoubletFinder: Doublet Detection in Single-Cell RNA Sequencing Data Using Artificial Nearest Neighbors. *Cell Syst* **8**, 329–337.e324 (2019). https://doi.org/10.1016/j.cels.2019.03.003

194 Wolock, S. L., Lopez, R. & Klein, A. M. Scrublet: Computational Identification of Cell Doublets in Single-Cell Transcriptomic Data. *Cell Systems* **8**, 281–291.e289 (2019). https://doi.org/10.1016/j.cels.2018.11.005

195 Becht, E. *et al.* Dimensionality reduction for visualizing single-cell data using UMAP. *Nature biotechnology* **37**, 38–44 (2019). https://doi.org/10.1038/nbt.4314

196 Zhao, R. *et al.* A systematic evaluation of highly variable gene selection methods for single-cell RNA-sequencing. *Genome Biology* **26**, 424 (2025). https://doi.org/10.1186/s13059-025-03887-x

197 Korsunsky, I. *et al.* Fast, sensitive and accurate integration of single-cell data with Harmony. *Nat Methods* **16**, 1289–1296 (2019). https://doi.org/10.1038/s41592-019-0619-0

198 Hie, B. L., Kim, S., Rando, T. A., Bryson, B. & Berger, B. Scanorama: integrating large and diverse single-cell transcriptomic datasets. *Nature Protocols* **19**, 2283–2297 (2024). https://doi.org/10.1038/s41596-024-00991-3

199 Luecken, M. D. *et al.* Benchmarking atlas-level data integration in single-cell genomics. *Nat Methods* **19**, 41–50 (2022). https://doi.org/10.1038/s41592-021-01336-8

200 Traag, V. A., Waltman, L. & van Eck, N. J. From Louvain to Leiden: guaranteeing well-connected communities. *Scientific reports* **9**, 5233 (2019). https://doi.org/10.1038/s41598-019-41695-z

201 McInnes, L., Healy, J., Saul, N. & Großberger, L. UMAP: Uniform Manifold Approximation and Projection. *Journal of Open Source Software* **3** (2018). https://doi.org/10.21105/joss.00861

202 Li, T. *et al.* An overview of computational methods in single-cell transcriptomic cell type annotation. *Briefings in Bioinformatics* **26**, bbaf207 (2025). https://doi.org/10.1093/bib/bbaf207

203 Pasquini, G., Rojo Arias, J. E., Schäfer, P. & Busskamp, V. Automated methods for cell type annotation on scRNA-seq data. *Computational and Structural Biotechnology Journal* **19**, 961–969 (2021). https://doi.org/https://doi.org/10.1016/j.csbj.2021.01.015

204 McMurray, J. L. *et al.* Transcriptional profiling of human V delta 1 T cells reveals a pathogen-driven adaptive differentiation program. *Cell reports* **39** (2022). https://doi.org/10.1016/j.celrep.2022.110858

205 Zhang, B. *et al.* Multimodal single-cell datasets characterize antigen-specific CD8+ T cells across SARS-CoV-2 vaccination and infection. *Nature immunology* **24**, 1725–1734 (2023). https://doi.org/10.1038/s41590-023-01608-9

206 Schattgen, S. A. *et al.* Influenza vaccination stimulates maturation of the human T follicular helper cell response. *Nature immunology* **25**, 1742–1753 (2024). https://doi.org/10.1038/s41590-024-01926-6

207 Mold, J. E. *et al.* Divergent clonal differentiation trajectories establish CD8+ memory T cell heterogeneity during acute viral infections in humans. *Cell reports* **35**, 109174 (2021). https://doi.org/https://doi.org/10.1016/j.celrep.2021.109174

208 Pan, Y.-G. *et al.* Vaccination reshapes the virus-specific T cell repertoire in unexposed adults. *Immunity* **54**, 1245–1256.e1245 (2021). https://doi.org/https://doi.org/10.1016/j.immuni.2021.04.023

209 Yost, K. E. *et al.* Clonal replacement of tumor-specific T cells following PD-1 blockade. *Nat Med* **25**, 1251–1259 (2019). https://doi.org/10.1038/s41591-019-0522-3

210 Park, S. L. *et al.* Tissue-resident exhausted and memory CD8+ T cells have distinct ontogeny, function and roles in disease. *Nature immunology* **27**, 110–125 (2026). https://doi.org/10.1038/s41590-025-02352-y

211 Wu, C. *et al.* Clonal expansion and compartmentalized maintenance of rhesus macaque NK cell subsets. *Science Immunology* **3**, eaat9781 (2018). https://doi.org/doi:10.1126/sciimmunol.aat9781

212 Rückert, T., Lareau, C. A., Mashreghi, M.-F., Ludwig, L. S. & Romagnani, C. Clonal expansion and epigenetic inheritance of long-lasting NK cell memory. *Nature immunology* **23**, 1551–1563 (2022). https://doi.org/10.1038/s41590-022-01327-7

213 Rückert, T. & Romagnani, C. Extrinsic and intrinsic drivers of natural killer cell clonality. *Immunological reviews* **323**, 80–106 (2024). https://doi.org/https://doi.org/10.1111/imr.13324

214 Melenhorst, J. J. *et al.* Decade-long leukaemia remissions with persistence of CD4(+) CAR T cells. *Nature* **602**, 503–509 (2022). https://doi.org/10.1038/s41586-021-04390-6

215 Mei, Y. *et al.* Identifying ADGRG1 as a specific marker for tumor-reactive T cells in acute myeloid leukemia. *Exp Hematol Oncol* **13**, 92 (2024). https://doi.org/10.1186/s40164-024-00560-0

216 Mathioudaki, A. *et al.* The remission status of AML patients post alloSCT is associated with a distinct single-cell bone marrow T cell signature. *Blood* (2024). https://doi.org/10.1182/blood.2023021815

217 Maurer, K. *et al.* Coordinated immune networks in leukemia bone marrow microenvironments distinguish response to cellular therapy. *Sci Immunol* **10**, eadr0782 (2025). https://doi.org/10.1126/sciimmunol.adr0782

218 Obermayer, B. *et al.* Single-cell clonal tracking of persistent T-cells in allogeneic hematopoietic stem cell transplantation. *Frontiers in immunology* **14**, 1114368 (2023). https://doi.org/10.3389/fimmu.2023.1114368

219 Halary, F. *et al.* Shared reactivity of Vδ2neg γδ T cells against cytomegalovirus-infected cells and tumor intestinal epithelial cells. *The Journal of experimental medicine* **201**, 1567–1578 (2005). https://doi.org/10.1084/jem.20041851

220 Weiden, P. L. *et al.* Antileukemic effect of graft-versus-host disease in human recipients of allogeneic-marrow grafts. *N Engl J Med* **300**, 1068–1073 (1979). https://doi.org/10.1056/nejm197905103001902

221 Weiden, P. L., Sullivan, K. M., Flournoy, N., Storb, R. & Thomas, E. D. Antileukemic effect of chronic graft-versus-host disease: contribution to improved survival after allogeneic marrow transplantation. *N Engl J Med* **304**, 1529–1533 (1981). https://doi.org/10.1056/nejm198106183042507

222 Zaslavsky, M. E. *et al.* Disease diagnostics using machine learning of B cell and T cell receptor sequences. *Science* **387**, eadp2407 (2025). https://doi.org/doi:10.1126/science.adp2407

223 Sidhom, J.-W. *et al.* Deep learning reveals predictive sequence concepts within immune repertoires to immunotherapy. *Sci. Adv.* **8**, eabq5089 (2022). https://doi.org/doi:10.1126/sciadv.abq5089

224 Mukhopadhyay, M. Learning the immunological repertoire. *Nature Methods* **22**, 651–651 (2025). https://doi.org/10.1038/s41592-025-02673-8

225 O'Donnell, T. J. *et al.* Reading the repertoire: Progress in adaptive immune receptor analysis using machine learning. *Cell Systems* **15**, 1168–1189 (2024). https://doi.org/https://doi.org/10.1016/j.cels.2024.11.006

226 Cowell, L. G. *et al.* The Adaptive Immune Receptor Repertoire Knowledge Commons: An invitation to the community. *Cell Systems* **16** (2025). https://doi.org/10.1016/j.cels.2025.101401

227 Yu, X. *et al.* Quantifiable TCR repertoire changes in prediagnostic blood specimens among patients with high-grade ovarian cancer. *Cell Reports Medicine* **5** (2024). https://doi.org/10.1016/j.xcrm.2024.101612

228 Li, Y. *et al.* Circulating T-cell receptor repertoire for cancer early detection. *npj Precision Oncology* **9**, 245 (2025). https://doi.org/10.1038/s41698-025-01036-y

229 Mayer, L. S. *et al.* Single-cell profiling reveals diverse γδ T cell subsets in ulcerative colitis. *Science Immunology* **11**, eadx8474 https://doi.org/10.1126/sciimmunol.adx8474

230 Daley, D. *et al.* γδ T Cells Support Pancreatic Oncogenesis by Restraining αβ T Cell Activation. *Cell* **166**, 1485–1499.e1415 (2016). https://doi.org/https://doi.org/10.1016/j.cell.2016.07.046

231 Siegers, G. M. & Lamb, L. S. Cytotoxic and Regulatory Properties of Circulating Vδ1+ γδ T Cells: A New Player on the Cell Therapy Field? *Molecular Therapy* **22**, 1416–1422 (2014). https://doi.org/10.1038/mt.2014.104

232 Zaidi, I. *et al.* γδ T Cells Are Required for the Induction of Sterile Immunity during Irradiated Sporozoite Vaccinations. *Journal of immunology (Baltimore, Md. : 1950)* **199**, 3781–3788 (2017). https://doi.org/10.4049/jimmunol.1700314

233 Hao, Q. *et al.* A pan-cancer single cell landscape reveals heterogeneity and functional diversity of double-negative T cells. *Mol Cancer* (2026). https://doi.org/10.1186/s12943-025-02548-8

Curriculum Vitae and List of Publications

Zheng SONG	
Affiliation	Institute of Systems Immunology, Hamburg Center for Translational Immunology, University Medical Center Hamburg-Eppendorf
Address	Room 01.2.010, Building N25, Martinistraße 52, 20251 Hamburg
Date of Birth	13 January, 1996
Nationality	China
Phone	+49 (0) 40 7410 - 57262
E-mail	z.song@uke.de

References	
Name	Prof. Dr. Immo PRINZ
Position	Professor, Director of the institute
Affiliation	Institute of Systems Immunology, Hamburg Center for Translational Immunology, University Medical Center Hamburg-Eppendorf
Address	Room 01.2.013, Building N25, Martinistraße 52, 20251 Hamburg
Phone	+49 (0) 40 7410 - 55028
E-mail	i.prinz@uke.de

Research Fields of Interest

Elucidating human αβ and γδ T cell receptor repertoire dynamics in cancer and inflammation to guide novel immunotherapies.

Education and Appointment	
2013 - 2018	Sun Yat-sen University, China Bachelor of Medicine in Public Health
2018 - 2021	Sun Yat-sen University, China Master of Medicine in Basic Medicine
2021 - 2026	University Medical Center Hamburg-Eppendorf, Germany Ph.D. student

Publications

First-author Peer-reviewed Publications

1. Song, Z., Klyuchnikov, E., Badbaran, A., Tan, L., Dress, R. J., Czajkowski, E., Wessler, S., Massoud, R., Wolschke, C., Schimrock, A., Zhang, Y., Ly, C., Gagelmann, N., Rathje, K., Fehse, B., Bonn, S., Ravens, S., Gagliani, N., Krebs, C. F., Panzer, U., Ayuk, F., Kroger, N., and Prinz, I. Mega-scale single-cell profiling reveals novel biomarkers associated with acute GvHD after allogeneic hematopoietic stem cell transplantation. *Biomark Res*. 2025;13:155.
2. Song, Z., Henze, L., Casar, C., Schwinge, D., Schramm, C., Fuss, J., Tan, L., and Prinz, I. Human γδ T cell identification from single-cell RNA sequencing datasets by modular TCR expression. *J Leukoc Biol*. 2023;114(6):630–638.

Co-author Peer-reviewed Publications

1. Schröter, P. E., Steppich, K. S., Carera, F. L., Song, Z., Klein, S., Souleiman, R., Urbanek-Quaing, M., Lietzau, A. D., Schnieders, A., Freyer, E., Bremer, B., León-Lara, X., Almeida, V., Gutierrez Jauregui, R., von Kaisenberg, C., Wedemeyer, H., Prinz, I., Ravens, S., Bartsch, Y., Kraft, A. R. M., and Cornberg, M. $CD16^{+}$ γδ T cells mediate antibody-dependent cellular cytotoxicity and associate with viral control in chronic hepatitis B virus infection. *Accepted for publication in Gut*, 2026.
2. Zhang, Y., Chen, Y., Li, Y., Huang, F., Luo, B., Yuan, Y., Xia, B., Ma, X., Yang, T., Yu, F., Liu, J., Liu, B., Song, Z., Chen, J., Yan, S., Wu, L., Pan, T., Zhang, X., Li, R., Huang, W., He, X., Xiao, F., Zhang, J., and Zhang, H. The ORF8 protein of SARS-CoV-2 mediates immune evasion through down-regulating MHC-I. *Proc Natl Acad Sci U S A*. 2021;118(23):e2024202118.
3. Zhang, J., Huang, F., Xia, B., Yuan, Y., Yu, F., Wang, G., Chen, Q., Wang, Q., Li, Y., Li, R., Song, Z., Pan, T., Chen, J., Lu, G., and Zhang, H. The interferon-stimulated exosomal hACE2 potently inhibits SARS-CoV-2 replication through competitively blocking virus entry. *Signal Transduct Target Ther*. 2021;6:189.
4. Ma, X., Zou, F., Yu, F., Li, R., Yuan, Y., Zhang, Y., Zhang, X., Deng, J., Chen, T., Song, Z., Qiao, Y., Zhan, Y., Liu, J., Zhang, J., Zhang, X., Peng, Z., Li, Y., Lin, Y., Liang, L., Wang, G., Chen, Y., Chen, Q., Pan, T., He, X., and Zhang, H. Nanoparticle vaccines based on the receptor binding domain (RBD) and heptad repeat (HR) of SARS-CoV-2 elicit robust protective immune responses. *Immunity*. 2020;53(6):1315–1330.e9.

5. Pan, T., Song, Z., Wu, L., Liu, G., Ma, X., Peng, Z., Zhou, M., Liang, L., Liu, B., Liu, J., Zhang, J., Zhang, X., Huang, R., Zhao, J., Li, Y., Ling, X., Luo, Y., Tang, X., Cai, W., Deng, K., Li, L., and Zhang, H. USP49 potently stabilizes APOBEC3G protein by removing ubiquitin and inhibits HIV-1 replication. *eLife*. 2019;8:e48318.
6. Ma, X., Yang, T., Luo, Y., Wu, L., Jiang, Y., Song, Z., Pan, T., Liu, B., Liu, G., Liu, J., Yu, F., He, Z., Zhang, W., Yang, J., Liang, L., Guan, Y., Zhang, X., Li, L., Cai, W., Tang, X., Gao, S., Deng, K., and Zhang, H. TRIM28 promotes HIV-1 latency by SUMOylating CDK9 and inhibiting P-TEFb. *eLife*. 2019;8:e42426.

Submitted / Under Revision

1. Sibbertsen, F., Song, Z., Ly, C., Sandrock, I., Bonn, S., Koenecke, C., Tan, L., Schultze-Florey, C., and Prinz, I. TCR barcoding reveals distinct anti-CMV responses of γδ T cell clones after stem cell transplantation. *Submitted*, 2026.
2. Ly, C., Schaub, D. P., Khatri, R., Sultana, Z., Boxnick, A., Song, Z., Huber, T., Wiech, T., Tolosa, E., Panzer, U., Bonn, S., Krebs, C., and Prinz, I. Spatial analysis of T cell clonality in autoimmune kidney disease using TRV probes. bioRxiv. 2025.08.29.673064. *Resubmitted after revision*, 2026.
3. Yang, T., León-Lara, X., Almeida, V., Wang, Z., Abu, Y. E., Janssen, A., Kleine-Wechelmann, C., Hassan, A., Song, Z., Dempsey, M. M., Tan, L., Boehne, M., von Kaisenberg, C., Prinz, I., Förster, R., and Ravens, S. Transcriptomic profiling of human γδ T cells reveals non-linear immune aging characterized by childhood transitions and relative stability in adulthood. bioRxiv. 2026.01.15.699622. *Submitted*, 2026.

Erklärung des Eigenanteils

The individual contribution to each publication included in this dissertation is specified at the beginning of the respective chapter.

Eidesstattliche Versicherung

Ich versichere ausdrücklich, dass ich die Arbeit selbständig und ohne fremde Hilfe, insbesondere ohne entgeltliche Hilfe von Vermittlungs- und Beratungsdiensten, verfasst, andere als die von mir angegebenen Quellen und Hilfsmittel nicht benutzt und die aus den benutzten Werken wörtlich oder inhaltlich entnommenen Stellen einzeln nach Ausgabe (Auflage und Jahr des Erscheinens), Band und Seite des benutzten Werkes kenntlich gemacht habe. Das gilt insbesondere auch für alle Informationen aus Internetquellen.

Soweit beim Verfassen der Dissertation KI-basierte Tools („Chatbots“) verwendet wurden, versichere ich ausdrücklich, den daraus generierten Anteil deutlich kenntlich gemacht zu haben. Die „Stellungnahme des Präsidiums der Deutschen Forschungsgemeinschaft (DFG) zum Einfluss generativer Modelle für die Text- und Bilderstellung auf die Wissenschaften und das Förderhandeln der DFG“ aus September 2023 wurde dabei beachtet.

Ferner versichere ich, dass ich die Dissertation bisher nicht einem Fachvertreter an einer anderen Hochschule zur Überprüfung vorgelegt oder mich anderweitig um Zulassung zur Promotion beworben habe.

Ich erkläre mich damit einverstanden, dass meine Dissertation vom Dekanat der Medizinischen

Fakultät mit einer gängigen Software zur Erkennung von Plagiaten überprüft werden kann.

Datum Unterschrift

Danksagung

I would like to express my sincere gratitude to my supervisor, **Prof. Dr. Immo Prinz**, for his patience, guidance, support, and opened doors throughout my PhD. I could hardly have asked for more—except perhaps a beer now and then.

I would also like to thank **Prof. Dr. Likai Tan** and my colleagues at the **Institute of Systems Immunology**, **UKE**, for the supportive working environment, helpful discussions, and companionship throughout my time there.

I am also very grateful to all my collaborators for the inspiring collaboration and scientific exchange. My special thanks go to all the patients who participated in the studies. Without their contribution, this work would not have been possible.

Finally, I would like to thank my grandmother, **Junying Liu**, and my brother, **Xingchen Song**, for their constant love, encouragement, and unwavering support throughout my life. I would also like to acknowledge my own perseverance, resilience, and dedication throughout this journey. Completing this PhD marks both a scientific and a personal milestone, and I look forward to the next chapter.